LEVEL II 12

ESL-TR-80-56

EVAPORATION AND GROUNDFALL OF JP-4 JET FUEL JETTISONED BY USAF AIRCRAFT

HARVEY J. CLEWELL III
ENVIRONICS DIVISION
ENVIRONMENTAL SCIENCES BRANCH

SEPTEMBER 1980

FINAL REPORT
FEBRUARY 1972 - JUNE 1980

APPROVED FOR PUBLIC RELEASE; DISTRIBUTION UNLIMITED

AIR FORCE ENGINEERING AND SERVICES CENTER

AFESC

ENGINEERING & SERVICES LABORATORY
AIR FORCE ENGINEERING & SERVICES CENTER
TYNDALL AIR FORCE BASE, FLORIDA 32403

NOTICE

Please do not request copies of this report from HQ AFESC/RD (Engineering and Services Laboratory). Additional copies may be purchased from:

National Technical Information Service
5285 Port Royal Road
Springfield, Virginia 22161

Federal Government agencies and their contractors registered with Defense Technical Information Center should direct requests for copies of this report to:

Defense Technical Information Center
Cameron Station
Alexandria, Virginia 22314

UNCLASSIFIED

SECURITY CLASSIFICATION OF THIS PAGE *(When Data Entered)*

REPORT DOCUMENTATION PAGE		READ INSTRUCTIONS BEFORE COMPLETING FORM
1. REPORT NUMBER ESL-TR-80-56	2. GOVT ACCESSION NO. AD-A10 9307	3. RECIPIENT'S CATALOG NUMBER
4. TITLE *(and Subtitle)* Evaporation and Groundfall of JP-4 Jet Fuel Jettisoned by USAF Aircraft		5. TYPE OF REPORT & PERIOD COVERED Final Technical Report Feb 78 - Jun 80 6. PERFORMING ORG. REPORT NUMBER
7. AUTHOR(s) Harvey J. Clewell, III, Capt, USAF, BSC		8. CONTRACT OR GRANT NUMBER(s)
9. PERFORMING ORGANIZATION NAME AND ADDRESS HQ AFESC/RDVC Engineering and Services Laboratory Tyndall AFB, FL 32403		10. PROGRAM ELEMENT, PROJECT, TASK AREA & WORK UNIT NUMBERS Program Element 62601F Project 19004C02
11. CONTROLLING OFFICE NAME AND ADDRESS Air Force Engineering and Services Center Tyndall AFB, FL 32403		12. REPORT DATE September 1980 13. NUMBER OF PAGES 131
14. MONITORING AGENCY NAME & ADDRESS *(if different from Controlling Office)*		15. SECURITY CLASS. *(of this report)* UNCLASSIFIED 15a. DECLASSIFICATION/DOWNGRADING SCHEDULE

16. DISTRIBUTION STATEMENT *(of this Report)*

Approved for public release; distribution unlimited.

17. DISTRIBUTION STATEMENT *(of the abstract entered in Block 20, if different from Report)*

18. SUPPLEMENTARY NOTES

Availability of this report is specified on verso front cover.

19. KEY WORDS *(Continue on reverse side if necessary and identify by block number)*

Fuel Jettisoning	Aircraft Emissions	Dispersion Modeling
Fuel Dumping	Environmental Quality	Droplet Evaporation
Evaporation Modeling	Hydrocarbons	Droplet Fall Rates
Environics	Environmental Chemistry	Jet Fuel Composition

20. ABSTRACT *(Continue on reverse side if necessary and identify by block number)*

An experimental and modeling effort was undertaken to determine the physical fate of JP-4 jet fuel discharged from an aircraft in flight. A computer model was developed to simulate evaporation and free-fall of fuel droplets in the atmosphere. In order to apply this model to jettisoned fuel, an experimental study was performed to determine the droplet size distribution produced by the jettisoning process. This study featured in-flight sampling of the fuel plume from a KC-135 tanker aircraft. Sampling was also performed at ground level to determine whether the jettisoned fuel reached the ground in significant

DD FORM 1 JAN 73 1473 EDITION OF 1 NOV 65 IS OBSOLETE

UNCLASSIFIED

SECURITY CLASSIFICATION OF THIS PAGE *(When Data Entered)*

concentrations. For fuel jettisoning as low as 750 meters above the ground at temperatures around 11°C, no liquid fuel could be detected by ground observers and no significant hydrocarbon concentrations (greater than a few ppm C) were measured by the sampling.

The predictions of the fuel droplet model concerning the evaporation and groundfall of jettisoned fuel are presented along with an estimate of the atmospheric dispersion which takes place. For JP-4 fuel jettisoned higher than 1,500 meters at ground-level temperatures above freezing (0°C), more than 98% of the fuel should evaporate before reaching the ground. Droplets and vapor are widely dispersed by atmospheric turbulence, quickly resulting in a fuel density too low to create any perceptible environmental changes.

Formulas and graphs are included for estimating the likelihood of significant ground-level concentrations of fuel vapor or liquid following a specific fuel jettisoning incident.

PREFACE

This report was prepared by HQ AFESC Engineering and Services Laboratory, Tyndall Air Force Base, Florida. It documents work performed during the period February 1972 through June 1980 under Program Element 62601F, Project 19004C02. The author and project officer since June 1976 was Capt Harvey J. Clewell; previous project officers were Captains James T. Haney and Edward R. Ricco.

This report describes the work which was performed to determine the physical fate of JP-4 jet fuel discharged from an aircraft in flight. The principal results of this effort have already been included in a general analysis of the environmental effects of fuel jettisoning by Air Force aircraft (Reference 1). This report is intended to document the experimental basis for part of that analysis. In addition, the information presented in this report can be used to estimate the likelihood of significant ground-level concentrations of fuel vapor or liquid following a fuel jettisoning incident.

The author acknowledges the contributions of several co-investigators in this effort. Development of the fuel droplet model was initiated by Captain Edward R. Ricco. Dr Daniel A. Stone helped plan the experimental study at Edwards Air Force Base, and along with A1C Gregory A. Urda, was instrumental in carrying out the ground sampling. The gas-chromatographic analysis of the samples was developed and performed by Mr. Thomas B. Stauffer. The airborne sampling was performed by Meteorology Research, Incorporated,

under contract to the Air Force Geophysics Laboratory, Dr R. E. Good and Mr Charles A. Forsberg project officers.

This report has been reviewed by the Public Affairs Office and is releasable to the National Technical Information Service (NTIS). At NTIS it will be available to the general public, including foreign nations.

This technical report has been reviewed and is approved for publication.

HARVEY J. CLEWELL, III, Capt, USAF, BSC
Air Quality Research Chemist

JOHN T. SLANKAS, Maj, USAF
Chief, Environmental Sciences Branch

MICHAEL J. RYAN, Lt Col, USAF, BSC
Chief, Environics Division

FRANCIS B. CROWLEY, III, Colonel, USAF
Director, Engineering and Services Laboratory

TABLE OF CONTENTS

TABLE OF CONTENTS (CONTINUED)

LIST OF FIGURES

LIST OF FIGURES (CONTINUED)

LIST OF TABLES

(The reverse of this page is blank)

SECTION I

INTRODUCTION

Due to in-flight emergencies or other unforseen events it occasionally becomes necessary for Air Force aircraft to discharge unburned fuel directly into the atmosphere while airborne. The primary reason for jettisoning fuel is to reduce the aircraft's gross weight to facilitate a safe landing. As a result of a growing awareness of fuel jettisoning's potential for environmental degradation, the Air Force initiated a study in 1972 to determine the nature, the extent and the environmental affects of fuel jettisoning by Air Force aircraft. The overall results of that study are reported in Reference 1. The present report documents the experimental and modelling efforts which were undertaken to determine the physical fate of the jettisoned fuel in support of one aspect of that study.

Jet fuel, when jettisoned from an aircraft, readily breaks up into small droplets and begins to evaporate. The fuel vapor and droplets are subject to entrainment in the aircraft wake, dispersion by atmospheric turbulence, and (in the case of droplets) gravitational settling. The principal question to be answered by the work described in this report was what fraction of the jettisoned fuel can be expected to reach the ground in liquid form. The environmental affects due to liquid fuel contamination of the ground are very different from those associated with the airborne fuel vapors. Therefore, a knowledge of the fraction of

fuel in each form is essential for estimation of the overall impact of fuel jettisoning.

Section II describes a computer model which was developed to simulate the evaporation and free-fall of fuel droplets in the atmosphere. In order to apply this model to fuel jettisoning it is necessary to know the distribution of droplet sizes which is produced by the jettisoning process; the experimental study which was performed to determine this information is described in Section III. As noted there it was necessary to use the droplet evaporation model to interpret the experimental findings. During this experiment, sampling was also performed at ground level to determine whether the jettisoned fuel reached the ground in significant concentrations. The results of the ground-sampling are also presented in this section.

In Section IV the predictions of the droplet model concerning the evaporation and groundfall of jettisoned fuel are presented along with an estimate of the atmospheric dispersion. A detailed description of the droplet model, together with a program listing and sample output, is provided in the appendices.

SECTION II

FUEL DROPLET FREE-FALL AND EVAPORATION MODELLING

The evaporation of a fuel droplet is complicated by the fact that as the droplet evaporates its composition changes. The lighter, more volatile components are stripped away preferentially while the denser, slower-evaporating components remain. Also, as the droplet evaporates it becomes smaller, reducing the surface area available for evaporation. Therefore the evaporation rate decreases markedly at first, but later levels off. A further complication arises when the droplet is allowed to fall. As it falls the droplet experiences changing atmospheric temperature, pressure, and viscosity, since these properties are a function of altitude. These changing atmospheric properties modify the droplet's evaporation rate as well as its rate of fall. In addition, the rate of fall varies with the droplet's size and density, which in turn depend on its evaporative history. As a result, the evaporation and free-fall of the droplet are interdependent processes.

2.1 DESCRIPTION OF THE MODEL

The model which was developed to simulate the simultaneous evaporation and free-fall of a fuel droplet is based on the pioneering work of Lowell (References 2 and 3). Lowell's method has been refined and extended chiefly by the incorporation of experimental data provided by the Arnold Engineering Development Center (AEDC)

and by the use of a more detailed fuel composition. The data obtained by AEDC (Reference 4) includes measurements of the drag coefficients and evaporation rates of JP-4 fuel droplets as well as the physical properties of JP-4 as a function of temperature. Data on the composition of JP-4 provided by the Air Force Aero-Propulsion Laboratory was used to prepare a theoretical 33 component "synthetic JP-4" mixture as shown in Table 1. The calculated physical properties of this mixture (density, average carbon number, and Reid vapor pressure) agree well with typical analyses of JP-4. Each component in the synthetic mixture represents a class of compounds in real JP-4. Lowell used ten equal volume distillate fractions to represent JP-4; the more detailed composition allows modelling of the droplet to continue until virtually all (99.9%) of the mass is gone. Additional refinements include a complete energy balance, and an initial droplet temperature estimate. The effect of these two calculations is assessed in Appendix A.

Essentially, the model breaks up a droplet's fall into a series of small time intervals. The distance of fall during each interval is calculated assuming the droplet is falling at the terminal velocity for its current diameter, density and altitude. Loss of mass through evaporation is calculated assuming Raoult's law; that is, each component evaporates independently. An energy balance routine adjusts the droplet temperature to allow for evaporative cooling, radiation, conduction, and insolation effects. The new droplet composition, mass and altitude are used as initial

TABLE 1. SYNTHETIC JP-4

Compound	Volume Percent	Molecular Weight	Boiling Point(C)	Density (g/ml)
iso-pentane	3.9	72.2	27.9	.62
iso-hexane	8.1	86.2	60.2	.66
cyclohexane	2.1	84.2	80.7	.78
benzene	0.3	78.1	80.1	.88
3-methylhexane	9.4	100.2	91.8	.69
methylcyclohexane	7.1	98.2	100.9	.77
toluene	0.7	92.1	110.8	.87
4-methylheptane	10.1	114.2	117.7	.70
cis-1,4-diethylcyclohexane	7.4	112.2	124.3	.78
m-xylene	1.6	106.2	139.1	.87
4-methyloctane	9.1	128.3	142.4	.72
isopropylcyclohexane	4.3	126.2	154.5	.80
1-ethyl-2-methylbenzene	2.4	120.2	165.2	.88
2,7-dimethyloctane	7.3	142.3	159.6	.72
p-menthane (cis)	3.7	140.3	170.9	.80
p-cymene	1.8	134.2	177.1	.86
napthalene	0.2	128.2	217.9	1.03
undecane	4.8	156.3	195.9	.74
3-methylbutylcyclohexane	2.5	154.3	196.5	.80
2-methylenedecalin (trans)	3.4	150.3	201.0	.89
1-butyl-3-methylbenzene	1.1	148.2	205.0	.86
1-methylnapthalene	0.2	142.2	244.6	1.02
dodecane	2.8	170.3	216.3	.75
3-ethylbutylcyclohexane	1.2	168.3	211.0*	.80*
1,3,5-triethylbenzene	0.5	162.3	216.0	.86
2,3-dimethylnapthalene	0.2	156.2	268.0	1.00
tridecane	1.1	184.4	235.4	.76
3-isopropylbutylcyclohexane	0.4	182.4	225.0*	.80*
3,5-diethyl-1-propylbenzene	0.1	176.3	234.0*	.87*
tetradecane	0.2	198.4	253.7	.76
pentadecane	0.1	212.4	270.6	.77
perhydrophenanthrene	1.8	192.4	290.0*	.94
pyrene	0.1	202.3	393.0	1.27

Density = 0.75 g/ml
Average Carbon # = 8.7
Reid vapor pressure (100F) = 2.5 psia
Aromatics = 9.2%
Napthalenes = 0.7%

NOTE: Olefins can be considered present in the paraffinic fractions at a level of 1%.

*estimated

conditions for the next interval. This stepwise approximation continues until the droplet impacts on the ground or loses 99.9 percent of its initial mass. The initial conditions which must be known are the droplet's original composition, altitude and diameter, the temperature at local ground level, and the aircraft's air speed. The initial droplet temperature is then taken as the corresponding stagnation temperature, assuming equilibration of the fuel tanks with the skin of the aircraft. In the early intervals the droplet is then allow to cool through evaporation until an energy balance is achieved.

A more detailed description of the model is presented in Appendix B, and a listing of the computor program is included as Appendix C. The program reports the droplet's status at the end of each time interval or a selected period of time. Output for a single-droplet case includes the elapsed time since release; the droplet altitude, velocity, diameter and fraction of initial mass remaining; and the fractional mass of each component. Sample output for several single-droplet cases as well as for a distribution of droplets is provided in Appendix D.

2.2 SINGLE-DROPLET RESULTS

Figure 1 shows the predicted evaporation and free-fall of a 270-micron droplet released at 1500 meters for three different ground-level temperatures. Initially evaporation dominates, and in the first few minutes the droplet loses from 60 to 90 percent of its mass, depending on the temperature. Thereafter evaporation becomes less important, and the droplet falls without a substantial

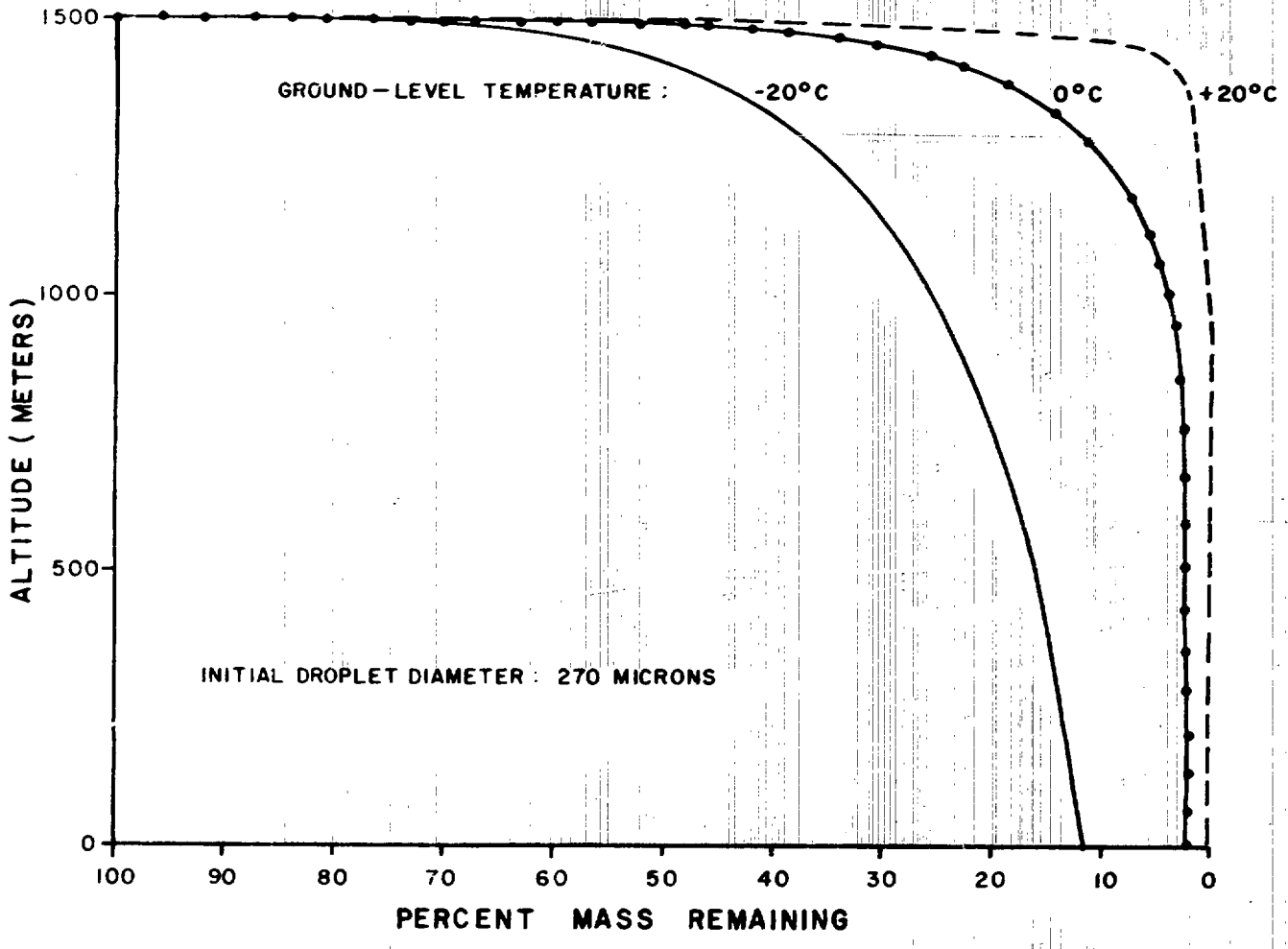

Figure 1. Evaporation and Free-Fall of a JP-4 Fuel Droplet

change in mass. The duration of the evaporation phase for all three temperatures is around five minutes, while the free-fall phase ranges from 50 minutes at -20°C to over 11 hours at +20°C. At the higher temperature the droplet evaporates more completely in the first phase; and therefore, being smaller, it falls more slowly during the second phase. The dots on the curve for 0°C show the actual intervals used by the model in performing its stepwise simulation. The model maintains roughly constant increments of mass and then altitude by increasing the duration of the intervals from less than a tenth of a second initially to more than 30 minutes at the end.

The effect of a droplet's initial size is shown in Figure 2 for an initial altitude of 1500 meters and a ground-level temperature of 0°C. On a relative basis, a 100-micron droplet appears to evaporate more quickly than a 500-micron droplet. However, this is only an artifact, caused by the fact that the mass of a droplet is proportional to its diameter cubed while the evaporation rate is proportional to the diameter squared. On an absolute basis, the larger droplet is actually evaporating much faster than the smaller droplet, as can be seen from the more rapid change in diameter. Due to its larger size, the 500-micron droplet also falls much faster than the 100-micron droplet.

As mentioned earlier, the more volatile components in the fuel evaporate preferentially. Figure 3 demonstrates this effect for

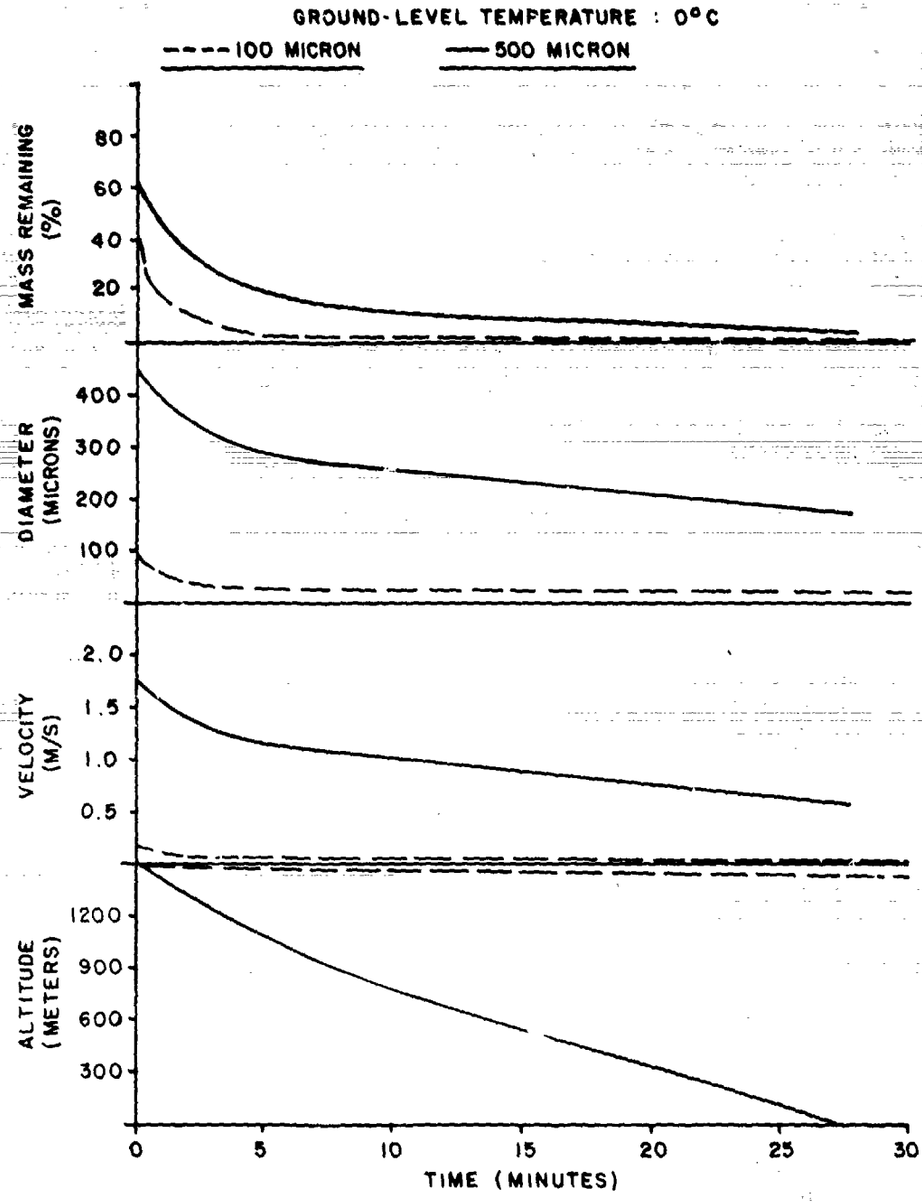

Figure 2. Effect of Initial Droplet Diameter on Evaporation and Free-Fall

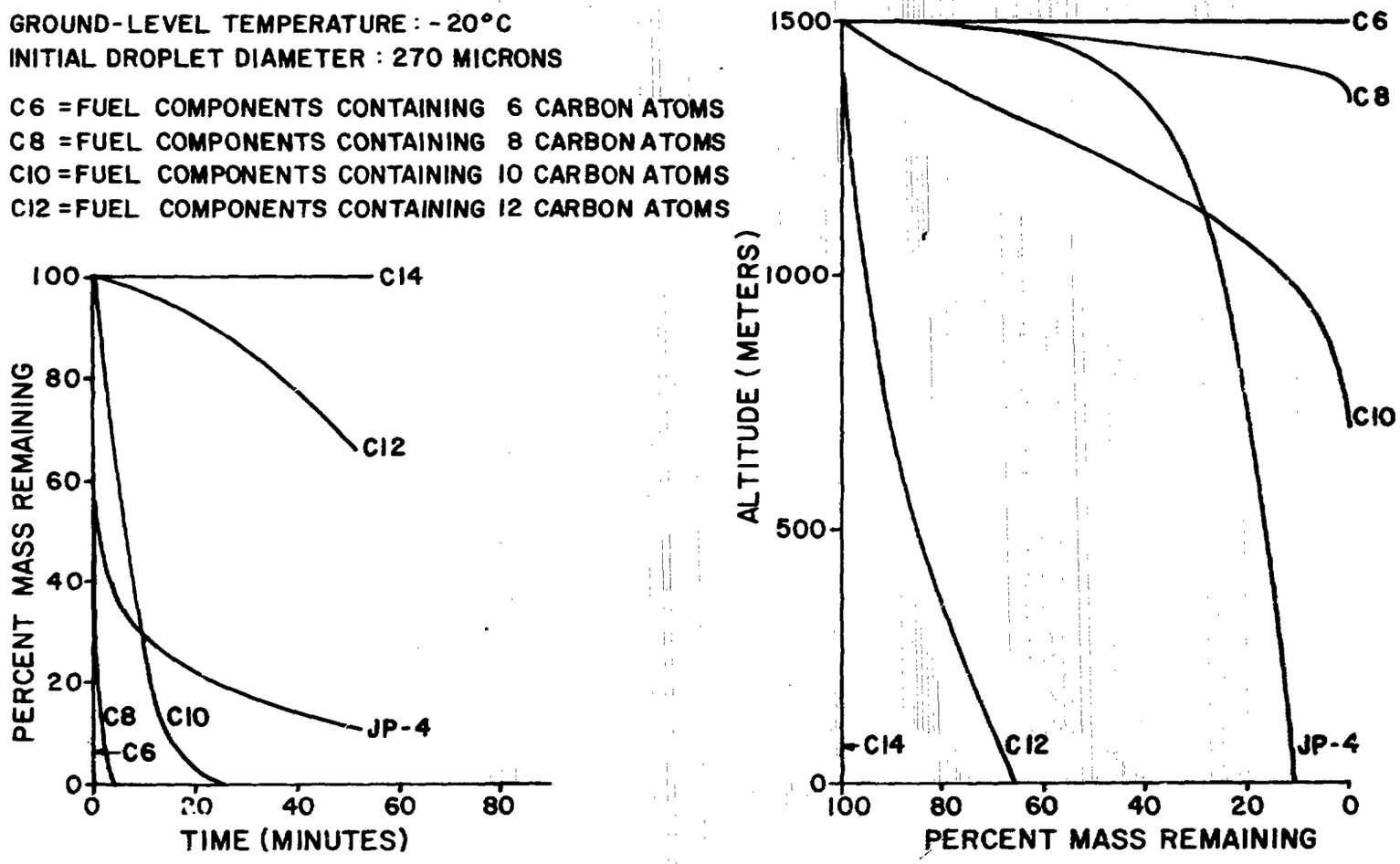

Figure 3. Differential Evaporation of Fuel Components from a Droplet of JP-4

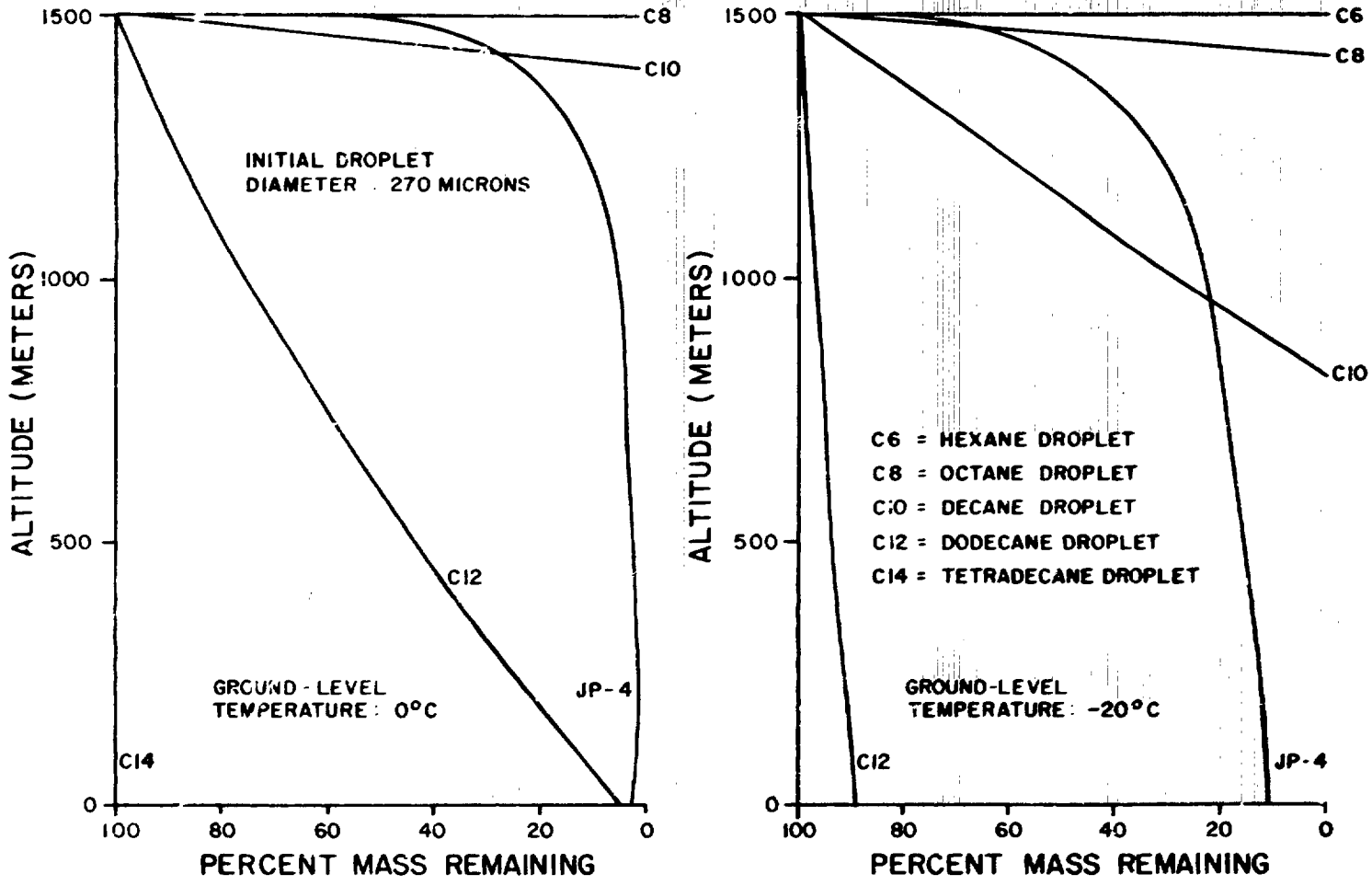

Figure 4. Evaporation of Single-Component Droplets Versus a Mixture

a 270-micron droplet released at 1500 meters when the ground-level temperature is -20°C. The lighter compounds (containing less than eight carbon atoms) are lost almost immediately, while the heavier components (containing more than twelve carbons) hardly evaporate at all. This results in the different fuel components being distributed vertically: the lighter compounds are left at the initial release height, the heavier compounds reach the ground, and the intermediate compounds are spread out in between.

Finally, Figure 4 examines the related question of whether the evaporation of a complex mixture can be approximated by a single compound. In Figure 3 the curves C6 through C14 represented different components in the same droplet. In Figure 4, however, curves C6 through C14 represent different droplets, each of which contain only one component. These curves show that no single-component droplet matches the behavior of a droplet of JP-4. During the early stages of evaporation, a JP-4 droplet resembles hexane or octane. But then the JP-4 droplet evaporation slows down until it eventually parallels that of a dodecane or tetradecane droplet. From inspection of the results for 0°C and -20°C it can be seen that no single-component droplet could be used to predict the fraction of JP-4 reaching the ground under different conditions. For the same reason, the ability of a mixture of several compounds to represent JP-4 is limited when the number of compounds in the mixture is small. For example, a mixture of ten equal fractions could not simulate a JP-4 droplet beyond 90 percent evaporation, because at that point the simulated droplet would essentially consist of just one component.

2.3 COMPARISON WITH EXPERIMENTAL DATA

One of the experiments carried out by AEDC in support of this fuel jettisoning study consisted of suspending small droplets of JP-4 from a glass filament and measuring their rates of evaporation when subjected to a controlled airflow (Reference 4). The results obtained for several droplets are shown as points in Figure 5. These data were obtained at a temperature of 20°C and with an airflow of 3 meters per second, which is close to the terminal velocity of the size droplets studied. The curves in Figure 5 show the predictions of the fuel droplet model under the same conditions. The agreement is excellent.

The AEDC effort also attempted to measure evaporation rates in cooled airflows (-10° to -20°C). Unfortunately, water condensation at these temperatures led to severe experimental problems, bringing the validity of the few results obtained into question. The reported evaporation rates are extremely low, roughly a factor of five lower than the fuel droplet model would predict. Since the temperature dependent parameters in the fuel droplet model have been checked against experimental values (see Appendix B), the disagreement solely with AEDC's low-temperature data indicates that the low-temperature experiments may have been compromised by the water condensation problems. However, these problems were not encountered during the tests at +20°C, so the use of the room-temperature results to validate the fuel droplet model appears to be justified.

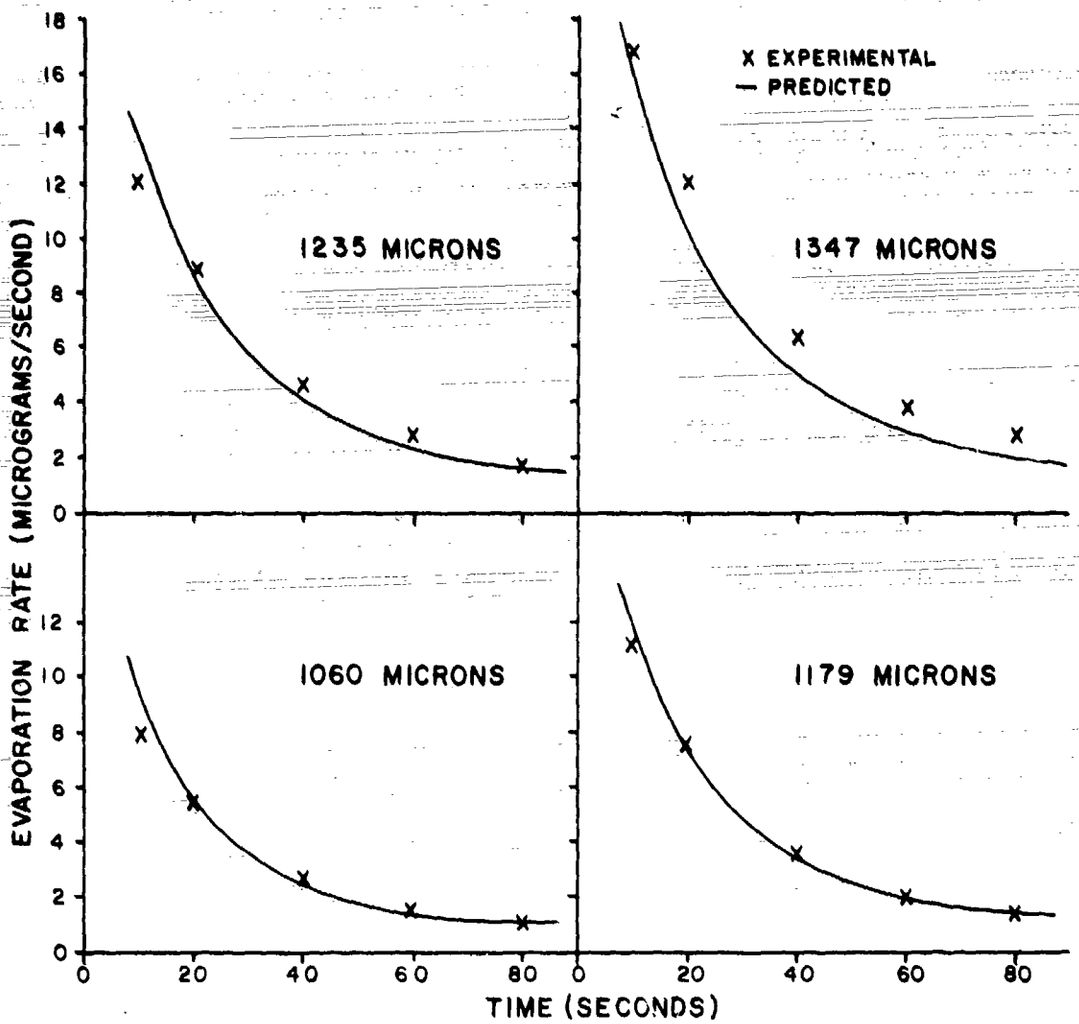

Figure 5. Comparison of Model Predictions with Experiment

SECTION III

EXPERIMENTAL FUEL JETTISONING STUDY

The fuel droplet model described in the previous section begins with an initial droplet diameter, altitude and temperature and predicts the ensuing history of the droplet. Therefore the application of this model to the question of fuel jettisoning requires a knowledge of the droplet sizes involved. It can be assumed that in the process of being discharged through an orifice into a high velocity airstream, the fuel would be atomized into a distribution of droplet sizes. However, the droplets produced could range from only a few microns in diameter (the size that scatter light) up to several thousand microns in diameter (the size of raindrops). The actual droplet size distribution produced by the jettisoning process cannot be predicted from theory. Therefore it must be determined experimentally.

3.1 BACKGROUND

An initial attempt to determine the droplet size distribution produced by fuel jettisoning was performed in 1973 (Reference 5). This study, which was conducted at the AEDC, simulated the fuel jettisoning process by injecting JP-4 into a high-velocity airstream in a wind tunnel. Airflows of 100 to 200 meters per second were used, representing typical aircraft airspeeds during jettisoning. The droplets produced were then measured using holography. The observed droplet size distribution is shown in

Figure 6 ("AEDC-experimental"). All of the droplets detected were less than 100 microns in diameter, with a mass median diameter of only 32 microns. However, due to the constraints imposed by the size of the wind tunnel these tests were conducted with fuel flow rates of only 0.02 to 2.2 kilograms per second, compared to typical aircraft jettisoning rates of 5 to 50 kilograms per second. Therefore, it was not certain that these results were representative of full-scale fuel jettisoning, where the airstream might not possess sufficient energy to thoroughly atomize all of the fuel.

During the same period another study was conducted in England by Cross and Picknett (Reference 6). In this study a small jet aircraft (a British "Buccaneer") jettisoned fuel at 7.5 kilograms per second from wing tanks while flying at 120 meters per second. The aircraft was flown less than 15 meters above the ground, and the fuel spray was sampled by filter papers laid on the ground. A fluorescent dye was added to the fuel so that the droplet spots on the filter paper could be visualized. The fuel used was Avtur, a British commercial fuel similar to JP-8 and much less volatile than JP-4. A typical droplet size distribution observed for one of their flights is shown in Figure 6 ("Cross and Picknett - experimental"). The mass median diameter was 240 microns with droplets ranging from 40 to 400 microns. Cross and Picknett considered this distribution to be a lower bound for fuel jettisoning, since the fuel was jettisoned perpendicular to the airstream. As an upper bound, they presented a composite distribution based on

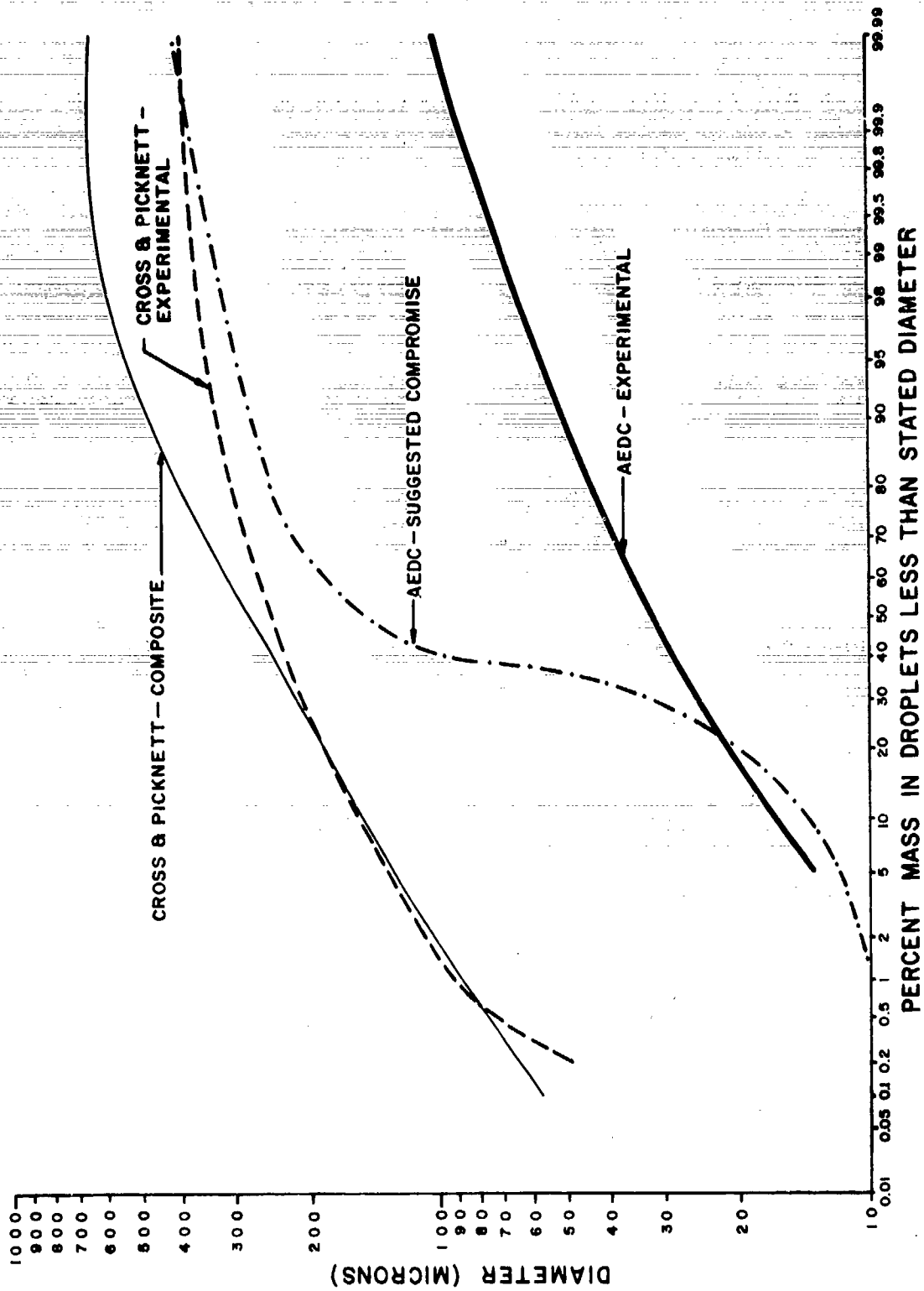

Figure 6. Reported Fuel Droplet Size Distributions

previous studies for other aircraft with rearward projecting jettison-tubes. This distribution is also shown in Figure 6 ("Cross and Picknett - Composite"). The mass median diameter in this case is 270 microns, with some droplets as large a 650 microns.

Although the aircraft-generated droplet size distributions measured by Cross and Picknett were more likely to be representative of aircraft fuel jettisoning than the wind tunnel data from AEDC, there was still some concern about the wide disparity of the two results. Also, the Cross and Picknett study suffered from two shortcomings: first, the technique used to visualize the droplets could not detect droplets less than 40 microns in diameter; and second, in all of the trials, no more than 55 percent of the jettisoned fuel could ever be accounted for. In an attempt to resolve the discrepant results, Dawbarn (Reference 4) suggested that the actual fuel droplet distribution was somewhere between the two extremes. His proposed intermediate distribution is shown in Figure 6 as "AEDC - Suggested Compromise." Due to the uncertainty still surrounding the size distribution question, the decision was made to perform another study in which an aircraft would be used to jettison the fuel. The distinguishing feature of this study would be in-flight sampling by a second aircraft.

3.2 DESCRIPTION OF THE EXPERIMENTAL PROGRAM

The in-flight sampling program was conducted jointly by the Air Force Engineering and Services Center and the Air Force Geophysics

Laboratory, at Edwards Air Force Base, California, in December 1976. A sampling aircraft equipped with optical droplet-sizing instrumentation and a hydrocarbon vapor analyzer was flown directly into the cloud of fuel jettisoned by an Air Force KC-135 tanker aircraft. Direct measurements of the fuel droplet size distribution and density were obtained and average droplet fall rates were estimated. Flights were conducted at three altitudes (approximately 1500, 3600, and 6000 meters above mean sea level) to determine whether the fuel droplet size distribution was a function of release height. Ground-level sampling for hydrocarbons was also performed during the low-level flights (which were roughly 750 meters above the ground) to determine whether any of the jettisoned fuel reached the ground. In all cases, typical KC-135 jettisoning practices were followed. Table 2 lists the conditions under which the fuel was jettisoned in this program.

TABLE 2. KC-135 FUEL JETTISONING PARAMETERS

Fuel:	JP-4
Dump-nozzle diameter:	10.1 centimeters
Aircraft airspeed:	170 meters per second
Jettison rate:	56 kilograms per second or 330 grams per meter
Duration of dump:	15-30 seconds

The KC-135 jettisons fuel through the boom normally used to refuel other aircraft. Usually the boom is lowered for jettisoning as well as refueling, but in some emergency situations fuel might be

jettisoned with the boom stowed. Therefore, the experimental program included jettisoning in both configurations.

3.3 IN-FLIGHT SAMPLING RESULTS

The in-flight sampling was carried out by Meteorology Research, Incorporated (MRI), using a specially instrumented Piper Navajo aircraft. The droplet sizing instrumentation consisted of three particle spectrometers manufactured by Particle Measuring Systems, Incorporated. These spectrometers, which size particles as they intercept a beam of laser light, cover the size ranges 2-30, 20-300, and 300-4500 microns. A foil impactor was also used on some flights to provide a larger cross-section for detecting droplets greater than 250 microns in diameter. Other instrumentation included a hydrocarbon analyzer and an integrating nephelometer to detect vapor and fine particles, respectively. A two-volume report describes the MRI sampling effort and presents in detail the data obtained (Reference 7).

After the tanker performed each fuel dump, the sampling aircraft was vectored in for perpendicular passes through the fuel dump plume. In the later sorties, better sampling results were obtained by flying the sampling aircraft directly down the length of the fuel dump. Flying at 80 meters per second, the aircraft was then able to obtain continuous particle counts for as long as 30 to 45 seconds on a single pass. The fuel dump could be seen initially as a long, white cloud resembling a contrail. For favorable sun angles the fuel cloud was still visible more than 10

minutes after the dump, but usually the sampling aircraft could no longer follow the cloud visually after the first two to four minutes. Real-time radar tracking of the tanker's position during the fuel dump and of the location of the sampling aircraft during successful passes through the plume was used to direct the search after visual sighting was no longer possible. Unexpectedly, drizzle-sized droplets (around 100 microns) could be detected even after the fuel cloud was no longer visible. In fact "splash on the windshield" of the Navajo became the most definitive mark of entry into the fuel cloud.

Figure 7 shows a typical plume produced by fuel jettisoning. During the first minute the plume quickly expands to nearly 100 meters in diameter and takes on a markedly coiled appearance under the influences of the aircraft wake vortex. This long spiral tube maintains its integrity for several minutes, but eventually begins to fold on itself as the plume dissipates. The position of the refueling boom greatly affects the initial growth of the fuel dump plume. When the boom is up in the stowed position, the fuel is immediately engulfed in one of the expanding wing tip vortices, leading to rapid expansion and coiling. However, with the boom lowered the plume initially lies below the aircraft wake and, therefore, expands more slowly with little sign of coiling. Finally, after approximately 60 seconds the plume does become entrained in one of the wake vortices and from then on is identical to the boom-up plume. The pilot of the Navajo reported that visually there appeared to be greater vertical dispersion of the

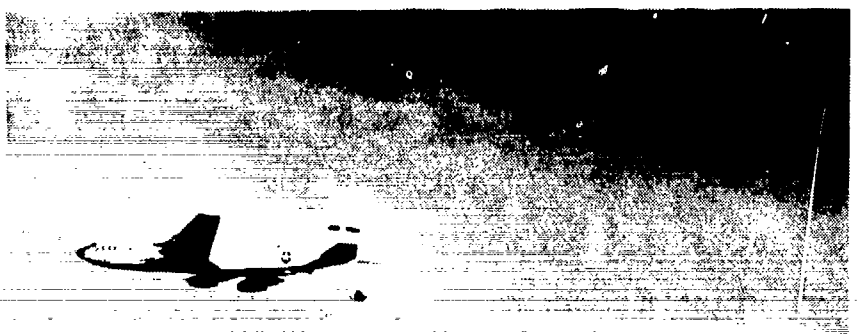

a. KC-135 Tanker Jettisoning JP-4 Jet Fuel

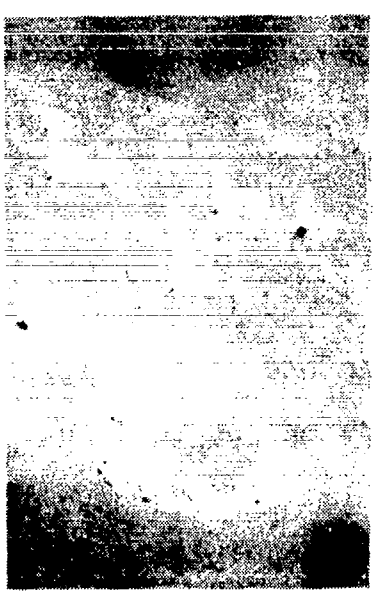

b. Sampling Aircraft in the Plume Two Minutes Later

Figure 7. Fuel Dump Plume

plume and possible "rainout" of larger droplets with the boom down, but no sampling or photographic evidence of this effect could be obtained. Sampling passes below the visible fuel clouds were performed to search for any rainout of larger droplets, but no such phenomenon was ever detected.

Overall planning, direction and analysis of the MRI sampling effort was performed by the Air Force Geophysics Laboratory (AFGL). Using a statistical analysis, AFGL was able to distinguish actual droplet encounters from fluctuations in the atmospheric particulate background. The droplet size distribution observed in these encounters was then corrected for evaporation (using the droplet evaporation model described in Section II of this report) to obtain an estimate of the "original" droplet size distribution. This correction was necessary to allow for the length of time the fuel droplets were free to evaporate before the sampling aircraft entered the fuel dump plume. Due to flying safety considerations, the first pass by the sampling aircraft through the fuel dump usually occurred as much as 90 seconds after the tanker had passed. Based on the evaporation model, a typical fuel droplet had lost more than 80 percent of its original mass by this time and had been reduced to about half of its original size.

Composite experimental and corrected droplet size distributions based on all of the sampling flights are shown in Figure 8. (The curve entitled "This Report" will be discussed later.) No clear distinction was found between results for different altitudes and

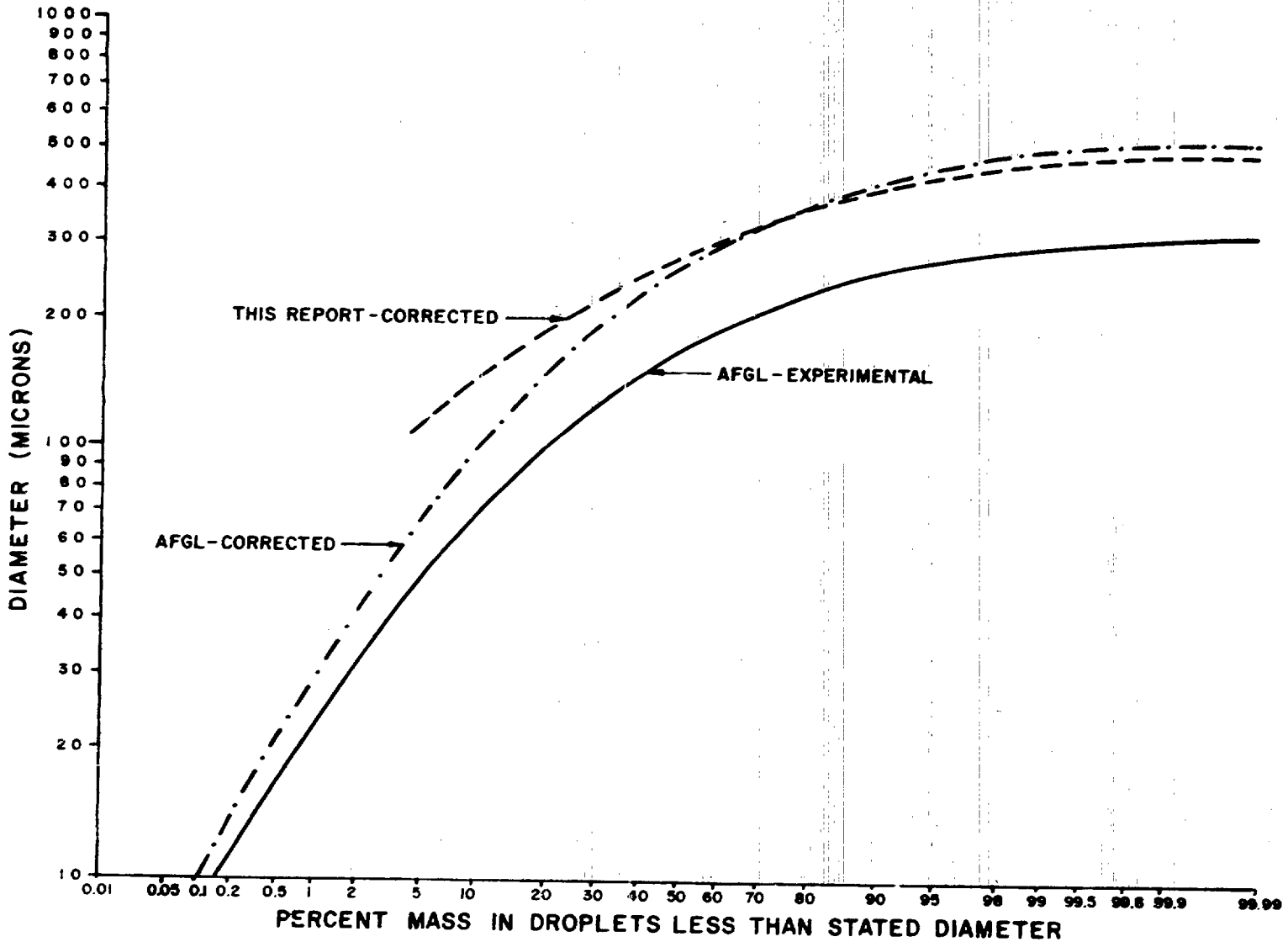

Figure 8. KC-135 Droplet Size Distributions

boom configurations; therefore, all of the encounters were averaged together to obtain these composites. Individual sampling results for each fuel dump plume encounter are included in the AFGL report (Reference 8). A full range of droplets from 2-600 microns were observed, with a composite mass median diameter of 165 microns. After correcting for evaporation, the mass median diameter becomes 265 microns, with a significant number of droplets as large as 500 microns.

Ground-level photography was used by AFGL to estimate the dimensions of the fuel dump plume during the sampling operation. Their analysis indicates that the fuel dump plumes were typically 100 meters in diameter after 90 seconds. For a jettisoning rate of 330 grams per meter, the nominal density of fuel dumped would then be 0.042 grams per cubic meter. Correcting the observed fuel droplet densities for evaporation, AFGL was able to account for only 0.010 grams per cubic meter, or about 25 percent of the known mass. Similarly, assuming the fuel droplets were 80 percent evaporated at the time the plume was sampled, the measured JP-4 vapor density should have been 80 percent of the nominal fuel density, or 0.034 grams per cubic meter (about 6.4 part per million). The highest concentration recorded by the hydrocarbon analyzer on the Navajo was only 4 parts per million, and average concentrations for passes down the length of the plume were closer to 2 parts per million. Since both of these discrepancies diminished confidence in the validity of the sampling results, they will be examined further in the following sections.

3.3.1 ANALYSIS OF THE DROPLET MEASUREMENTS

During the first experimental sortie, only perpendicular passes through the fuel dump plume were performed. However, it soon became apparent that these perpendicular encounters were too short to provide significant particle counts. Thereafter, parallel passes down the length of the fuel dump plume were also carried out. The parallel passes are preferred not only because they encountered a larger number of particles, but also because they would tend to average out any local fluctuations in the fuel dump plume density. The longest continuous encounter with each fuel dump plume is listed in Table 3. Fuel dumps not listed did not include any long sampling passes.

Two of the fuel dump encounters listed in Table 3 were not used in the mass balance calculation that follows. In fuel dump 3/5, the plume rose above the initial jettisoning height under the influence of a high level inversion with a vertical wind component. Apparently, in pushing the plume upward, the inversion also compressed it vertically, because the observed fuel droplet density was considerably greater than that observed in any of the other fuel dumps. In fuel dump 3/6, the only lengthy encounter with the plume recorded an anomalous droplet distribtuion. All of the observed mass was in very large droplets (between 230 and 300 microns). Since these results are contradictory to the observations of all the other fuel dumps, they were rejected.

The mass densities listed in Table 3 are those observed by the Cloud Particle Spectrometer (CPS) only. This instrument sizes

TABLE 3. MAJOR FUEL DUMP PLUME ENCOUNTERS

Dump Altitude (meters)	Sortie/Dump	Start of Encounter (hr:min:sec)	Elapsed Time Since Dump (seconds)	Duration of Encounter (seconds)	Observed Mass Density (g/m^3)	Boom Position
1500	2/2	22:31:53	90	22	.007	Up
	2/3	22:46:56	88	37	.007	Up
	2/4	23:00;46	49	10	.002	Up
	2/5	23:17:40	106	12	.006	Up
	3/2	21:09:29	69	22	.004	Up
	3/3	21:29:12	90	29	.010	Up
	Average		82		.006	
3600	3/4	22:17:46	76	27	.013	Up
	3/5	22:44:17	(96)*	20	(.037)*	Down
	3/6	23:06:08	(101)*	25	(.013)*	Down
	4/1	19:12:46	91	57	.009	Down
	Average		84		.011	
6000	4/3	20:29:32	52	45	.006	Down
	4/5	21:29:43	208	21	.007	Down
	Average		130		.007	
	Overall Average		92		.007	

*excluded from calculations (see text)

droplets with diameters ranging from 10 to 310 microns by sorting the droplets into 15 channels, each of which includes a particle diameter range of 20 microns. As can be seen from the experimental curve in Figure 8, practically all of the observed droplet mass was within the range of the CPS. Eliminating consideration of the small (2-20 micron) and large (300-4500 micron) particle instruments simplifies the mass balance calculations without significantly changing the result.

Calculation of the average intial droplet mass density for the six fuel dumps at 1500 meters is shown in Table 4. The average mass density observed in each CPS channel, taken directly from Reference 7, was multiplied by a correction factor. This factor was necessary because in converting from corrected (raw minus background) droplet counts to mass of JP-4, MRI used the wrong density for JP-4 (0.92 instead of 0.76). Also, their conversion to mass neglected the effect of the median diameter offset which they had noted for the first five channels. These discrepancies were also corrected in the AFGL analysis (cf. Table 2 in Reference 8 versus Table 2 in Reference 7). The fuel droplet evaporation model was used to determine the initial droplet diameter which would evaporate to each channel's median diameter in the time available and at the observed ambient temperature. Using the percent mass remaining calculated by the model, the observed mass density for each channel was then scaled up to obtain the initial droplet mass densities.

TABLE 4. CALCULATION OF THE INITIAL DROPLET MASS DENSITY FOR THE FUEL DUMPS AT 1500 METERS

CPS Channel	Median Diameter (microns)	Correction Factor*	Observed Density ($g/m^3 x 10^5$)	Cumulative Percent	Initial † Diameter (microns)	Percent † Mass Remaining	Calculated Initial Density ($g/m^3 x 10^3$)	Cumulative Percent
1	24	1.43	4.98	0.84	90	2.9	1.72	3.97
2	44	1.1	10.21	2.56	130	4.5	2.27	9.22
3	64	1.0	15.95	5.24	160	6.2	2.57	15.16
4	83	.93	25.24	9.48	190	8.5	2.97	22.02
5	103	.90	39.46	16.12	220	10.7	3.69	30.55
6	120	.83	51.02	24.70	250	12.5	4.08	39.97
7	140	.83	64.73	35.59	280	13.9	4.66	50.74
8	160	.83	62.74	46.15	310	15.1	4.15	60.33
9	180	.83	77.37	59.16	340	16.6	4.66	71.10
10	200	.83	75.63	71.88	370	17.6	4.29	81.01
11	220	.83	43.07	79.13	400	18.6	2.32	86.37
12	240	.83	33.57	84.78	430	19.6	1.71	90.32
13	260	.83	29.48	89.74	460	20.6	1.43	93.62
14	280	.83	30.55	94.87	490	21.6	1.41	96.88
15	300	.83	30.47	100	520	22.6	1.35	100
		TOTAL:	0.006 g/m^3				0.043 g/m^3	

* factor used to correct masses reported in Reference 7 (see text)

† calculated with fuel droplet evaporation model

The resulting mass balance at all three altitudes is shown in Table 5. The ratio of the calculated initial mass density to the nominal density, based on a plume diameter of 100 meters, ranges from 0.6 to 1.8, with an average of 1.1. The composite initial distribution for all ten encounters is shown in Figure 8 ("This Report - Corrected"). This distribution differs from the initial distribution derived by AFGL only in the smaller droplet diameter range. Where they differ, the AFGL distribution is probably the more accurate for two reasons: first, the AFGL distribution is based on data obtained by all three spectrometers, not just the CPS; and second, AFGL used a more sophisticated method of background subtraction to obtain the corrected droplet counts than that used by MRI in Reference 7.

The total initial density derived by AFGL was only 0.010 grams per cubic meter, compared to an average of 0.046 derived here. However, the curves of initial droplet density versus diameter in the AFGL report (Reference 8) are consistent with the results obtained here. For example, the initial droplet density curve in the AFGL report for the fuel dumps at 1500 meters rises from 1.5×10^{-3} grams per cubic meter at 100 microns to a maximum of 8.3×10^{-3} grams per cubic meter at 350 microns, and then falls to around 1×10^{-3} grams per cubic meter at 500 microns. From Table 4, the corresponding densities are 1.7×10^{-3} grams per cubic meter at 100 microns, 4.7×10^{-3} grams per cubic meter at 340 microns, and 1.41×10^{-3} grams per cubic meter at 500 microns. The discrepancy, then, only appears when these droplet density curves are integrated to obtain the total liquid density.

TABLE 5. SUMMARY OF DROPLET MASS DENSITY CALCULATIONS

Altitude:	1500 meters	3600 meters	6000 meters	Overall
Number of encounters:	6	2	2	10
Typical ambient temperature (C):	6	-1	-18	
Observed liquid density (g/m^3):	0.006	0.011	0.007	0.007
Calculated percent mass remaining when sampled:	14	15	26	15
Calculated initial liquid density (g/m^3):	0.043	0.074	0.026	0.046
Ratio to nominal density:	1.0	1.8	0.6	1.1
Mass median diameters (microns)				
- measured:	175	150	170	170
- initial:	290	250	260	270

As can be seen from Table 4, in the process of correcting for evaporation the significance of the actual instrument channel width is lost, and the question of what "bin size" to use in the integration arises. The analysis performed here was able to simply add the results for each channel of the CPS. Since the AFGL analysis was based on three overlapping spectrometers with different channel widths, it was necessary to perform the integration analytically. To accomplish this, expressions for the droplet density as a function of diameter (D) were fit to the curves. Based on discussions with the AFGL project officer, these expressions were then divided by D and integrated, yielding the total of 0.010 grams per cubic meter. The usual procedure would be to divide the density function by the bin size (if it were known) rather than by D. If the density functions from Reference 8 are integrated and divided by an "effective" bin size of 30 microns (from inspection of Table 4), the total initial liquid density becomes 0.088 grams per cubic meter. This alternative calculation is somewhat arbitrary, but the resultant density is more in line with the results in Table 5, and the proper way to arrive at an effective bin size for this case is not known. At any rate, the observed droplet mass densities, based on CPS data, appear to be within expectations.

As shown in Figure 9, the initial fuel droplet size distribution obtained for the KC-135 in this study agrees very well with the distributions reported by Cross and Picknett (Reference 6). The smaller droplet size distribution found by AEDC (Reference 5) is

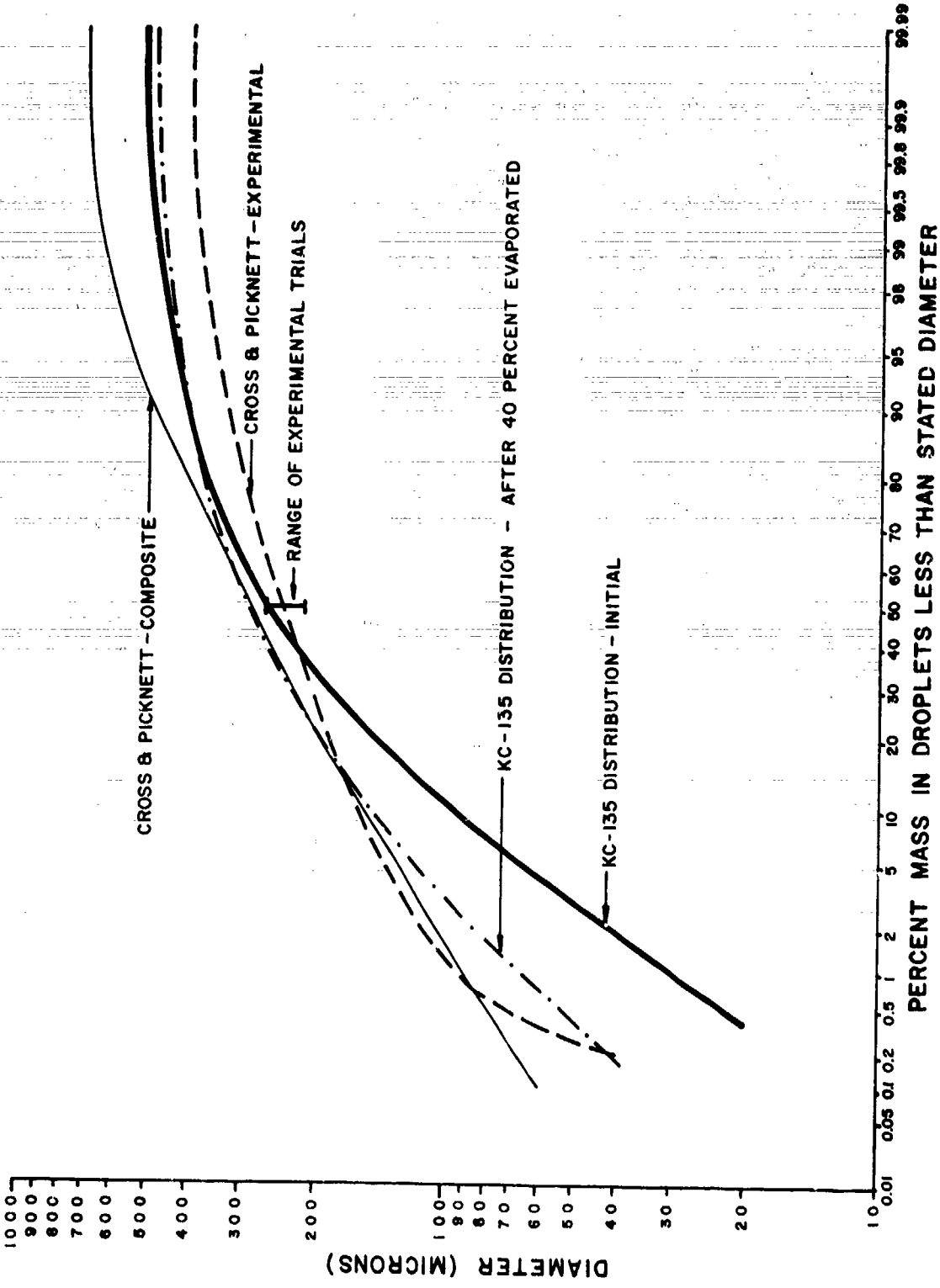

Figure 9. Comparison of Fuel Droplet Size Distributions for Different Aircraft

evidently not representative of full scale jettisoning by aircraft. The agreement with Cross and Picknett's results is even more remarkable if the possible effect of evaporation on their results is considered. As mentioned earlier, Cross and Picknett could never account for more than 55 percent of the jettisoned fuel. To investigate the extent of evaporation, they measured the concentration of dye in the spots on the filter paper and compared this with the amount of dye added to the fuel. On one trial it appeared that drops initially 117 microns in diameter had evaporated to 100 microns before being sampled, but they were unable to confirm this result in two subsequent trials. They therefore concluded that no significant evaporation took place. However, a change in size from 117 to 100 microns amounts to the loss of 40 percent of the droplet's mass. Therefore, to further examine the possibility of evaporation, the fuel droplet evaporation model was run for the conditions of their experiment.

Since Cross and Picknett's study was performed in August in England, an ambient temperature of 25°C was assumed. To simulate the relatively non-volatile Avtur fuel used in their study, a composition based on analyses of JP-8 and Jet A-1 was input to the model instead of the synthetic JP-4 composition shown in Table 1. The model was then run starting with the fuel droplet size distribution found for the KC-135. For a release height of 15 meters, the model predicts that approximately 40 percent of the fuel will have evaporated before it reaches the ground. The predicted droplet distribution at the ground is shown in Figure 9 ("KC-135

Distribution - After 40 Percent Evaporated"). Although the mass median diameter of the distribution is not significantly altered by the evaporation, the relative contribution from smaller droplets is greatly reduced. Thus allowing for the possibility of evaporation in Cross and Picknett's experiment not only accounts for their missing mass, but also reduces the difference between their distribution and the distribution observed in this study. Based on the agreement between these two studies it is postulated that the distribution obtained for the KC-135 aircraft is representative of most other aircraft as well.

3.3.2 ANALYSIS OF VAPOR MEASUREMENTS

The average hydrocarbon vapor concentrations measured during long passes through the fuel dumps were a factor of two to three below the levels calculated assuming 80 percent evaporation of the fuel and a plume diameter of 100 meters. Since the droplet measurements have been shown to be consistent with both of these assumptions, the discrepancy is probably due to some deficiency in the vapor measurements. Therefore, the adequacy of the technique used was re-examined.

The instrument used to obtain the hydrocarbon measurements was a Century Portable Organic Vapor Analyzer (OVA) Model 108. This instrument features a logarithmic scale covering the range from 1 to 10,000 parts per million and a response time under two seconds. For use in this study an in-line carbon filter was removed from the inlet hose and the inlet hose was then positioned in an

ambient air inlet on the skin of the aircraft. A reverse flow inlet was used to avoid sampling particulates larger than 60 microns. Also, to assure continuous operation of the OVA's flame ionization detector at the altitudes included in this study, it was necessary to increase the hydrogen supply pressure from 8 pounds per square inch to 15 pounds per square inch. Surprisingly, this modification resulted in about a ten-fold increase in response to methane standards.

Before the in-flight sampling program was performed, the OVA was calibrated in an altitude chamber at each of the planned altitudes. Aluminum clyinders containing three concentrations of methane in dry air were used: 10, 102.4, and 1054 parts per million. These standards were transferred to polyethlyene bags for sampling. These studies indicated a reduction in response of approximately 20 and 40 percent in going from sea-level to 3600 and 6000 meters, respectively. However, actual in-flight calibration with the same standards indicated much more severe reductions in response: 73 percent at 3600 meters and 96 percent at 6000 meters. The contractor assumed this difference was due to the low ambient temperatures encountered during the in-flight sampling. Therefore this "temperature effect" was incorporated into the OVA calibration equation.

The relative response of the OVA to JP-4 vapor was determined by injecting a known amount of JP-4 liquid into a plastic bag and allowing the J-P4 to evaporate. In calculating the concentration

thus obtained, the contractor unfortunately used an incorrect value for the density and mean molecular weight of JP-4. Instead of 0.92 grams per milliliter and 170 grams per mole, the contractor should have used 0.76 grams per milliliter and 127 grams per mole. However, the effects of these two errors partially cancel and the overall effect is to raise the concentrations reported in Reference 7 by only 9 percent. The relative response of the OVA to JP-4 vapor, as determined by the above method, is 92 percent of the response to methane.

After the sampling program, when it was found that observed hydrocarbon vapor levels had been less than expected, possible explanations for the discrepancy were studied. Although the actual instrument used in the in-flight sampling was no longer available, an identical OVA Model 108 was obtained and tested. A relatively flat response to hydrocarbons of varying molecular weight was verified, eliminating any concern about differences between the composition of the vapor sampled in flight and that produced during the calibration. The increase in response reported by the contractor when the hydrogen supply pressure was raised was also reproduced. However, the decrease in response with temperature suggested by the contractor to explain the difference between the in-flight and altitude chamber calibration results was not found. The response of this second OVA to methane and propane standards was unaffected by lowering the ambient temperature from 23°C to 2°C. Of course, this does not completely exclude the possibility that the instrument used by MRI did indeed possess a temperature dependence.

The in-flight calibrations were performed by filling plastic bags from the standards in aluminum cylinders. The OVA inlet hose was then removed from the air inlet on the skin of the aircraft and introduced into the bag. If, as suggested by the contractor, the response of their OVA was a function of temperature, then the in-flight calibration would not be completely accurate. Although the sampling aircraft's heater was not on, the warming effect of the personnel and equipment on board would tend to keep the interior of the aircraft well above ambient temperatures, particularly at the higher altitudes where outside temperatures were below 0°C. Thus the response of the instrument to the standards inside the aircraft would be greater than its response to the JP-4 vapor outside where it was colder. This effect would then explain the failure to observe the anticipated vapor levels. On the other hand, if the response of the OVA was not affected by temperature, as was the case for the second OVA studied later, then there is no explanation why the response of the OVA during in-flight calibration was so much lower than during the altitude chamber runs. In this case it could only be assumed that some unidentified instrument malfunction occurred, compromising the in-flight measurements.

3.3.3 EFFECT OF IGNORING THE WAKE IN THE MODEL

During the first few minutes after being jettisoned, fuel droplets are subject to the complex forces present in the aircraft wake. Therefore, the droplets are not in "free-fall" until the wake dissipates. The fuel droplet evaporation and free-fall model,

however, assumes that from the start gravitational settling is the only force acting on the droplets. Nevertheless, this model was used to estimate the evaporation which occurred during the first few minutes before the droplets were sampled, in order to arrive at an initial droplet size distribution. It is reasonable then to question the propriety of ignoring the effect of the wake in the model. This question will be considered from two viewpoints: first, the empirical evidence for the sufficiency of the model is given; and second, the theoretical basis for this sufficiency is suggested.

From the standpoint of using the model to predict the later history of the fuel droplets, the accuracy of the calculated initial distribution is of secondary importance. Since the model that was used to work backwards from the observed distribution at 90 seconds to an initial distribution is the same model used to obtain the later predictions, the purpose of obtaining an initial distribution is only to assure that the model passes through the observed distribution and mass remaining at the obervation time. After this point the droplets are essentially in free fall and the model assumptions are valid. The calculated fuel droplet distributions at 90 seconds (the typical observation time) for the three altitudes included in this study are compared in Figure 10 with the experimentally observed distributions. The calculated initial distribution is also shown for contrast. At all three altitudes the agreement is considered satisfactory. The percentage of mass remaining at 90 seconds calculated by the droplet evaporation

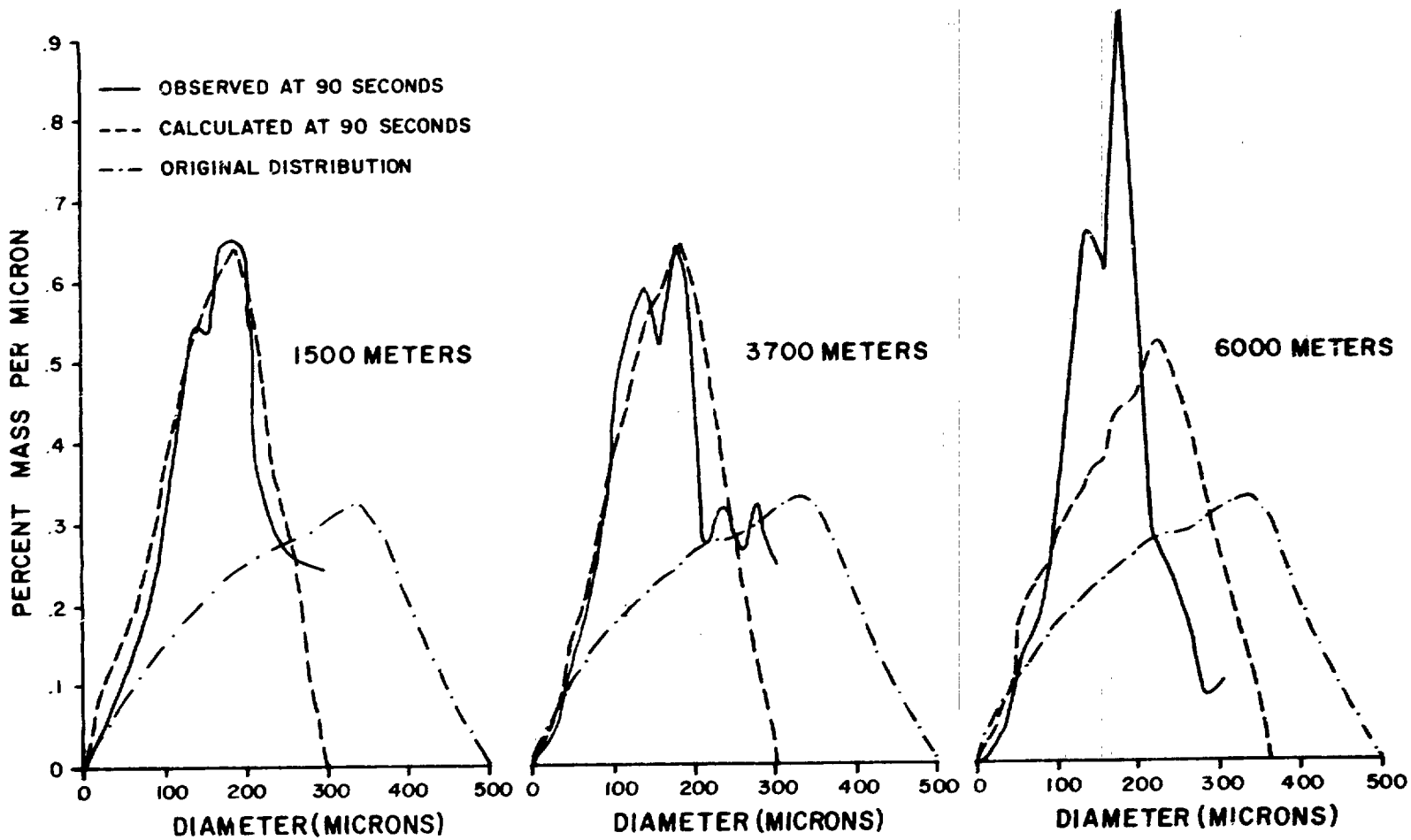

Figure 10. Comparison of Observed and Calculated Fuel Droplet Size Distributions 90 Seconds after Jettisoning

model for the 1500, 3600, and 6000 meter cases is 12, 15, and 30 percent, respectively. The corresponding observed values, based on a nominal dump rate of 330 grams per meter and a plume diameter of 100 meters at 90 seconds, were 14, 26, and 17 percent. Once again, this rough agreement is considered satisfactory, given the variability of the experimental results.

In order to explain the apparent similarity of droplet evaporation in the wake and in free-fall, it is necessary to consider the forces involved in each case. As discussed in Appendix A, the rate of evaporation of a droplet is the product of the vapor pressure of its components, the surface area available for evaporation, and the mass transfer coefficient. The mass transfer coefficient depends in part on the droplet's terminal velocity, which is determined by the external forces acting on the droplet. Whether the droplet is experiencing the wake vortex or just gravitational settling, an equilibrium is reached between the forces accelerating the droplet and the drag resisting its motion. This equilibrium determines the droplet's terminal velocity and thus, indirectly, its evaporation rate. During free-fall the acceleration is simply that due to gravity, or 9.8 meters per square second. For a stable orbit in the wake, the centripetal acceleration is V^2/r, where V is the angular velocity in the wake, and r is the orbit radius. This stable orbit is maintained by the strong influx of air being entrained into the growing vortex.

TABLE 6. ESTIMATION OF TYPICAL DROPLET ACCELERATION IN WAKES

Aircraft	Orbit Radius (meters)	Angular Velocity (m/s)	Centripetal Acceleration (m/s^2)
DC-6B	1	8	64
(wake age = 25 sec)	4	4	4
	6	3	1.5
	8	3	1.1
	12	2	0.3
C-141	1	15	225
(wake age = 10 sec)	2	11	60
	4	7	12
	6	6	6
	8	5	3
	12	3	0.8
C-141	2	5	12
(older wake)	14	3	0.6

Table 6 shows typical values of acceleration that a droplet can experience in an aircraft wake (Reference 9). The aircraft shown are roughly the same size and weight as a KC-135, and therefore the wake energies should be similar. Although the range of acceleration appears large, the net effect on the droplet evaporation rate is small. If the droplet evaporation calculations in Appendix A are carried out using the centripetal accelerations from Table 6 instead of the gravitational acceleration (g), the resulting evaporation rates range from 0.6 to 2.1 times the rate for free-fall, with typical values lying near unity. In other words, the average environment experienced by fuel droplets while in the aircraft wake does not significantly alter their evaporation rate from that which occurs during simple gravitational settling.

Ignoring the aircraft wake does substantially underestimate the initial fall rate of the droplets, however. From windshield splash encounters and radar records the initial fall rate of the fuel droplets was around 150 centimeters per second, but after approximately 100 seconds the observed fall rate had reduced to around 35-50 centimeters per second (Reference 8). The faster initial fall rate is due to the downward force of the aircraft wake. Thereafter, the droplets are in free-fall and the observed fall rate is consistent with the predictions of the model for droplets on the order of 120 to 160 microns in diameter. Thus, ignoring the wake effect only underestimates initial droplet fall-rates, and the overall error of about 100 meters is not significant for most uses of the model.

3.4 GROUND-LEVEL SAMPLING

In parallel with the in-flight sampling program, a separate program of ground-level sampling was also performed. Whereas the purpose of the in-flight sampling was to measure the initial fuel droplet size distribution, the ground-level sampling was designed to determine whether any of the jettisoned fuel reached the ground in significant concentrations, either as vapor or liquid. For this purpose 18 sampling stations were set up in a two-mile square grid, as shown in Figure 11. Several of the low-altitude fuel dumping sorties for the in-flight sampling were positioned so that the fuel would reach the ground in the area of the sampling grid. Air samples were obtained with small diaphram pumps, using

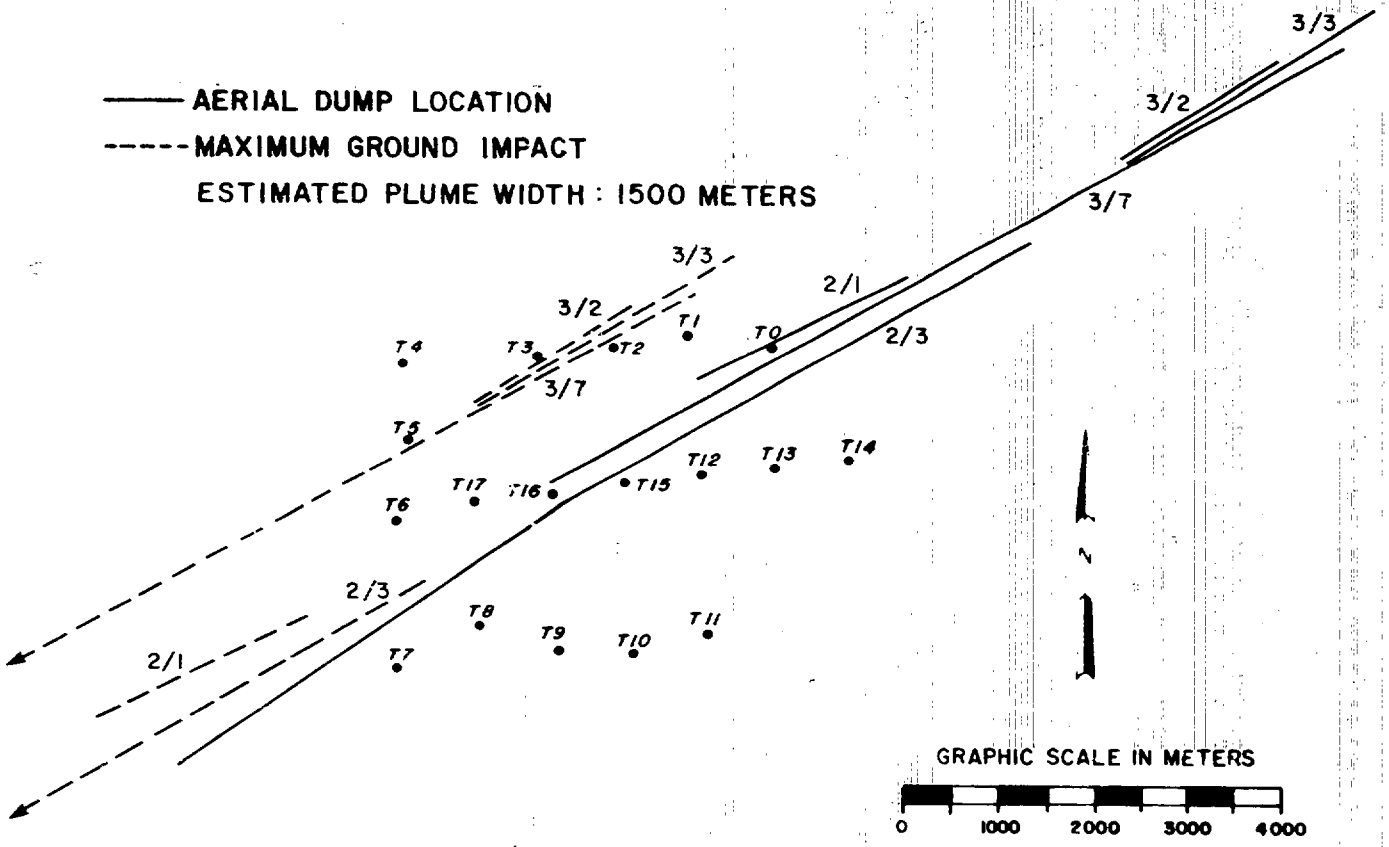

Figure 11. Calculated Ground Imprint of Fuel Dumps

charcoal adsorption tubes to collect any hydrocarbons present. The hydrocarbons were later desorbed from the charcoal in the laboratory and analyzed by gas chromatography.

The positioning of the fuel dumps was excellent, and in all cases personnel on the ground at the sampling grid were able to smell JP-4 vapor approximately 13 minutes after release. However, none of the ground observers were ever able to detect any sign of liquid fuel at ground-level. These observations, which are for fuel dumped approximately 750 meters above the ground at temperatures around 11°C, substantiate the prediction of the fuel droplet evaporation and free-fall model that under such conditions essentially all of the fuel will evaporate before it reaches the ground.

3.4.1 PREDICTED CONCENTRATION AND LOCATION OF THE FUEL AT THE GROUND

Four ground-sampling runs were performed in all. During the second in-flight sampling sortie on 6 December, ground samples were obtained for fuel dumps 2/1 and 2/3 (using the notation from Reference 8). On 10 December, fuel dumps 3/2 and 3/3 were sampled together and a final dump, which will be referred to as 3/7, was performed (with the boom down) for the ground-level sampling alone. The winds and temperatures at the time of the sampling are shown in Table 7.

TABLE 7. ATMOSPHERIC CONDITIONS DURING GROUND-SAMPLING STUDIES

Date and Local Time	Altitude (meters, MSL)	Temperature (C)	Wind Direction (degrees)	Wind Speed (m/s)
6 Dec, 1430	1500	7.5	62	7.3
	1200	8.4	65	5.0
	900	12.7	53	4.0
	725*	15.4	45	3.5
10 Dec, 1300	1500	4.5	61	8.5
	1200	7.1	72	7.0
	900	11.1	72	4.5
	725*	14.3	70	3.0

*local ground-level

Based on a Gaussian dispersion model, the maximum concentration of fuel at ground-level can be expected to occur when the vertical standard deviation (σ_z) of the fuel cloud is equal to 0.707 H, where H is the height of the release above the ground (Reference 10). In this case H is 775 meters, making the desired σ_z 548 meters. For a sunny winter day in Southern California with surface winds around 3 meters per second, the atmospheric stability category is probably B or C. From Reference 10, for stability B-C, σ_z will equal 548 meters when the plume has been blown approximately 7 kilometers downwind, and at this point the width of the central plume at the ground will be at least 1500 meters. That is, the maximum concentration of fuel at ground level will occur 7 kilometers downwind of the aerial dump location.

Figure 11 shows the aerial location of each of the fuel dumps and the predicted location of the maximum ground-level concentrations for each. The locations of the ground imprints were determined

by integrating the effects of the wind direction and speed from the release height to the ground. The maximum ground imprints for the fuel dumps performed on 10 December cross the northwest corner of the sampling grid. The maximum ground concentrations for the fuel dumps performed on 6 December fall beyond the grid. However, initial contact of the fuel cloud with the ground would occur well before the point where the maximum concentration was reached. Therefore, some of the fuel could be expected to reach the sampling grid, as is supported by the ability of personnel in the sampling area to smell JP-4 after each dump.

Based on the fuel droplet evaporation and free-fall model, the fuel will have been more than 99 percent evaporated before it reaches the ground. Nevertheless, the droplets that still remain are predicted to reach the ground after about 20 minutes. For the wind profiles shown in Table 7, in 20 minutes the droplets will be blown roughly 7 kilometers downwind. Thus the maximum ground imprints shown in Figure 11 are indicative of droplet impact as well. While the fuel dumps on 10 December are better positioned to look for the predicted maximum ground impact, those on 6 December serve as a check for anomalously high ground contamination. If the fuel were to reach the ground sooner than expected, either from slower evaporation leading to faster fall rates or from an unexpected mechanism mixing the fuel to the ground prematurely, much greater ground impact would result. However, in this event, the early ground-fall could be detected in dumps 2/1 and 2/3.

The highest ground concentrations which can be anticipated for these fuel dumps can be calculated following the procedure from Reference 10:

$$Xmax = Q/\pi \sigma_y \sigma_z Ue$$

Where Q = the emission rate
= 56 kilograms per second
σ_y = the horizontal standard deviation
= 730 meters at 7 kilometers
σ_z = the vertical standard deviation
= 548 meters at 7 kilometers
U = the windspeed (here the aircraft speed)
= 175 meters per second

The maximum concentration calculated in this way is 0.11 milligrams per cubic meter, which is equivalent to 0.021 parts per million of JP-4, or 0.19 parts-per-million-carbon (ppmC). The duration of this concentration at a sampling point depends on the length of the fuel plume and the rate at which the wind sweeps the plume past the sampling point. The longest imprint of a fuel plume on the sampling grid is about 3 kilometers. For a surface wind of 3 meters per second, the duration would be roughly 17 minutes. The shortest sampling times used in this study were around 30 minutes. Therefore, the highest time-weighted average concentration that could be obtained with the charcoal tubes is predicted to be on the order of 0.1 ppmC.

3.4.2 DESCRIPTION OF THE ANALYTICAL TECHNIQUE

Small diaphragm pumps of the type used for personnel monitoring were used to draw air samples through standard charcoal sampling tubes. The sampling rate of each pump was calibrated to 1.0 liters per minute using a soap-bubble burette. The pumps were started before, or within ten minutes after, the fuel was jettisoned, and were allowed to run until approximately 30 minutes after the jettisoning. On 10 December, background samples were also obtained before any fuel had been jettisoned.

The hydrocarbons adsorbed on the charcoal were analyzed by gas chromatography. The technique used to transfer the hydrocarbons from the charcoal to the gas chromatograph is shown in Figure 12. The charcoal tube was flushed with inert gas and was heated to approximately 200°C in a heater block to desorb any hydrocarbons present. The desorbed hydrocarbons were trapped in a sample loop cooled to liquid nitrogen temperatures before the inert gas stream was vented to the atmosphere. To analyze the sample, the gas flow through the sample loop was diverted into the chromatograph, while the sample loop itself was heated with a hot air gun to revolatilize the trapped hydrocarbons. The hydrocarbons were then separated on a Porapak-Q micro-column programmed from 50° to 240°C at 5°C per minute. The flame ionization detector response was output to an electronic integrator to provide quantification.

Standards containing 13 ppmC of JP-4 vapor were prepared by injecting 0.5 microliters of liquid JP-4 into a 50 liter bag and allowing the fuel to vaporize. A typical gas chromatogram is

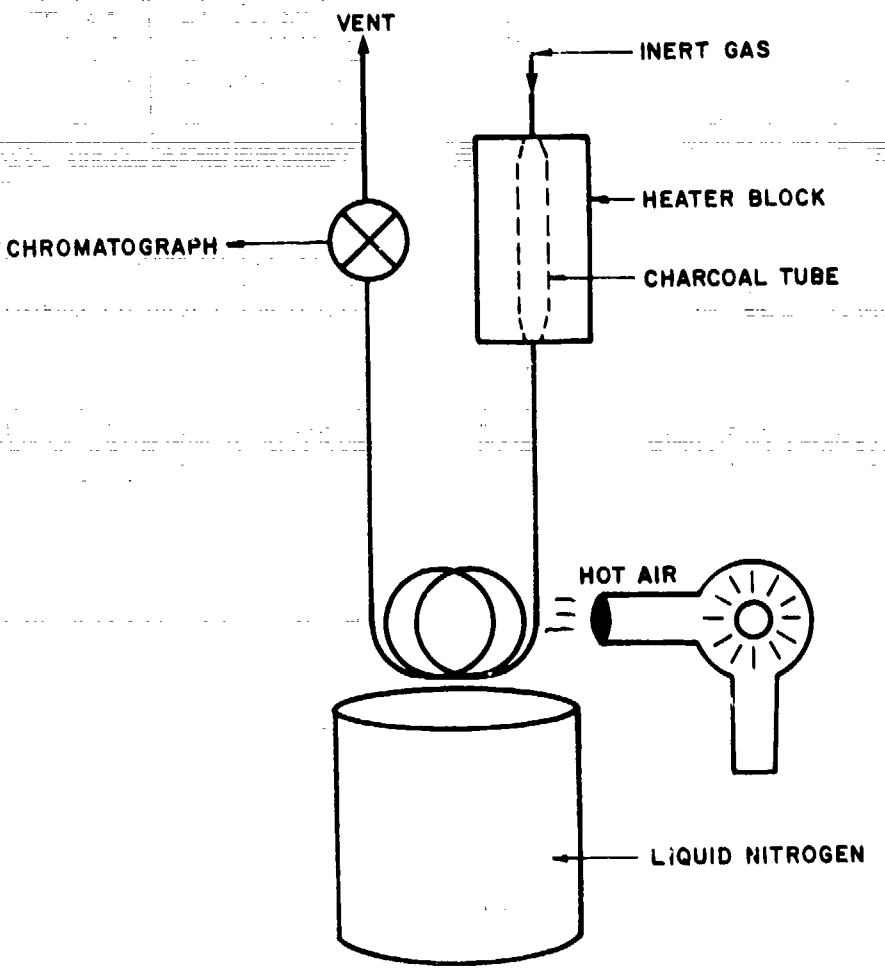

Figure 12. Diagram of Charcoal Tube Desorption Technique

shown in Figure 13a. The three major peaks have retention times of approximately 60, 240, and 860 seconds. The response and standard deviation for the calibration runs are shown in Table 8. Due to the excessive variability of the peak at 860 seconds, this peak was not used to quantify the experimental results.

TABLE 8. CALIBRATION OF HYDROCARBON ANALYSIS

	Response (area/ppmC/liter)
Total Area:	110 ± 12
Major Peaks	
60 seconds:	24 ± 4
240 seconds:	31 ± 9
860 seconds:	11 ± 8

The results for the four ambient backgrounds collected on 10 December appear in Table 9. Three of these samples resembled Figure 13b. Note that all of the major peaks for JP-4 are also present in ambient air. The background taken at T4 had several additional peaks, notably ones at 180, 210, 430, and 730 seconds. Many of the samples collected during the ground-sampling on both 6 and 10 December contained these additional peaks, and they were also present in ambient air samples collected in the Los Angeles basin as well as near the flightline at Tyndall Air Force Base. A typical chromatogram is shown in Figure 13c. It appears that these additional peaks may be indicative of hydrocarbon pollutants from automobile and aircraft exhaust. Their appearance in some of the ground samples on 6 and 10 December could be due to the

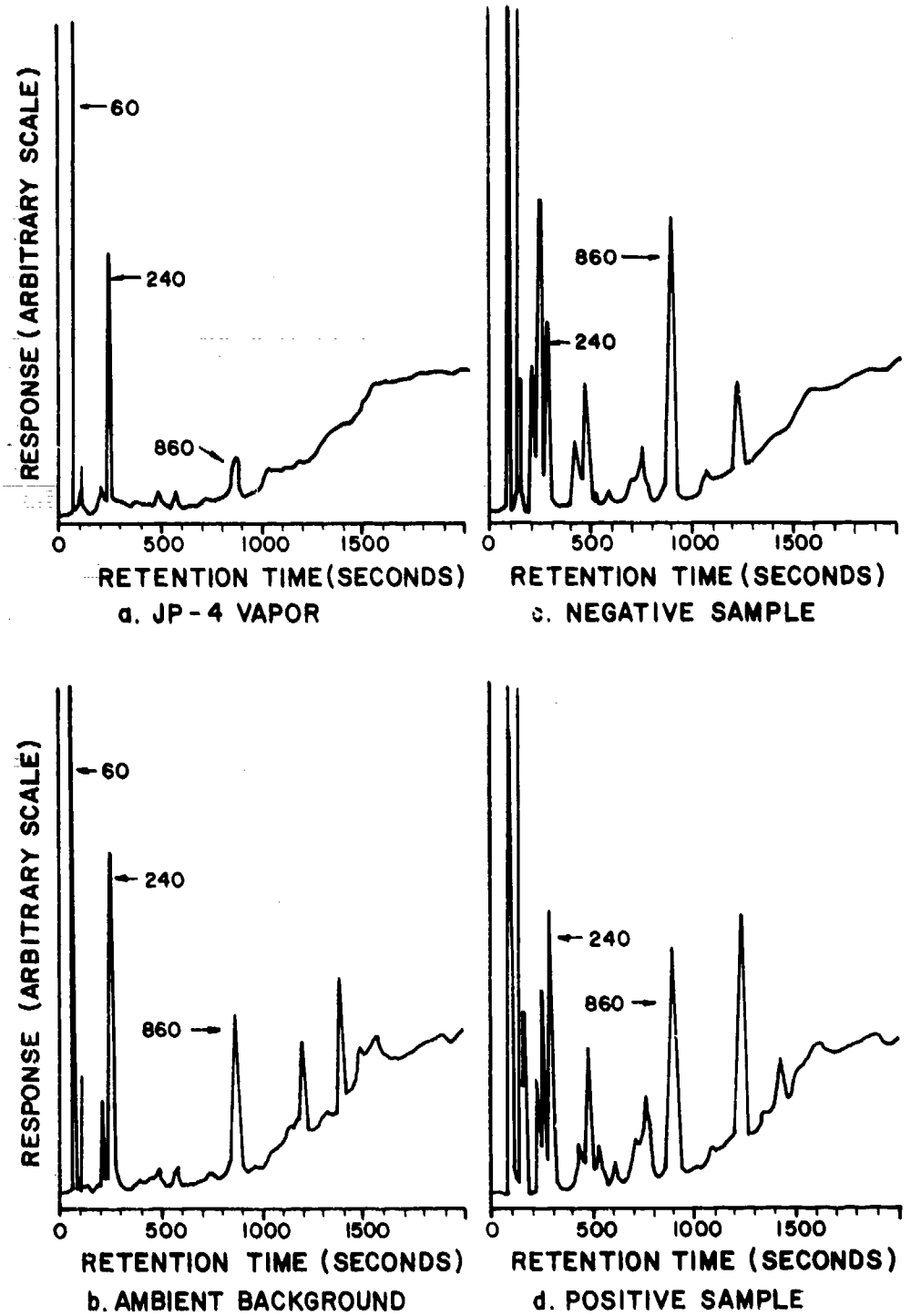

Figure 13. Typical Gas-Chromatograms of Hydrocarbon Samples

exhaust from the trucks used to get between sampling stations. The background in the Los Angeles basin calculated for the peaks of interest is also shown in Table 9. Fortunately, although the presence of these additional hydrocarbons does of course increase the total hydrocarbon concentration, it does not appear to affect the peaks at 60 and 240 seconds. These two peaks were therefore used to analyze the ground-sampling results.

TABLE 9. AMBIENT BACKGROUND SAMPLES

Sampling Location	Background Concentration (ppmC) Based On: Total Area	Peak 60	Peak 240	Peak 860
T1	0.70	0.70	0.43	1.07
T2	0.63	0.42	0.29	2.15
T4*	3.46	1.06	0.37	4.62
T7	1.19	1.15	0.50	3.86
Average	1.50	0.83	0.40	2.93
Pasadena*	†	0.29	0.53	13.35

*includes additional peaks associated with automobile exhaust.
†integrator overflow

3.4.3 ANALYSIS OF SAMPLING RESULTS

The results of the four sampling runs are summarized in Table 10. Only on the last run were concentrations greater than the background obtained. From the negative results on 6 December we can conclude that there is no evidence for the premature arrival of the fuel at the ground and the increased ground concentrations which would result. The fact that higher concentrations were observed on the second 10 December run but not the first may be due to the difference in sampling times. While all the other samples and backgrounds were obtained over 30-50 minutes, the

samples for the first run on 10 December were collected for 90 minutes in order to encompass two fuel dumps. However, later studies indicated that increasing sampling time from 50 to 90 minutes decreased the apparent concentrations by roughly a factor of three. This decrease is probably due to saturation of the charcoal or displacement of the hydrocarbons by other compounds in ambient air.

TABLE 10. SUMMARY OF GROUND-SAMPLING RESULTS

	Background Concentration (ppmC) Based On:		
	Total Area	Peak 60	Peak 240
6 December - fuel dump 2/1			
average:	0.57	0.18	0.14
maximum:	1.02	0.25	0.24
6 December - fuel dump 2/3			
average:	0.35	0.26	0.37
maximum:	0.75	0.26	0.37
10 December - fuel dump 3/1 and 3/2			
average:	0.62	0.45	0.19
maximum:	0.98	0.77	0.37
10 December - fuel dump 3/7			
average:	2.04	1.77	0.53
maximum:	4.79	3.15	1.09

The chromatogram for station T4 obtained in the final run is shown in Figure 13d. The quantitative results from this run for all of the stations are listed in Table 11. Here the average background levels from Table 9 have been subtracted out. Concentrations greater than the variation of the background have been underlined for emphasis. Depending on the peak used, concentrations on the order of several tenths of a ppmC or even as high as 2 ppmC were seen at several sampling stations. The highest

Table 11. ESTIMATED JP-4 CONCENTRATIONS AT THE GROUND FROM FUEL DUMP 3/7

Station	Total Hydrocarbon Concentration (ppmC)	JP-4 Concentration (ppmC) Based on: Peak 60	Peak 240
Background:	1.5 ± 2.0†	0.8 ± 0.4†	0.4 ± 0.1†
Sample minus background:			
T0	-	0.4	-
T2	-	0.8	-
T3*	1.0	1.6	0.1
T4*	1.8	2.0	0.4
T6*	1.3	1.8	0.3
T7*	3.3	2.4	0.7
T8*	1.3	1.2	0.2
T9*	1.0	0.4	-
T12	-	-	-
T13	0.2	1.2	0.15
T14	-	0.6	-
T15*	-	-	0.1
T16	-	1.4	0.2
T17	-	0.2	-

†Total range of background samples.

*Sample includes additional species associated with polluted air.

NOTE: Underlined concentrations are greater than variation in background samples.

results were obtained along the western edge of the sampling grid (T4-T8), but positive results were also seen along the centerline (T16 and T13). These observations indicate that the wind direction probably shifted slightly from the time it was measured (13:00) to the time of the last fuel dump (15:15). It is interesting that some stations saw concentrations well above the expected levels while adjacent stations saw nothing. This variation is probably due in part to the non-uniformity of the fuel dump plume after the vortex structure begins to break-up and fold on itself under the influence of large scale atmospheric eddies. The overall results are felt to be in general agreement with expectations, demonstrating that only minimal concentrations of fuel vapor are reached at the ground, even for very low altitude releases.

SECTION IV

PREDICTED GROUNDFALL OF JETTISONED JP-4

Coupling the fuel droplet evaporation and free-fall model with the experimentally determined initial size distribution, it is now possible to predict the fate of fuel jettisoned under differing circumstances. In all cases these predictions apply only for jettisoning of JP-4 fuel, although estimates for other fuels will be provided where possible. Atmospheric dispersion, which is not considered in the droplet model, will also be treated in order to fully describe the physical fate of the fuel.

4.1 FRACTION OF THE FUEL REACHING THE GROUND

Figures 14 and 15 show the percentage of JP-4 fuel which can be expected to reach the ground before evaporating, based on the release altitude and the temperature at ground-level. These curves indicate that except for very low altitude releases, the fraction of fuel reaching the ground as liquid droplets is primarily determined by the temperature. For JP-4 fuel jettisoned higher than 1500 meters and at temperatures above freezing (0°C), more than 98 percent of the fuel should evaporate before reaching the ground. For less volatile fuels, such as the Air Force's JP-8, commercial Jet-A, or the Navy's JP-5, much more of the fuel will reach the ground as liquid droplets than would be the case for JP-4 under the same conditions. Preliminary calculations suggest that the percentage of JP-8, Jet-A, or JP-5 reaching the ground at, for

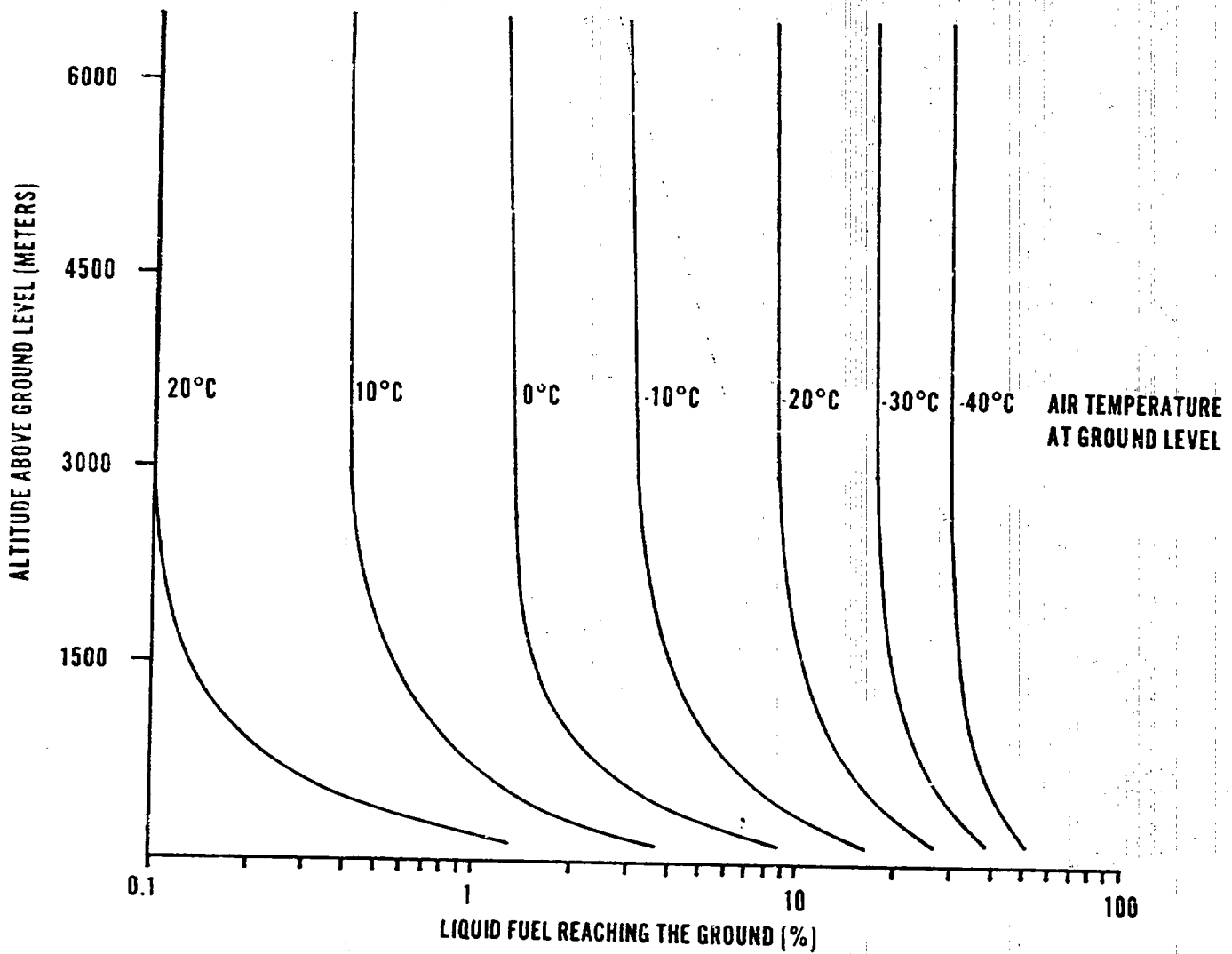

Figure 14. Percent of Jettisoned Fuel Reaching the Ground

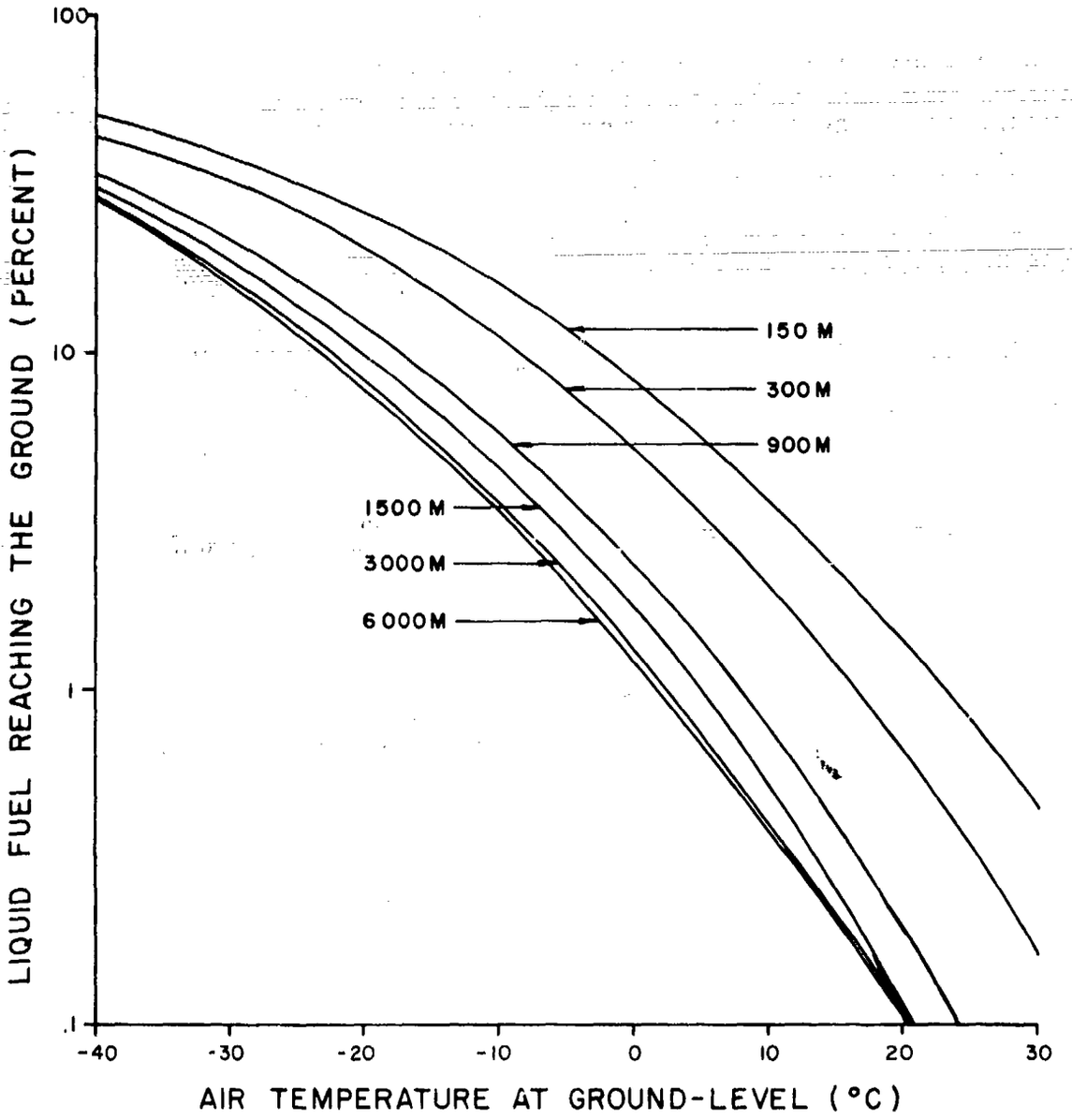

Figure 15. Effect of Temperature on the Percent of Fuel Reaching the Ground

example, 0°C would be somewhat between the curves for JP-4 at -20°C and -40°C in Figure 14.

Figure 16 compares the fuel droplet size distribution for the KC-135 ("Good - Corrected") which was used in these calculations, with the smallest experiment distribution obtained for the Buccaneer ("Cross and Picknett - Experimental") and the suggested larger distribution for other aircraft ("Cross and Picknett - Composite") from Reference 6. These distributions probably represent the range of droplet sizes that can be expected for most aircraft. The effect of these different distributions on the predicted amount of liquid fuel reaching the ground is shown in Figure 17. Also shown are the predictions for a single droplet whose diameter is equal to the mass median diameter of the KC-135 distribution (270 microns). The difference between the predictions based on the KC-135 distribution and those obtained with the other aircraft distributions is generally less than 40 percent. That is, the ground-fall of fuel from different aircraft should not vary more than 0.6 to 1.4 times the estimates shown in Figures 14 and 15. The surprising agreement of the predictions for a single droplet at the mass median diameter with those for the whole distribution indicates that the central tendency or spread of the droplet sizes is relatively unimportant for determing the composite evaporation and free-fall of the distribution.

In addition to experimentally determining an initial droplet size distribution for fuel jettisoning, Cross and Picknett also estimated the fraction of fuel reaching the ground as a function of

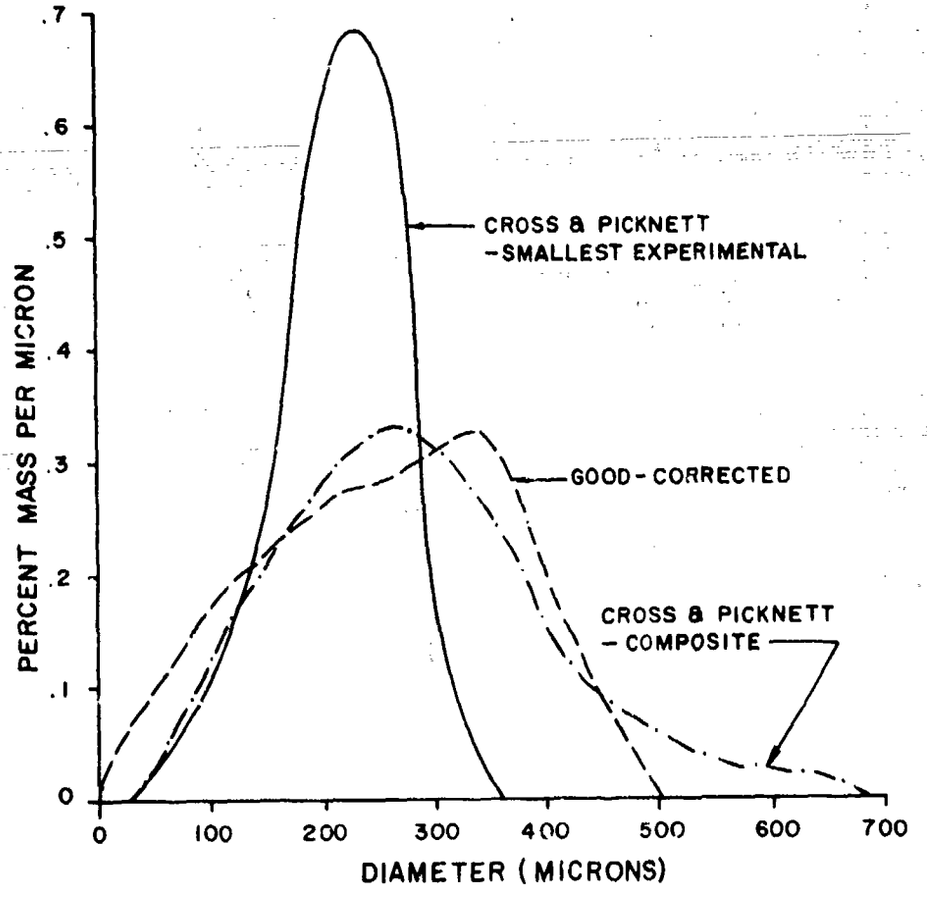

Figure 16. Experimental Fuel Droplet Size Distribution for Aircraft Fuel Jettisoning

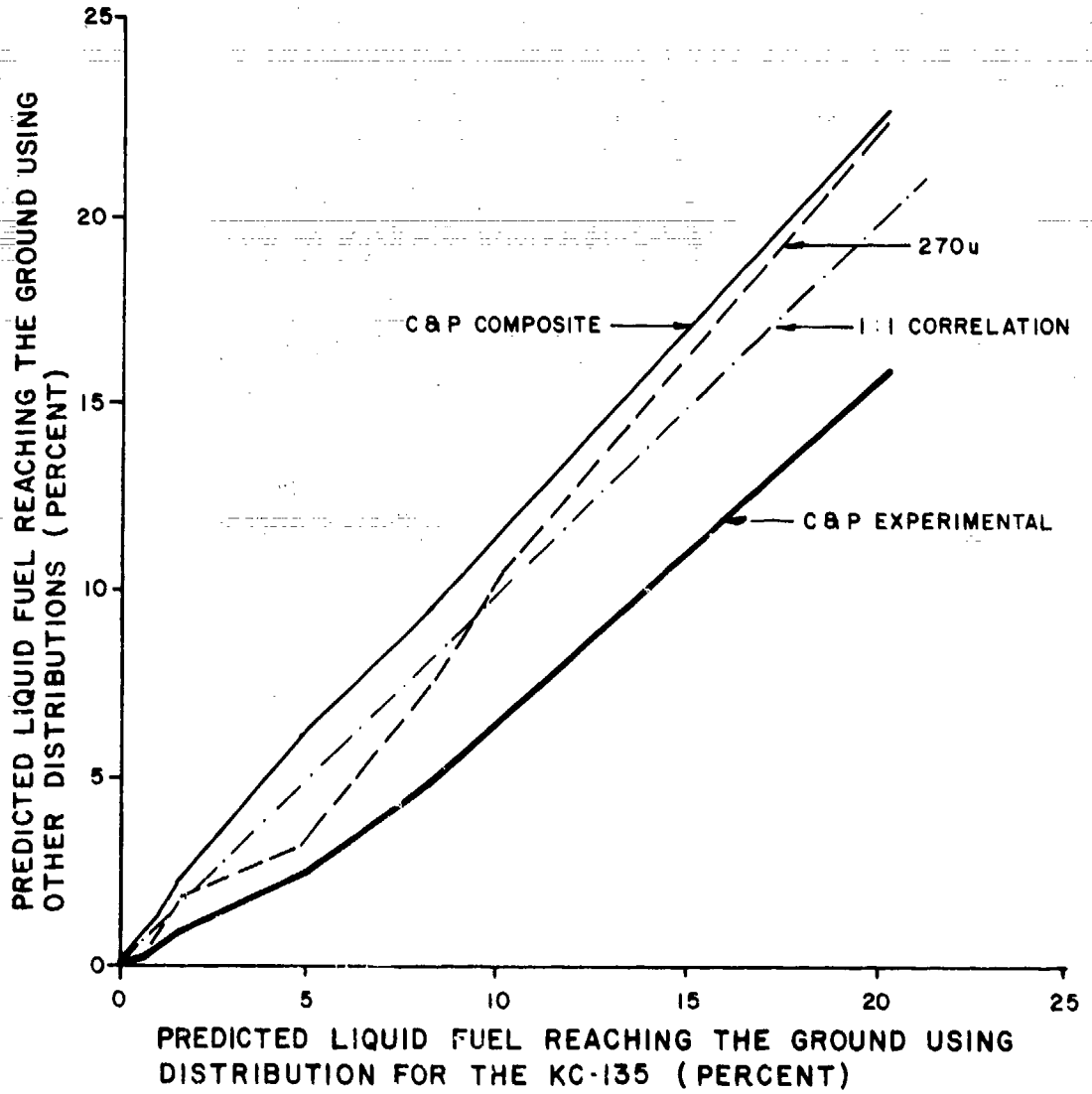

Figure 17. Effect of Initial Droplet Size Distribution on the Percent of Fuel Reaching the Ground

release height and temperature (Reference 6). Their estimates were based on the droplet modelling results of Lowell (Reference 2) for a fall of 300 meters. Unfortunately, to model release heights greater than 300 meters they calculated the evaporation during successive 300 meter intervals by assuming that the droplets would follow the same curve of percent evaporation versus diameter used for the first 300 meters. However, as discussed in Section 2.2 of this report the evaporation of a fuel droplet changes not only due to its decreasing diameter, but also due to its changing composition. The more volatile components are stripped away in the early evaporation, leaving only the slower evaporating components in the droplet. By ignoring composition changes Cross and Picknett grossly underestimated the fraction of fuel reaching the ground for release heights of greater than 300 meters; therefore, their predictions cannot be used.

4.2 OTHER MODEL PREDICTIONS

As can be seen in Figure 18, the vast majority of the fuel evaporates in the first few minutes after release. For fuel released at 1500 meters when the ground-level temperature is above freezing, less than 10 percent of the fuel remains after 10 minutes. During this short time interval even the largest droplets only fall 700-900 meters, and most of the vapor is generated within a few hundred meters of the release height. The implication of these calculations for dispersion modeling is that the fuel dump can be

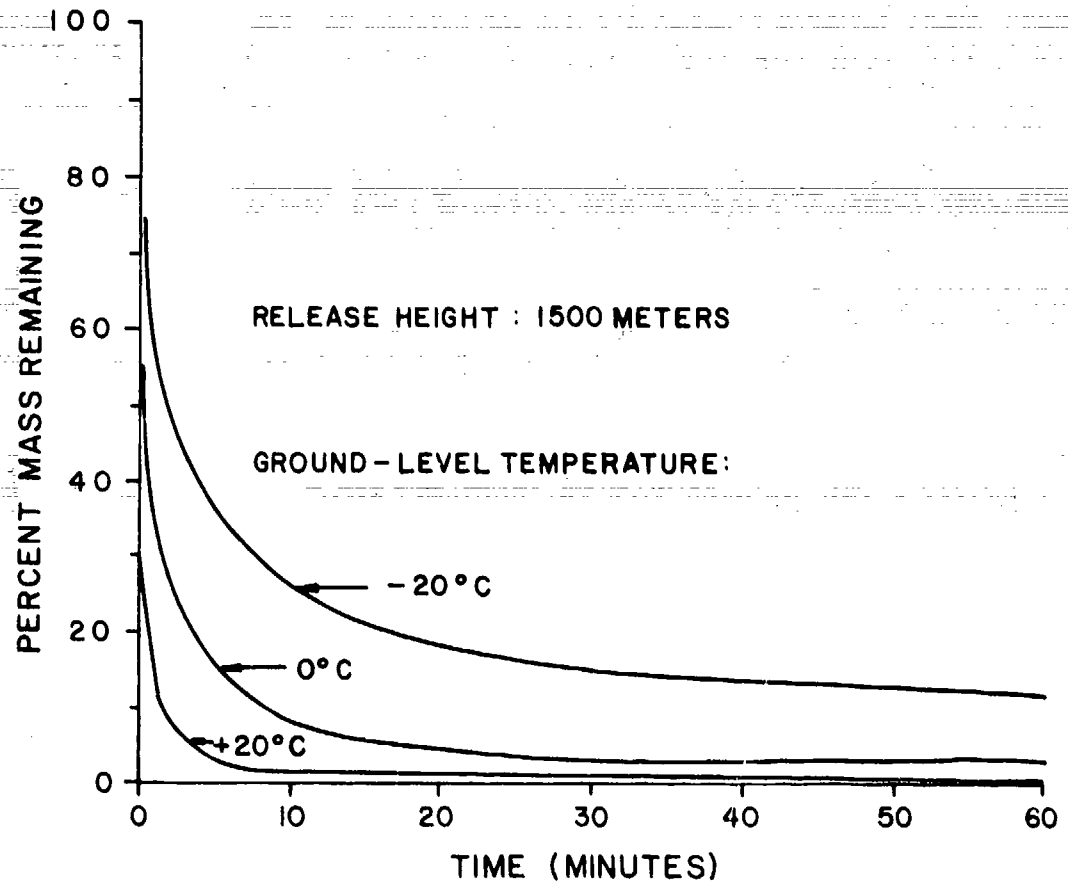

Figure 18. Evaporation of a Distribution of Droplets

approximated as an elevated vapor source at the release height without seriously degrading the accuracy of the estimated ground-level concentrations. This approximation was used for the dispersion calculations in this report.

Due to the different settling velocities of droplets with varying diameters, not all of the liquid fuel reaches the ground at the same time. Two examples of the time spread over which liquid fuel reaches the ground from 1500 meters are shown in Figure 19. At a ground-level temperature of -20°C, 10 percent of the fuel reaches the ground in liquid form. The largest droplets, on the order of 300 microns, reach the ground in less than 20 minutes. Most of the unvaporized fuel reaches the ground during the first hour after release, but a significant fraction takes much longer.

Raising the ground-level temperature reduces the fraction of fuel reaching the ground in liquid form, and also delays the onset of ground-fall. Although increasing the release altitude above 1500 meters does not substantially lower the fraction of liquid fuel reaching the ground, it greatly increases the time required for the droplets to reach the ground. The time of fall for the first droplets to reach the ground at several altitudes and temperatures is shown in Table 12. These predictions of the fuel droplet model can be approximated by the formula $T = NH$, where T is the time of fall in minutes, H is the release height in kilometers, and N is 18, 12, and 10 minutes per kilometer for ground-level temperatures of 0°C, -20°C, and -40°C, respectively. These results can be used

TABLE 12. TIME OF FALL FOR THE FIRST DROPLETS TO REACH THE GROUND

Ground-Level Temperature (C)	Release Altitude (Kilometers)	Maximum Droplet Diameter (Microns)	Time of Fall (Minutes)	Average Fall Rate (Minutes/ Kilometer)
0	6	151	103	17
	3	154	60	20
	1.5	173	29	20
	.9	202	16	18
	.3	267	4.4	15
-20	6	286	65	11
	3	288	37	12
	1.5	301	19	13
	.9	317	11	12
	.3	359	3.5	12
-40	6	381	54	9
	3	381	30	10
	1.5	389	16	10
	.9	398	9.3	10
	.3	424	3.0	10

to estimate the effect of winnowing by the wind on the dispersion of the fuel.

For a ground-level temperature of -20°C, slightly over 10 percent of the fuel released at 1500 meters will reach the ground as droplets. The different size droplets will be distributed in time, as indicated by the upper scale in Figure 19. This same distribution is shown on a linear scale in Figure 20. The modal diameter at -20°C is 190 microns. For a ground-level temperature of 0°C evaporation is more complete, and the modal diameter at the ground is less than 100 microns.

The composition of the fuel droplets which reach the ground is no longer the same as that of the JP-4 fuel which was jettisoned. The more volatile, lower molecular weight components will have evaporated off, leaving a residual mixture of the higher molecular weight components. A typical composition for a distribution of droplets which has evaporated to 10 percent of the original mass is shown in Table 13. As can be seen in this table, the final droplet composition resembles kerosene rather than JP-4, in that it is composed chiefly of hydrocarbons having a molecular weight greater than 150 grams per mole.

4.3 DISPERSION OF THE FUEL

Once the fraction of fuel reaching the ground in liquid form has been determined, the fate of the liquid and vapor fractions can be investigated separately. The next step in assessing the environmental consequences of a jettisoning incident is to estimate the

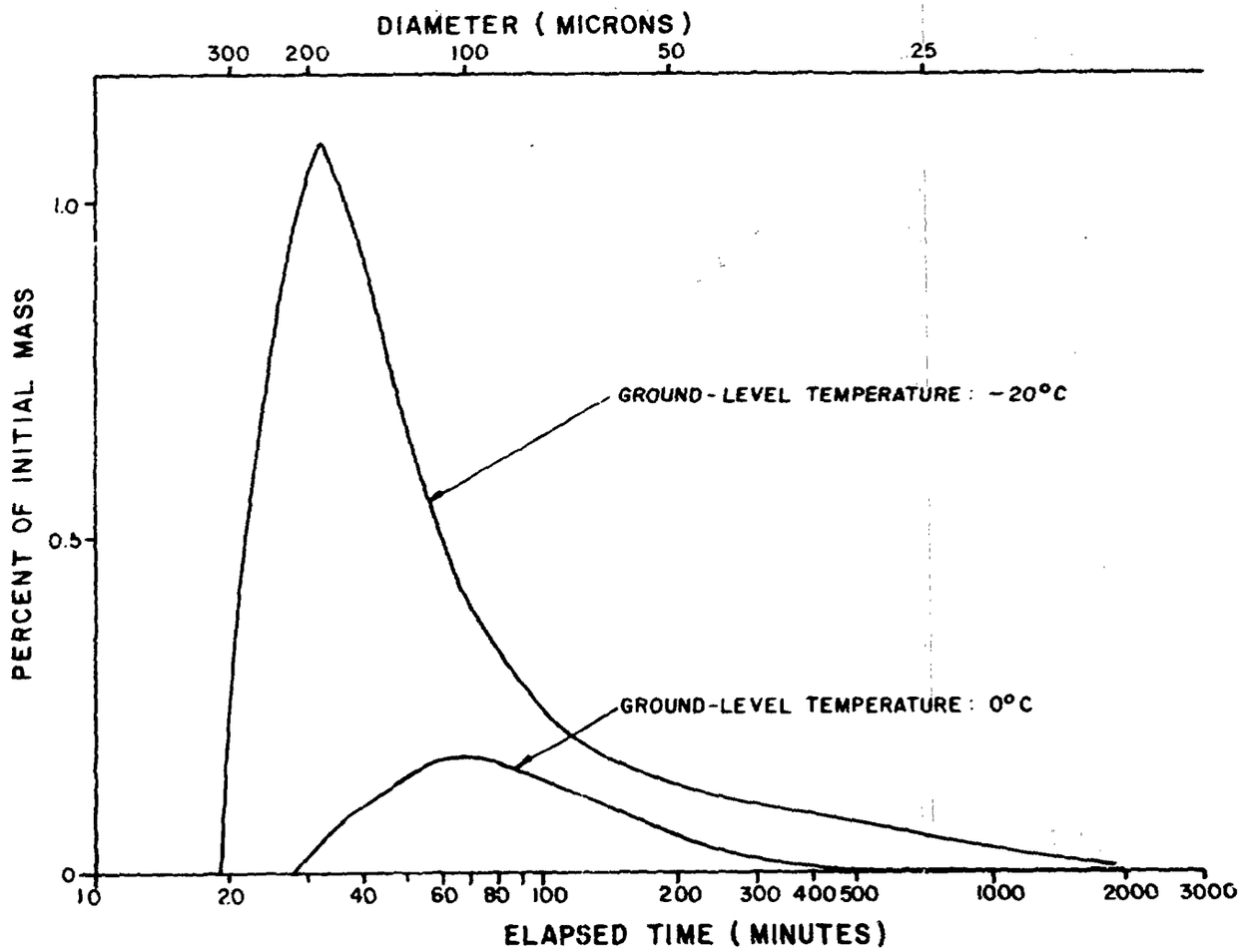

Figure 19. Time-Spread of Liquid Fuel Reaching the Ground from 1500 Meters

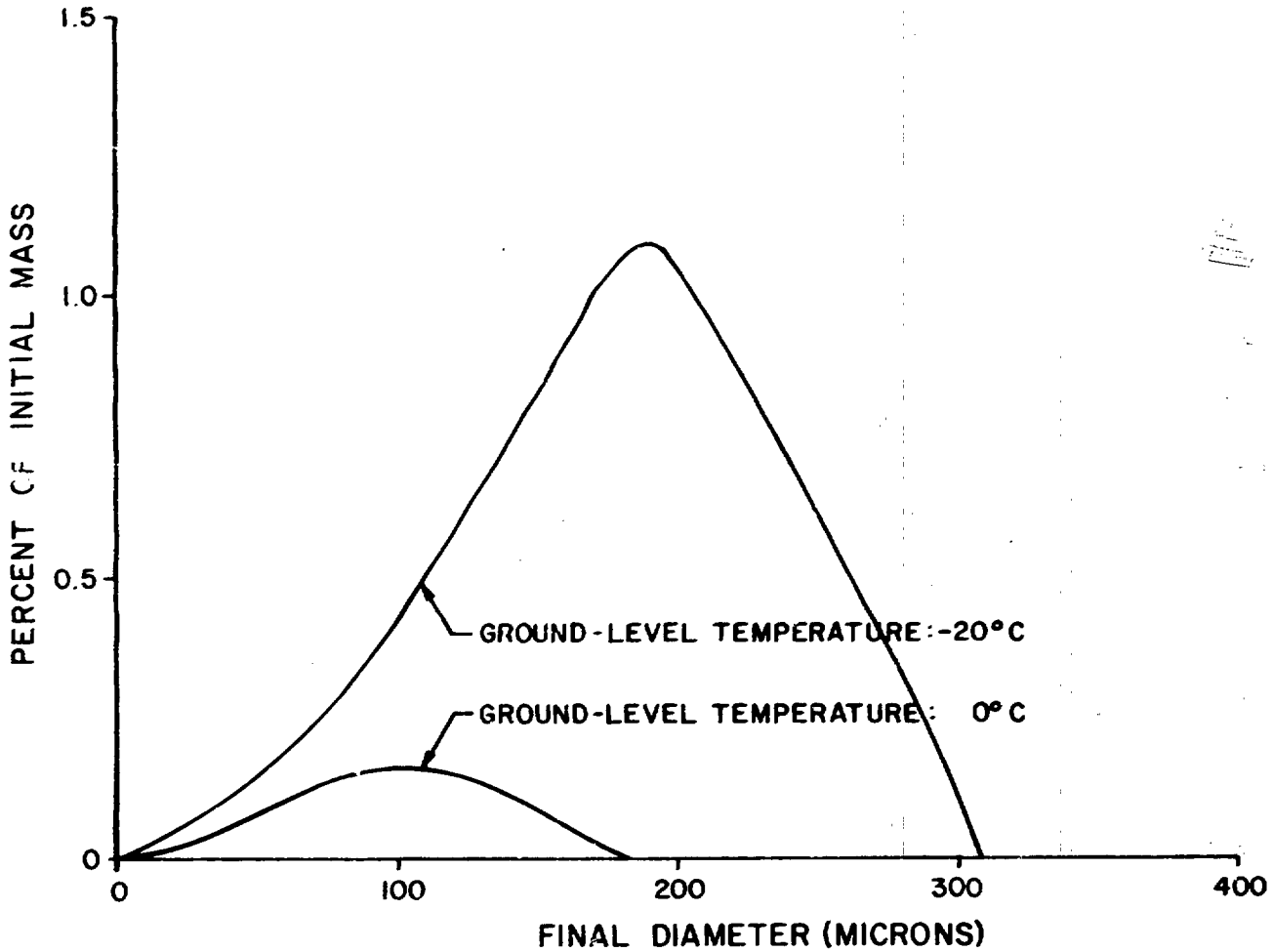

Figure 20. Droplet Size Distribution at the Ground for Fuel Released at 1500 Meters

TABLE 13. RESIDUAL COMPOSITION OF FUEL DROPLETS AFTER 90 PERCENT OF THE ORIGINAL MASS HAS EVAPORATED

Component	Original Percent of Droplet Mass	Percent Remaining of Component	Percent of Initial Droplet Mass	Percent of Final Droplet Mass
iso-pentane	3.2	0	-	-
iso-hexane	7.1	0	-	-
cyclohexane	2.2	0	-	-
benzene	0.3	0	-	-
3-methylhexane	8.6	0	-	-
methylcyclohexane	7.3	0	-	-
toluene	0.8	0	-	-
4-methylheptane	9.4	0	-	-
cis-1, 4-dimethyl-cyclohexane	7.7	0	-	-
m-xylene	1.8	0	-	-
4-methyloctane	8.7	0	-	-
isopropyl-cyclohexane	4.6	0.3	0.01	0.1
1-ethyl-2 methyl-benzene	2.8	1.6	0.05	0.5
2,7-dimethyloctane	7.0	1.0	0.07	0.7
p-methane (cis)	3.9	4.2	0.17	1.6
p-cymene	2.1	7.4	0.15	1.5
napthalene	0.3	46.4	0.13	1.3
undecane	4.7	26.9	1.29	12.6
3-methylbutyl-cyclohexane	2.7	27.0	0.73	7.1
3-methylenedecalin (trans)	4.0	31.0	1.26	12.3
1-butyl-3-methyl-benzene	1.2	35.4	0.45	4.4
1-methylnapthalene	0.3	66.8	0.18	1.7
dodecane	2.8	48.3	1.36	13.3
3-ethylbutyl-cyclohexane	1.3	42.9	0.55	5.4
1,3,5-triethyl-benzene	0.6	47.0	0.27	2.6
2,3-dimethyl-napthalene	0.3	78.9	0.21	2.0
tridecane	1.1	63.2	0.71	6.9
3-isopropylbutyl-cyclohexane	0.4	55.7	0.24	2.3
3,5-diethyl-1-propylbenzene	0.1	61.6	0.07	0.7
tetradecane	0.2	73.8	0.15	1.5
pentadecane	0.1	81.4	0.08	0.8
perhydro-phenanthrene	2.2	86.7	1.96	19.1
residual	0.2	99.8	0.16	1.6

extent to which the fuel vapor and droplets are dispersed prior to reaching ground-level.

4.3.1 VAPOR DISPERSION

Since most of the fuel jettisoned from an aircraft will evaporate within a few hundred meters of the release height, the concentration of hydrocarbons at ground-level is primarily determined by the ability of atmospheric diffusion processes to transport the vapors downward. The highest ground-level concentrations will be obtained under unstable atmospheric conditions, since the vertical transport is then a maximum. The longest exposures will occur when the fuel is jettisoned parallel to the wind.

The gradient-transfer (K) theory of atmospheric diffusion can be used to estimate the "worst-case" vapor concentrations at the ground. According to K theory, the vertical spread of a plume (as measured by its standard deviation, σ_z) can be related to the vertical component of the atmospheric eddy diffusivity, K_z, by the formula $K_z = \sigma_z^2/2T$, where T is the time since release (Reference 11). A profile of eddy diffusivity in the mixing layer (Reference 12) shows that K_z is generally less than 100 square meters per second, even under relatively unstable conditions. For a Gaussian plume profile, the maximum ground concentration is reached when $\sigma_z = 0.707H$, where H is the release height. Using a value for K_z of 100 square meters per second to represent strong vertical mixing, the time at which the maximum ground concentration is reached

is given by $T_{max} = \sigma_z^2/2K_z = H^2/400$. Expressing T in minutes and H in kilometers, this formula becomes $T = 40H^2$.

The horizontal spread (σ_y) of the plume during this period can be estimated by $\sigma_y = 0.5t$ (Reference 13). This value provides a good fit to experimental data on σ_y for plume travel periods from 1-100 hours (Reference 11). Assuming that the highest concentrations in the plume occur over a width $W = 2\sigma_y$, the width of the plume at the time the maximum ground-level concentrations are reached is $W = H^2/400$. For W and H in kilometers, $W = 2.4H^2$. Using a simple box model and ignoring upward diffusion of the plume, we can then conservatively estimate the ground concentration with the formula $X = 1000Q/VWH$, where X is the concentration in micrograms per cubic meter, Q is the jettison rate in kilograms per second, and V is the aircraft velocity in meters per second. Substituting for W from the formula derived above yields $X = 400Q/VH^3$. The predications of this box-model for several fuel jettisoning scenarios are shown in Table 14.

TABLE 14. WORST-CASE GROUND-LEVEL VAPOR CONCENTRATIONS

Release Height (kilometers)	Aircraft Velocity (m/s)	Jettison Rate (kg/s)	Maximum Ground-Level Concentration (ug/m^3) K-Theory/Box	Gaussian
.3	175	17	1439	298
.775	175	56	275	147
1.5	175	5	3.4	3.5
6	175	56	0.6	0.4

An alternative technique for estimating the worst-case concentrations of vapor at ground-level is to rely solely on a

Gaussian diffusion analysis (Reference 10). In this case the maximum ground-level concentration is given (as in Section 3.4.1) by $X = Q/\pi\sigma_y\sigma_z Ue$, where normally U is the windspeed, but here U = V. Then assuming $\sigma_y = \sigma_z$ (true within a factor of two for moderately unstable atmospheric conditions), $X = 2Q/\pi eVH^2$. For X in micrograms per cubic meter, Q in kilograms per second, and H in kilometers, this formula bedcomes $X = 276Q/VH^2$. The predictions of this Gaussian model are also shown in Table 14. The two models agree for a release height of 1.5 kilometers and diverge elsewhere. The theoretical basis for the two models is quite different: the Gaussian model is most valid for low altitudes, whereas the K-theory box-model applies best to high altitudes near the top of the mixing layer. Thus the two analyses are complimentary. As a means of comparison with a more exacting model, the Environmental Protection Agency's "Point-Area-Line" (PAL) computer dispersion model (Reference 14) was run for the case in Table 14 for 1.5 kilometers. Under moderately unstable conditions (stability category B) with a windspeed of 2 meters per second, the highest ground-level concentration predicted by the PAL model was 8.5 micrograms per cubic meter, in reasonable agreement with the two simplified approximation techniques.

4.3.2 DROPLET DISPERSION

At temperatures below freezing the fraction of fuel reaching the ground as liquid droplets can become significant. As in the case of fuel vapor, however, natural atmospheric dispersion would

reduce the droplet density at the ground. For jettisoning parallel to the wind, the droplets would be spread over nearly as wide a path as the vapor: $W = 2.4H^2$, where W and H are in kilometers. Therefore, the maximum liquid fuel contamination of the ground, C, (in milligrams per square meter) would be given approximately by the formula $C = 10PQ/(VW)$, where P is the percentage of fuel reaching the ground in liquid form from Figure 14 or 15.

For jettisoning in any direction other than parallel to the wind, the droplets would be further separated by the process of winnowing: as the droplets are carried along by the wind the larger droplets fall faster and are deposited sooner (closer to the jettisoning location) than the smaller droplets, which tend to be transported more like the vapor. The distance in kilometers that the fuel will be carried downwind before reaching the ground is given by $L = 0.06UT$, where U is the average windspeed (in meters per second) between the jettisoning altitude and the surface, and T is the time of fall in minutes. As stated earlier, $T = 40H^2$ for the vapor, while for the largest droplets $T = NH$, where N is 18, 12 and 10 minutes per kilometer at 0°C, -20°C, and -40°C, respectively. Therefore, for fuel jettisoned crosswind, the droplets will be spread by winnowing over a distance $W = 0.06U(40H^2 - NH)$. Several cases comparing jettisoning parallel and perpendicular to the wind are shown in Table 15. Generally, the average liquid-fuel ground contamination is reduced by a factor of three to four when jettisoning crosswind.

TABLE 15. EXAMPLES OF LIQUID FUEL CONTAMINATION OF THE GROUND

Aircraft:	F-4	F-111	FB-111	KC-135	F-111
Airspeed (m/s):	175	175	175	175	175
Jettison Rate (kg/s):	5	17	17	50	17
Release Height (km):	1.5	1.5	6	6	.3
Ground-Level Temperature (C):	0	0	-20	-20	20
Windspeed (m/s):	5	5	3	4	4
Parallel to Wind:					
Width at Ground (km):	5	5	90	90	.2
Concentration (mg/m^2):	.08	.28	.09	.27	3.1
Perpendicular to Wind:					
Width at Ground (km):	19	19	250	330	.2
Concentration (mg/m^2):	.02	.08	.03	.07	3.1

SECTION V

SUMMARY AND CONCLUSIONS

A computer model has been developed which simulates the evaporation and free-fall of fuel droplets in the atmosphere. This model gives good agreement with evaporation rates of fuel droplets measured experimentally. A study of fuel jettisoning by a KC-135 tanker aircraft was performed to obtain a fuel droplet size distribution for input to the model. The droplet size distribution was measured directly in flight, but only after significant evaporation was known to have occurred. The observed droplet sizes were therefore corrected for evaporation using the fuel droplet evaporation model. Correcting the observed droplet mass densities for evaporation, all of the jettisoned fuel was accounted for. The original distribution thus obtained has a mass median diameter of 265 microns with a maximum droplet size of around 500 microns. During this study, sampling was also performed at ground level to determine whether the jettisoned fuel reached the ground in significant concentrations. For fuel jettisoned as low as 750 meters above the ground at temperatures around 11°C, no liquid fuel could be detected by ground observers and no significant hydrocarbon concentrations (greater than a few ppmC) were measured by the sampling.

Based on the fuel droplet evaporation and free-fall model, more than 98 percent of JP-4 fuel will evaporate before reaching the ground if jettisoned higher than 1500 meters when the ground-level

temperature is above freezing. The droplets and vapor will be widely dispersed by atmospheric turbulence, quickly resulting in a fuel density too low to create any perceptible environmental changes. The formulas and graphs in Section IV can be used to estimate the likelihood of significant ground-level concentrations of fuel vapor or liquid following a specific fuel jettisoning incident.

This report has dealt only with the short-term physical fate of the jettisoned fuel. The possible longer-term fates of the fuel vapor in the atmosphere are discussed in Reference 1. Since the vapor is quickly dispersed and diluted below the levels at which it could be harmful in itself (around 500 ppm), its environmental impact derives principally from its role in the production of photochemical oxidant pollution (ozone and smog). Studies of this role are currently in progress. The possible long-term fate of any liquid fuel which reaches the ground is also under study, with particular emphasis on the chemical and biological fate of the hydrocarbons in an aqueous environment. When these studies are completed the overall environmental consequences of fuel jettisoning can be determined.

REFERENCES

1. Clewell, H. J., "Fuel Jettisoning by US Air Force Aircraft. Volume I: Summary and Analysis," ESL-TR-80-17, March 1980. (Unclassified)

2. Lowell, H., "Free Fall and Evaporation of JP-4 Jet Fuel Droplets in a Quiet Atmosphere," NASA-TN-D-33, 1959. (Unclassified)

3. Lowell, H., "Free Fall and Evaporation of JP-1 Jet Fuel Droplets in a Quiet Atmosphere," NASA-TN-D-199, 1960. (Unclassified)

4. Dawbarn, F., Nutt, K. W., and Pender, C. W., "A Study of the Jettisoning of JP-4 Fuel in the Atmosphere," AEDC-TR-75-49, November 1975. (Unclassified)

5. Wasson, R. A., Darlington, C. R., and Billingsly, J. C., "Droplet Diameter and Size Distribution of JP-4 Fuel Injected into a Subsonic Airstream," AEDC-TR-74-117, April 1975. (Unclassified)

6. Cross, N. L., and Picknett, R. G., "Ground Contamination by Fuel Jettisoned from Aircraft," AGARD CP-125, 1972. (Unclassified)

7. Merritt, M. J., "Fuel Dump Plume Characterization," (Volume I and II), AFGL-TR-77-085, March 1977. (Unclassified)

8. Good, R. E., Forsberg, C. A., and Bench, P. M., "Breakup Characteristics of JP-4 Vented from KC-135 Aircraft," AFGL-TR-78-0190, August 1978. (Unclassified)

9. Donaldson, C. duP, Snedeker, R. S., and Sullivan, R. D., "Calculation of the Wakes of Three Transport Aircraft in Holding, Takeoff, and Landing Configurations and Comparison with Experimental Measurements," AFOSR-TR-73-1594, March 1973. (Unclassified)

10. Turner, D. B., "Workbook of Atmospheric Dispersion Estimates," Environmental Protection Agency Publication #AP-26, 1970. (Unclassified)

11. Slade, D. H., editor, Meteorology and Atomic Energy -- 1968, US Atomic Energy Commission/Division of Technical Information, Oak Ridge, Tennessee, July 1968. (Unclassified)

12. Pasquill, F., "The Dispersion of Material in the Atmospheric Boundary Layer -- The Basis for Generalization," Lectures on Air Pollution and Environmental Impact Analysis, Boston, Massachusetts, American Meteorological Society, 1975. (Unclassified)

13. Telegadas, K., "Estimation of Maximum Credible Atmospheric Radio - Activity Concentrations and Dose Rates from Nuclear Tests," Atmospheric Environment, Volume 13, Number 2, 1979. (Unclassified)

14. Petersen, W. B., "User's Guide for PAL -- a Gaussian-Plume Alogrithm for Point, Area, and Line Sources, " EPA-600/4-78-013, February 1978. (Unclassified)

B-1. US Standard Atmosphere, 1976, NOAA-S/T76-1562, 1976. (Unclassified)

B-2. Pasion, A., and Thomas, J., "Preliminary Analysis of Aircraft Fuel Systems for Use with Broadened Specification Fuels," NASA-CR-135198, 1977. (Unclassified)

B-3. Lowell, H., "Free Fall and Evaporation of JP-4 Jet Fuel Droplets in a Quiet Atmosphere", NASA-TN-D-33, 1959. (Unclassified)

B-4. Lowell, H., "Free Fall and Evaporation of JP-1 Jet Fuel Droplets in a Quiet Atmosphere," NASA-TN-D-199, 1960. (Unclassified)

B-5. Dawbarn, F., Nutt, K. W., and Pender, C. W., "A Study of the Jettisoning of JP-4 Fuel in the Atmosphere," AEDC-TR-75-49, November 1975. (Unclassified)

B-6. Bird, R. B., Stewart, W. E., and Lightfoot, E. N., Transport Phenomena, John Wiley and Sons Inc., New York, 1966. (Unclassified)

B-7. Perry, R. H., and Chilton, D. H., Chemical Engineers' Handbook, 5th Edition, McGraw-Hill, New York, 1973. (Unclassified)

B-8. Mackay, D., and Matzugo, R. S., "Evaporation Rates of Liquid Hydrocarbon Spills on Land and Water," Can J Ch Eng, pp. 434-439, 1973. (Unclassified)

APPENDIX A

EFFECT OF DROPLET TEMPERATURE CALCULATIONS IN THE FUEL DROPLET EVAPORATION MODEL

The evaporation rate of a fuel droplet depends in part on the vapor pressure of its components at the droplet temperature. As described in Appendix B, the fuel droplet model performs an energy balance to derive the steady state droplet temperature. This energy balance considers heat transfer by conduction with the air, absorbtion and emission of radiation, solar insolation, and evaporative cooling. In addition the model calculates an initial droplet temperature higher than that of the ambient air, assuming equilibration of the fuel in the tank with the skin of the aircraft before release. The model could be greatly simplified by eliminating these calculations and assuming instead that the droplet temperature is always equal to to the temperature of the ambient air. Therefore, it is worthwhile to investigate the importance of the energy balance and initial droplet temperature routines.

The effect of these two calculations on the droplet temperature is shown in Figure A-1. Due to the dominant effect of evaporative cooling in the energy balance, the droplet cools appreciably below the ambient air temperature during the initial moments when the highly volatile components are being stripped away. However, the combined effects of solar insolation and heat conduction from the air rapidly restore the droplet to the ambient temperature when

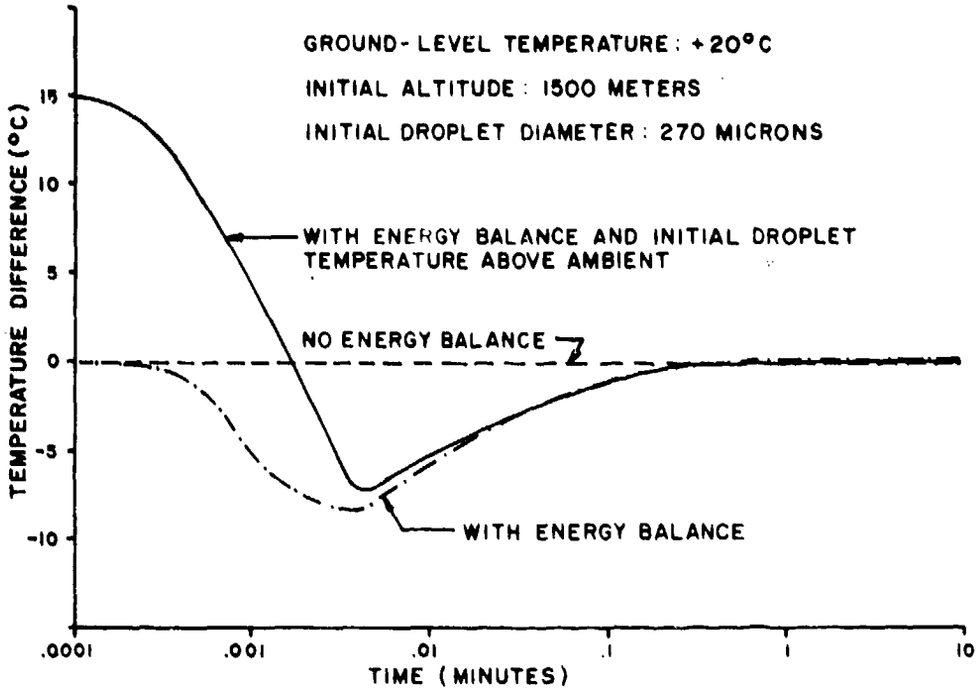

Figure A-1. Difference Between Droplet and Ambient Temperatures for Different Calculations

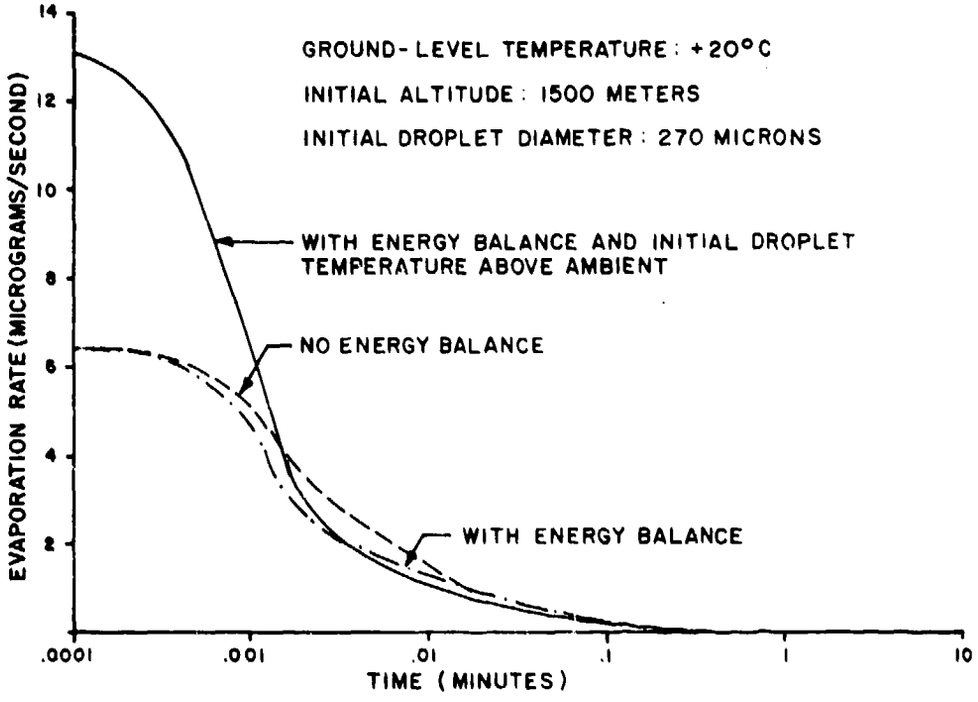

Figure A-2. Predicted Evaporation Rates for Different Droplet Temperature Calculations

evaporation slows. The entire droplet cooling and warming cycle lasts less than a minute in most cases. The assumption of an initial droplet temperature above ambient tends to delay and partially offset the maximum cooling effect, but does not eliminate it.

Figure A-2 shows the resulting variation in the droplet evaporation rates. Although assuming an initial droplet temperature above ambient produces a larger change in instantaneous evaporation rate, the opposing effect of the energy balance is of longer duration. The net effect on the predicted mass remaining in the droplet as a function of time is shown in Figure A-3. The raised initial temperature causes the droplet mass to fall off much more rapidly at first, but evaporative cooling quickly counters this effect, and after the first few seconds the droplet mass is greater than it would be if both effects were ignored. Regardless of the calculations used, the droplet mass remaining is essentially the same after the first minute. The reason the three different calculations come back together after initially diverging is that the changing composition of the droplet is a factor in the evaporation rate. For example if the droplet is made to evaporate more slowly, its composition will include more of the volatile components. Then when the restraint on evaporation is removed the more volatile composition of the droplet will accelerate its evaporation, counteracting the effect of the earlier restraint.

The primary conclusion which can be drawn from these results is that for predictions of droplet evaporation over periods greater

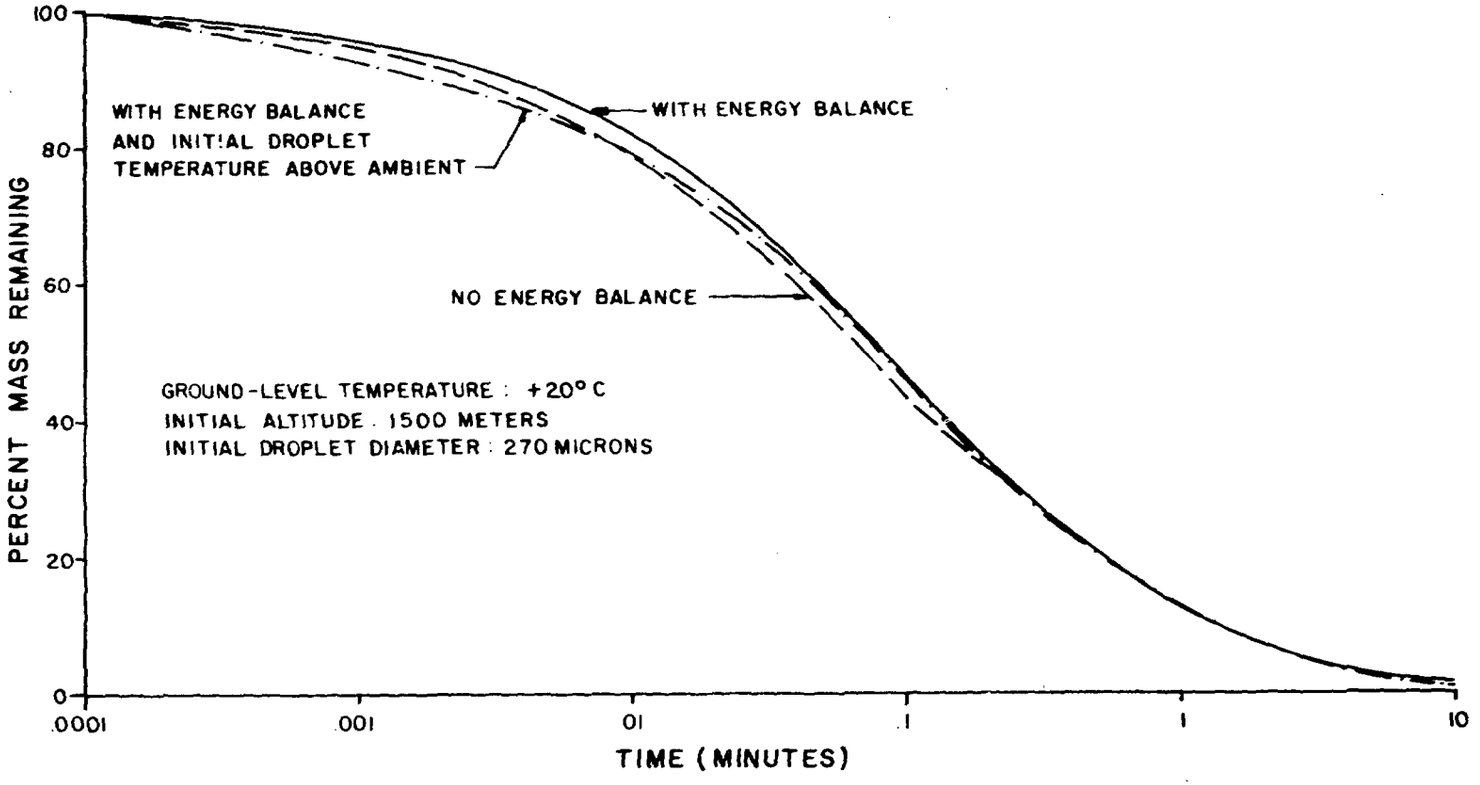

Figure A-3. Predicted Mass Remaining for Different Droplet Temperatures Calculations

than one minute, the droplet temperature can be assumed to be identical to the ambient air temperature. Only for predictions of the droplet evaporation rate and history during the first minute are the energy balance and initial droplet temperature calculation important.

APPENDIX B

DETAILED DESCRIPTION OF THE FUEL DROPLET MODEL

The fuel droplet evaporation and free-fall model breaks a given droplet's fall into a series of small time intervals. The distance of fall during each interval is calculated assuming the droplet is falling at the terminal velocity for its current diameter, density and altitude. Loss of mass through evaporation is calculated assuming Raoult's law; that is, each component evaporates independently. An energy balance routine adjusts the droplet temperature to allow for evaporative cooling, radiation, conduction and insolation effects. The new droplet composition, mass, and altitude are used as initial conditions for the next interval. This stepwise approximation continues until the droplet impacts on the ground or loses 99.9 percent of its initial mass.

The initial conditions which must be known are the droplet's original composition, altitude and diameter; the temperature and altitude at local ground level; and the aircraft's air speed. The initial droplet temperature is then taken as the corresponding stagnation temperature, assuming equilibration of the fuel tanks with the skin of the aircraft. In the early intervals the droplet is allowed to cool through evaporation until an energy balance is achieved.

At the beginning of each interval, the droplet's current mass composition and altitude are known. (For the first interval, the mass

is determined from the droplet's diameter and density; calculation of the latter is discussed below). The local air temperature is derived from the droplet altitude and the temperature at the ground using the standard lapse rate of 6.5 K/km. Atmospheric pressure, density, and viscosity are then calculated as recommended in the US Standard Atmosphere, 1976 (Reference B-1):

$$P_a = P_o \, (T_o/T_a)^{(gM_a/R_oL)}$$

where P_a = the local atmospheric pressure (N/m^2)

P_o = atmospheric pressure at sea level = 101325 N/m^2

T_o = sea level temperature (K)

T_a = local air temperature (K)

g = acceleration of gravity = 9.81 m/s^2

M_a = molecular weight of air = 28.96 kg/kmol

R_o = universal gas constant = 8314 N·m/K·kmol

L = standard lapse rate = 0.0065 K/m

$$\rho_a = P_a M_a / R_o T_a$$

where ρ_a = the local air density (kg/m^3)

$$\mu_a = \frac{1.458 \times 10^{-6} \, T_a^{1.5}}{110.4 + T_a}$$

where μ_a = the local air viscosity ($N.s/m^2$)

For the first interval the droplet temperature is assumed to be at the equilibrium temperature of the aircraft fuel tanks, which is approximately the stagnation temperature corresponding to the

aircraft velocity and local air temperature (Reference B-2). The stagnation temperature, T_s (K), can be calculated from the true air speed, V (m/s), and the local air temperature:

$$T_s = T_a (1 + V^2/5C_s^2)$$

where C_s is the local speed of sound (m/s) calculated as in Reference B-1:

$$C_s = (1.4 R_o T_a/M_a)^{1/2}$$

The density, ρ_i (kg/m^3) is calculated for each component in the mixture using a linear expansion coefficient:

$$\rho_i = {}^{20}\rho_i/(1 + 0.001 (T_d - 293.15))$$

where ${}^{20}\rho_i$ = the component's density at 20C (kg/m^3)

T_d = the droplet temperature (K)

An expansion coefficient of 0.001 was chosen to give the best fit for a variety of hydrocarbons. Assuming an ideal solution, the droplet's volume is then a sum of its components.

The droplet terminal velocity, U_t(m/s) is determined following the method of Lowell (References B-3 and B-4): A parameter "q" (equivalent to Lowell's $\phi^{1/2}$) is defined:

$$q = ReC_D^{1/2} = (4\rho_a\rho_d g d^3/3\mu_a^2)^{1/2}$$

where Re = the Reynolds number of the system

C_D = the drag coefficient

ρ_d = the droplet density (kg/m^3)

d = the droplet diameter (m)

An empirical relation between q and Re is then used to find Re:

$$\ln Re = -3.13 + 2.06 \ln q - 0.083(\ln q)^2$$

This relation was chosen to fit the AEDC data (Reference B-5) for Reynolds numbers over 100, while agreeing with Stoke's law ($Re = q^2/24$) for $Re < 1$. A plot showing the success of this fit is presented in Figure B-1. The droplet terminal velocity is then:

$$U_t = \mu_a Re/d\rho_a$$

and the distance the droplet falls during the interval is approximated by the product of U_t with the duration of the interval, $\Delta t(s)$.

The evaporation of a falling single-component drop is treated in Bird, Stewart, and Lightfoot (Reference B-6). To treat the multicomponent fuel droplet the contribution from each component is calculated separately assuming independent transport and ignoring any internal resistance:

$$\Delta m_i = \pi d^2 h_i p_i \varepsilon_i \Delta t$$

where Δm_i = the mass of component "i" evaporated during the time Δt (kg)

h_i = the mass transfer coefficient for the component (s/m)

p_i = the true vapor pressure of the component (N/m^2)

ε_i = the mole fraction of the component in the droplet

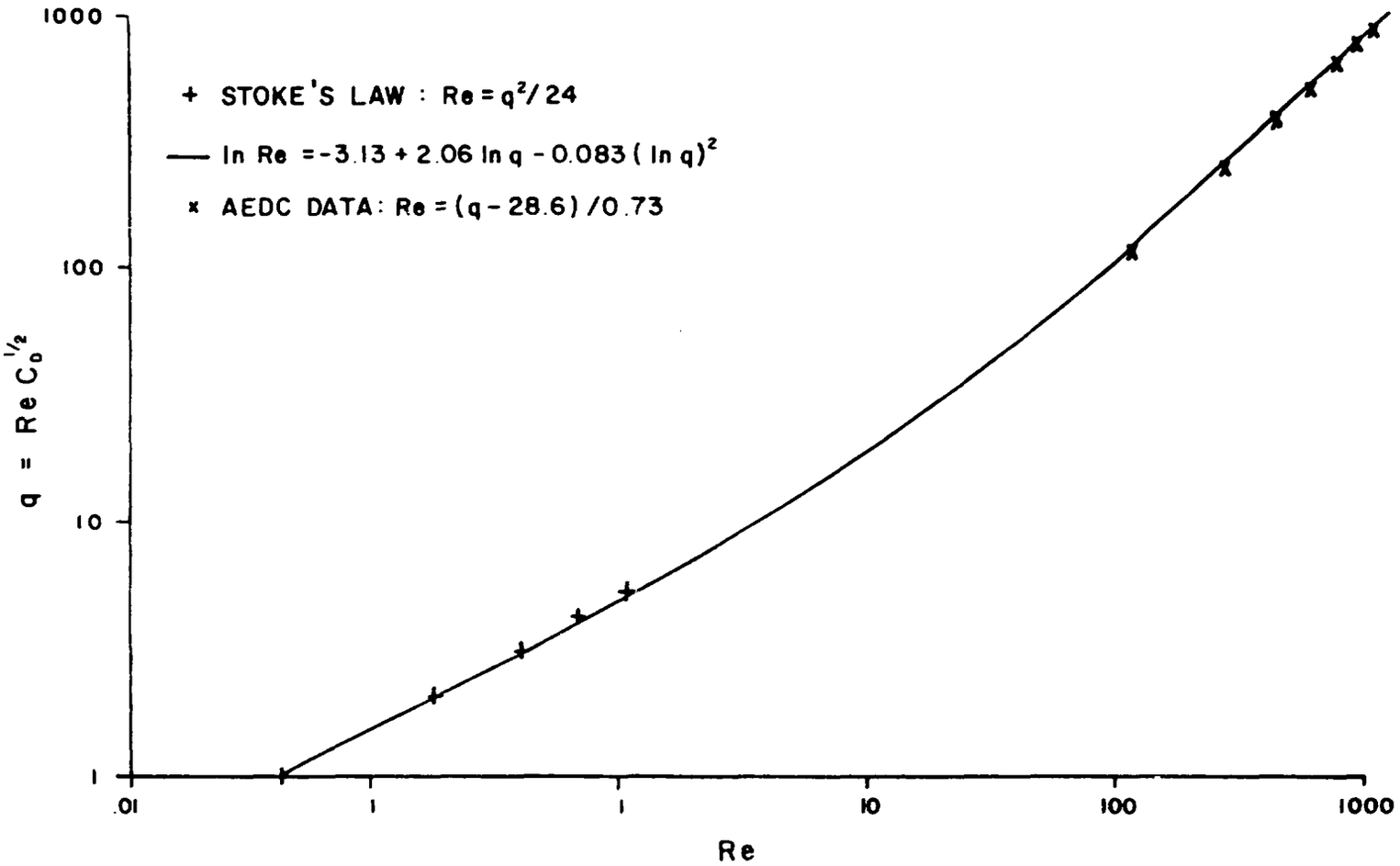

Figure B-1. Relation Between the Reynolds Number and the Drag Coefficient

The component vapor pressure is calculated using a modified Antoine equation:

$$\ln p_i = 20.53 - 2899/(385.15\ T_d/T_{b,i} - 62.3)$$

where $T_{b,i}$ = the normal boiling point of component "i" (K)

The constants is this equation were obtained by using 3,3-dimethylhexane as a reference compound. This single Antoine equation can be used for all of the components through the use of the Ramsey-Young Relation, which states that for similar substances (e.g. hydrocarbons) the ratio of the temperatures at which the substances exert equal vapor pressures is the same for any vapor pressure. As used in the Antoine equation, the relation takes the form:

$$T_r = T_{b,r}(T_d/T_{b,i})$$

where T_r is the temperature at which the reference compound (3,3-dimethylhexane) will have the same vapor pressure that component "i" has at the droplet temperature, and $T_{b,r}$ and $T_{b,i}$ are the normal boiling points of the reference compound and component "i", respectively. Table B-1 compares the vapor pressure predicted in this manner with experimental vapor pressures for several fuel components (from Reference B-7). The agreement is generally within 10 percent.

The mass coefficient is a function of the component's diffusivity, D (m^2/s), the Schmidt number, Sc, and the Nusselt number, Nu:

TABLE B-1. COMPARISON OF EXPERMENTAL AND CALCULATED VAPOR PRESSURES

Compound	Temperature(K)	Vapor Pressure (Pa) Experimental	Calculated	Calc/Exp
n-pentane	223	1333	1197	0.90
n-pentane	261	13332	13468	1.01
n-pentane	309	101325	103839	1.02
iso-hexane	214	133	109	0.82
iso-hexane	243	1333	1241	0.93
iso-hexane	284	13332	13594	1.02
cyclohexane	228	133	138	1.04
cyclohexane	257	1333	1326	0.99
cyclohexane	299	13332	13462	1.01
benzene	236	133	292	2.20
benzene	262	1333	1925	1.44
benzene	299	13332	13990	1.05
2-methylhexane	233	133	128	0.96
2-methylhexane	264	1333	1367	1.03
2-methylhexane	307	13332	13702	1.03
methylcyclohexane	237	133	98	0.74
methylcyclohexane	270	1333	1204	0.90
toluene	246	133	123	0.92
toluene	280	1333	1429	1.07
4-methylheptane	253	133	151	1.14
4-methylheptane	285	1333	1420	1.07
dimethylcyclohexane	254	133	113	0.85
dimethylcyclohexane	288	1333	1253	0.94
m-xylene	266	133	145	1.09
2,7-dimethyloctane	279	133	139	1.05
cis-decalin	296	133	94	
diethylbenzene	294	133	147	0.71
napthaline	326	133	255	1.92
undecane	306	133	180	1.35
triethylbenzene	321	133	184	1.38
tridecane	333	133	206	1.55
isopropylnapthalene	349	133	154	1.16

$$D_i = \frac{2.66 \times 10^{-5} T_F^{\,2} \left[\frac{1}{M_i} + \frac{1}{M_a}\right]^{\frac{1}{2}}}{Pa\,(V_b^{\,1/3} + 0.31)^2}$$

where T_F = the temperature of the evaporating film (K)

$= 1/2(T_a + T_d)$

M_i = the molecular weight of compound "i" (kg/kmol)

V_b = the molar volume of compound "i" at its normal boiling point

$= M_i\,(1 + 0.001\,(T_{b,i} - 293.15))/^{20}\rho_i$

$$Sc_i = \mu_a/(\rho_a B_i)$$

$$Nu_i = 2 + 0.6\,Re^{1/2}\,Sc_i^{\,1/3}$$

$$h_i = Nu_i D_i M_i/(dR_o T_a)$$

The equation for the diffusivity is derived from the one given in Bird, Stewart, and Lightfoot by using a typical value of the Lennard-Jones function, Ω, for hydrocarbon-air pairs at 273K and including the functional dependence of Ω on $T_F^{-1/2}$ (in the temperature range of interest) explicitly. The error introduced by these approximations is estimated to be less than 10 percent. A comparison of experimental and predicted diffusivities for several pure hydrocarbons is shown in Table B-2.

As the droplet falls it cools through evaporation and heat transfer until it is accommodated to the local air temperature. The mass lost through evaporation is included in a total energy balance equation (Reference B-8) to determine the new droplet temperature:

TABLE B-2. COMPARISON OF EXPERMENTAL AND CALCULATED DIFFUSIVITIES

Compound	Temperature(K)	Diffusivity ($m^2/s \times 10^6$) Experimental	Calculated	Calc/Exp
n-hexane	288	7.6	6.9	0.91
2,3-dimethylbutane	288	7.5	7.0	0.93
methylcyclopentane	288	7.6	7.4	0.97
cyclohexane	288	7.6	7.5	0.99
cyclohexane	318	8.6	9.0	1.05
benzene	273	7.7	7.2	0.94
toluene	273	7.6	6.5	0.86
toluene	303	8.8	8.0	0.91
n-octane	273	5.0	5.3	1.06
n-octane	303	7.1	6.6	0.93
2,2,4-trimethylpentane	303	7.1	6.6	0.93
ethylbenzene	273	6.6	6.0	0.91
mesitylene	273	5.6	5.5	0.98
propylbenzene	273	4.9	5.6	1.14
n-decane	363	8.4	8.4	1.00
napthalene	273	5.1	5.9	1.16
dodecane	399	8.1	9.2	1.14
diphenyl	273	6.1	5.0	0.82

$$Q = \pi d^2 \Delta t(e_a \sigma T_a^4 + 1/4(1-a)L + k(T_a - T_d) - e_d \sigma T_d^4) - \Delta H_v \Delta m$$

where e_a = the emissivity of air = 0.75

e_d = the emissivity of the droplet = 0.95

σ = the Stefan-Boltzmann constant

= 5.67×10^{-8} J/s·m^2·K^4

a = the droplet albedo = 0.14

L = the solar insolation rate (J/m^2·s)

k = the heat transfer coefficient (J/m^2·s·K)

= $k_a (2 + 0.6\ Re^{1/2} Pr^{1/3})/d$ (Reference 6)

where k_a = the thermal conductivity (J/m·s·K)

Pr = the Prandtl number

ΔH_v = the latent heat of vaporization (J/kg)

The values chosen for e_a, e_d, and a are those recommended in Reference B-8. For most calculations a fairly high solar rate of 1000 watts per square meter is used since the fuel droplets are released at high altitude. The thermal conductivity and Prandtl number at the evaporating film are essentially those of air, and these were approximated from tabular data by the expressions:

$$k_a = 0.024\ (1 + 0.0034\ (T_a - 273.15))$$

$$Pr = 0.713\ (1 - 4.6 \times 10^{-4}\ (T_a - 273.15))$$

From inspection of the heats of vaporization for a range of individual hydrocarbons as well as JP-4 itself, it was determined that in the temperature range of interest (-40° to +40°C), ΔH_v can be approximated quite well by the linear formula:

$$\Delta H_v = 3.7 \times 10^5 \ (1 - 0.0013 \ (T_d - 273.15))$$

Once Q has been calculated, the amount, T(K), that the droplet cools during the interval is simply:

$$T = Q/m_d \ C_p$$

where m_d = the droplet mass (kg)

C_p = the droplet heat capacity (J/kg/K)

The heat capacity of petroleum fuels can be estimated by (Reference B-7):

$$C_p = 4.84 \ (181 + 0.8 \ T_d)/\rho_d$$

The new droplet temperature, mass, composition, and height are then used as the initial conditions for the next interval. This process continues until the droplet has accommedated itself to the ambient air temperature. The steady-state difference, $\Delta T'$ (K), between the droplet temperature and the air temperature is determined by setting Q equal to zero and solving for $\Delta T'$ using the Newton-Raphson iterative method. The droplet temperature thus obtained is compared with the droplet temperature which was assumed for the evaporation calculations and if the discrepancy is greater than 0.5K the interval is rerun using the new value of T_d. This step is repeated until a self-consistent droplet temperature is obtained.

A flow chart of the model is shown in Figure B-2.

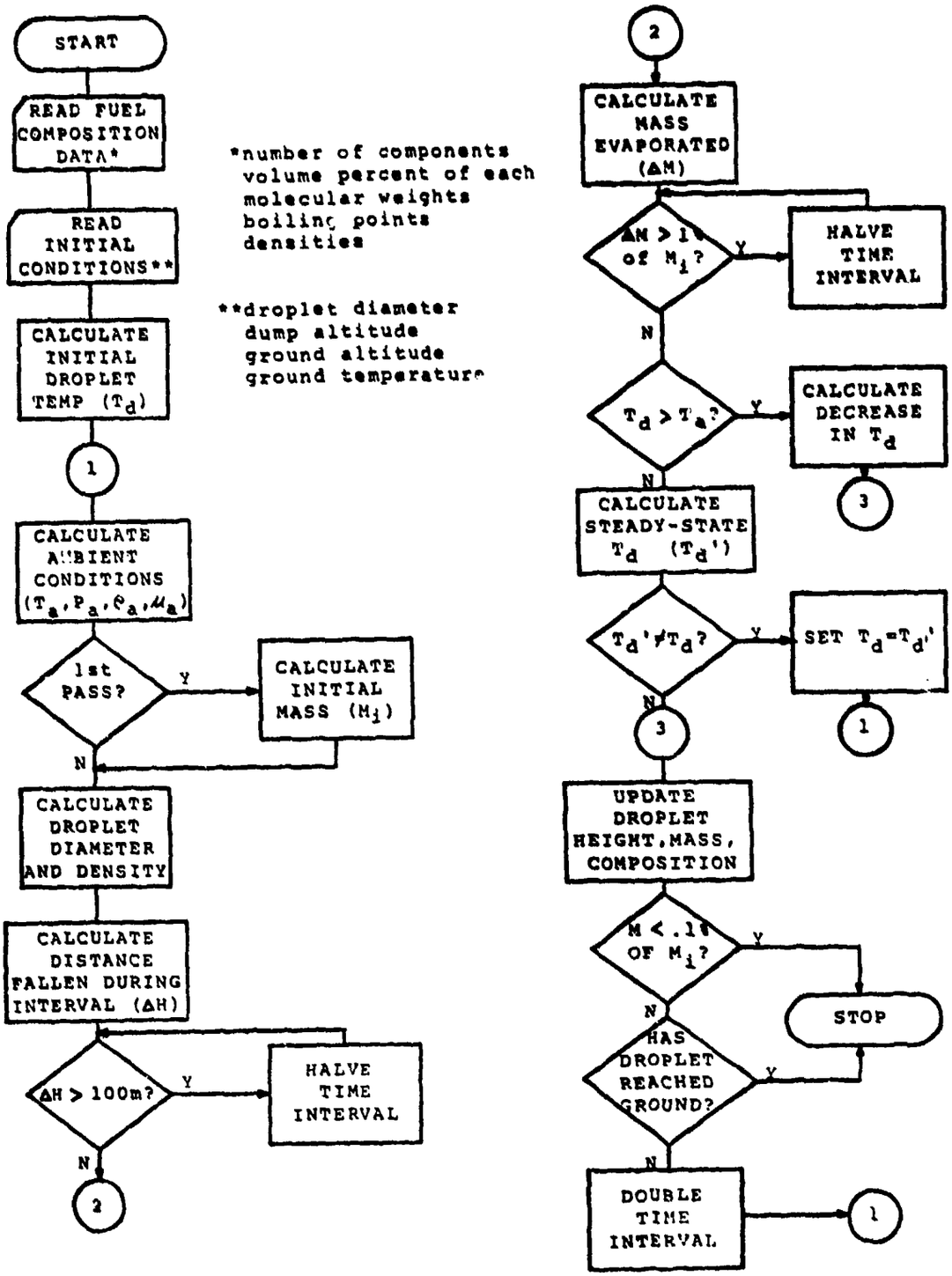

Figure B-2. Flow Chart of Fuel Droplet Model

APPENDIX C

FUEL DROPLET PROGRAM

The FORTRAN IV computer program developed to simulate the evaporation and free-fall of a fuel droplet is listed in this appendix. The variable names used in the program are described in Table C-1 which follows the listing.

```
      PROGRAM FREFAL(INPUT,OUTPUT,TAPE7=INPUT,TAPE6=OUTPUT)
C     SIMULATES THE FREE FALL AND EVAPORATION OF FUEL DROPLETS
      REAL M(40),MO,MEV(40),MI,MOLES,MOLF(40),MW(40),MREL,MS,MSAVE(40),
     2MSTEP,MW(40),NUM,NUB,NAM1,NAM2,NAM3
      DIMENSION DENS(40),PCV(40),TB(40),VC(40),K(9),PCT(50),PCR(40),
     2EPS(9)
C     SET CONSTANTS
      NMAX=10000
      TMAX=600000.
      RMMIN=.0005
      DMMIN=.005
      DMMAX=.05
      DHMIN=10.
      DHMAX=100.
      EA=.75
      ED=.95
      ALB=.14
      RS=1000.
C     INPUT COMPOSITION
  100 READ(7,10) NCOMP
      IF(EOF(7)) 330,105
  105 WRITE(6,5)
      DO 110 I=1,NCOMP
      READ(7,20) NAM1,NAM2,NAM3,PCV(I),MW(I),TB(I),DENS(I)
      WRITE(6,30) I,NAM1,NAM2,NAM3,PCV(I),MW(I),TB(I),DENS(I)
      TB(I)=TB(I)+273.15
      DENS(I)=1000.*DENS(I)
      DCFB=1./(1.+.001*(TB(I)-293.15))
  110 VC(I)=MW(I)/(DENS(I)*DCFB)
      READ(7,25)K
C     K CONTAINS THE LIST OF COMPONENT NUMBERS TO BE PRINTED OUT
      READ(7,31)IND
C     IND=1 FOR SINGLE DROP, 0 FOR DISTRIBUTION
      IF(IND.EQ.1) GO TO 122
C     INPUT DISTRIBUTION (MULTIPLE DROPLET CASE)
  115 READ(7,32)NB,DD,DX
      IF(EOF(7))330,116
  116 READ(7,34)(PCT(I),I=1,NB)
      DU=DD
      WRITE(6,36)
      DO 118 I=1,NB
      WRITE(6,38)DD,PCT(I)
  118 DD=DD+DX
      DMAX=DD-DX
      DMIC=DU
      DSAVE=DU
C     INPUT CASE TO BE RUN (MULTIPLE DROPLET)
  120 READ(7,40)HI,HG,TG,V
      IF(EOF(7)) 330,121
  121 IF(V.EQ.0.) V=175.
      WRITE(6,50)DX,HI,HG,TG,V
      WRITE(6,51)
      WRITE(6,55)K
      WRITE(6,56)
      GO TO 130
C     INPUT CASE TO BE RUN (SINGLE DROPLET)
  122 READ(7,42) DMIC,HI,HG,TG,V
      IF(EOF(7)) 330,123
  123 WRITE(6,44) DMIC,HI,HG,TG
      WRITE(6,46) K
      WRITE(6,48)
      TMAX=60000.
C     INITIALIZE VARIABLES
  130 TO=TG+.0065*HG+273.15
      IF(V.EQ.0.)V=175.
      J=1
      TOT=0.
      DO 132 I=1,NCOMP
  132 PCR(I)=0.
  137 DI=.000001*DMIC
      D=DI
      H=HI
      T=HSTEP=MSTEP=MI=UT=0.
      TSAVE=-1.
      IDONE=0
```

```
      TSTEP=1.
      NPAS=1
      TA=T0-.0065*H
      CS=20.*SQRT(TA)
      DTSAV=-TA*V*V/CS/CS/5.
      DT=DTSAV
      IDS=0
C     BEGINNING OF CALCULATION LOOP
  140 TA=T0-.0065*H
      PA=101315.*(TA/T0)**5.256
      DENSA=.003494*PA/TA
      VISCA=1.458E-6/(110.4+TA)*TA**1.5
      TD=TA-DT
      TF=.5*(TA+TD)
      DCFD=1./(1.+.001*(TD-293.15))
C     ON INTIAL PASS CALCULATE DROPLET VOLUME AND MASS
      IF(NPAS.GT.1) GO TO 160
      VD=.5236*D**3
      MI=0.
      DO 150 I=1,NCOMP
      M(I)=DENS(I)*DCFD*PCV(I)*VD/100.
      MSAVE(I)=M(I)
  150 MI=MI+M(I)
      MD=MI
      DENSI=MD/VD
C     CALCULATE COMPOSITION AND SIZE OF DROPLET
  160 MOLES=0.
      DO 170 I=1,NCOMP
  170 MOLES=MOLES+M(I)/MW(I)
      VD=0.
      DO 180 I=1,NCOMP
  180 VD=VD+M(I)/(DENS(I)*DCFD)
      D=(1.90986*VD)**(1./3.)
      DMIC=1000000.*D
      IF(IDONE.GE.1) GO TO 186
      DO 185 I=1,NCOMP
  185 MOLF(I)=M(I)/(MW(I)*MOLES)
      DENSD=MD/VD
  186 MREL=MD/MI
      DO 190 I=1,NCOMP
  190 MR(I)=M(I)/MSAVE(I)
C     DETERMINE WHETHER TO PRINT
  195 IF(IND.EQ.0) GO TO 200
      IF(IDONE.GE.1) GO TO 218
      IF(MREL.GE.RMMIN) GO TO 197
      IDONE=3
      GO TO 218
  197 IF(T.LE.TSAVE) GO TO 220
      TSAVE=T
      GO TO 218
  200 IF(IDONE.GE.1) GO TO 210
      IF(MREL.GE.RMMIN) GO TO 220
      IDONE=3
C     MULTIPLE DROPLET PRINTOUT
  210 WRITE(6,60)DU,DMIC,T/60.,H,MREL
      DO 211 I=1,9
      KK=K(I)
  211 PMR(I)=MR(KK)
      WRITE(6,61)(PMR(I),I=1,9)
      IF(IDONE.LT.2) GO TO 213
      IF(TMAX.LT.600000.) GO TO 213
      MREL=0.
      DO 212 I=1,NCOMP
  212 MR(I)=0.
  213 WRITE(6,65)PCT(J)*MREL
      IF(IDONE.EQ.2) GO TO 325
C     INCREMENT DROPLET SIZE AND UPDATE TOTALS (MULTIPLE DROPLET CASE)
  214 DU=DU+DX
      DMIC=DU
      DO 215 I=1,NCOMP
  215 PCR(I)=PCR(I)+MR(I)*PCT(J)
      TOT=TOT+MREL*PCT(J)
      J=J+1
C     IF NOT DONE, RE-INITIALIZE AND BEGIN NEXT DROPLET
      IF(DU.LE.DMAX)GO TO 137
```

```
C       IF DONE, PRINT TOTALS AND CHECK FOR ANOTHER CASE
        WRITE(6,70)TOT
  216   WRITE(6,75)(I,PCR(I)*PCV(I)*DENS(I)*DCFD/DENSI/100.,I=1,NCOMP)
        DU=DSAVE
        DMIC=DU
        GO TO 120
C       SINGLE DROPLET PRINTOUT
  218   WRITE(6,80)T/60.,H,DMIC,UT,MREL
        DO 219 I=1,9
        KK=K(I)
  219   PMR(I)=MR(KK)
        WRITE(6,81)(PMR(I),I=1,9)
        WRITE(6,82)DT
C       IF DONE, CHECK FOR ANOTHER CASE (SINGLE DROPLET)
        IF(IDONE.GE.1) GO TO 325
C       CALCULATE FREE FALL AND EVAPORATION
  220   Q=SQRT((4.*DENSA*DENSD*9.8*D**3)/3.)/VISCA
        QLN=ALOG(Q)
        REY=EXP(-3.13+2.06*QLN-.083*QLN*QLN)
        UT=VISCA*REY/(D*DENSA)
        HSTEP=UT*TSTEP
        MSTEP=0.
        DO 225 I=1,NCOMP
        DIFY=2.66E-5*SQRT(1./MW(I)+.0345)*TF*TF/(PA*(VC(I)**(1./3.)+.31)**
       12)
        NUM=2.+.6*SQRT(REY)*(VISCA/(DENSA*DIFY))**(1./3.)
        HM=NUM*DIFY*MW(I)/(8314.34*D*TA)
        PV=EXP(20.53-2899./(385.15*TD/TB(I)-62.3))
        MEV(I)=3.1416*D*D*HM*PV*MOLF(I)*TSTEP
        MS=MEV(I)
        IF(MS.GT.M(I)) MS=M(I)
  225   MSTEP=MSTEP+MS
        NPAS=NPAS+1
        IF(NPAS.LE.NMAX) GO TO 230
        IDONE=2
C       SKIP HEAT BALANCE IF CALCULATING DROPLET COOLING
  230   IF(IDS.EQ.1)GO TO 234
C       CALCULATE STEADY-STATE TEMPERATURE DIFFERENCE
        OLDT=DT
        TKA=.024+8.1E-5*(TA-273.15)
        PR=.713-3.3E-4*(TA-273.15)
        NUH=2.+.6*SQRT(REY)*PR**(1./3.)
        HH=TKA*NUH/D
        DHVAP=3.7E5*(1.-.0013*(TD-273.15))
  231   DTNW=5.67E-8*EA*TA**4-5.67E-8*ED*TD**4+.25*(1.-ALB)*RS+HH*DT-DHVAP
       1*MSTEP/(3.1416*D*D*TSTEP)
        TD=TD+DTNW/(HH+2.27E-7*ED*TD**3)
        IF (ABS(TA-DT-TD).LE..1) GO TO 232
        DT=TA-TD
        GO TO 231
  232   IF(ABS(TA-TD-OLDT).LE..5)GO TO 234
        DT=(TA-TD+OLDT)/2.
        GO TO 140
  234   DT=TA-TD
C       SKIP DROPLET COOLING AFTER STEADY-STATE TEMPERATURE IS REACHED
        IF(IDS.EQ.2)GO TO 240
        IF(IDS.EQ.1)GO TO 238
        IF(DT.GT.DTSAV)GO TO 236
C       SET INDICATOR THAT DROPLET COOLING IS NO LONGER NEEDED
        IDS=2
        GO TO 240
C       RESTORE DT AND SET INDICATOR TO CALCULATE DROPLET COOLING
  236   IDS=1
        DT=DTSAV
        GO TO 140
C       CALCULATE DROPLET COOLING AND RESET INDICATOR TO HEAT BALANCE
  238   IDS=0
        CP=4184.*(181.+.8*TD)*VD
        DHVAP=3.7E5*(1.-.0013*(TD-273.15))
        DCOOL=(EA*5.67E-8*TA**4-ED*5.67E-8*TD**4+.25*(1-ALB)*RS+TKA*NUH*
       2DTSAV/D)*3.1416*D*D*TSTEP
        DCOOL=(DCOOL-MSTEP*DHVAP)/CP
        DTSAV=DTSAV-DCOOL
        DCSAV=DCOOL
        DT=DTSAV
```

```
C     HALVE INCREMENT UNTIL WITHIN LIMITS
  240 IF(HSTEP.GT.DHMAX) GO TO 250
      IF(MSTEP/MI.LE.DMMAX) GO TO 275
  250 TSTEP=TSTEP/2.
      HSTEP=HSTEP/2.
      MSTEP=0.
      DO 260 I=1,NCOMP
      MEV(I)=MEV(I)/2.
      MS=MEV(I)
      IF(MS.GT.M(I)) MS=M(I)
  260 MSTEP=MSTEP+MS
      IF(IDS.EQ.2)GO TO 240
      DCSAV=DCSAV/2.
      DTSAV=DTSAV+DCSAV
      DT=DTSAV
      GO TO 240
C     UPDATE VARIABLES WITH RESULTS FOR INCREMENT
  275 HS=H
      H=H-HSTEP
      IF(H.LT.HG) GO TO 310
      T=T+TSTEP
      IF(T.GE.TMAX)GO TO 321
      MD=MD-MSTEP
      DO 280 I=1,NCOMP
      IF(MEV(I).GT.M(I)) MEV(I)=M(I)
  280 M(I)=M(I)-MEV(I)
C     INCREASE DURATION OF NEXT INCREMENT
      TSTEP=2.*TSTEP
      IF(MD/MI.GE.RMMIN) GO TO 285
      IDONE=3
      GO TO 140
  285 IF(HSTEP.LT.DHMIN) GO TO 290
      IF(MSTEP/MI.LT.DMMIN) GO TO 290
      GO TO 140
  290 TSTEP=2.*TSTEP
      GO TO 140
C     END OF CALCULATION LOOP
C     INTERPOLATE POINT OF GROUND IMPACT
  310 FAC=(HS-HG)/HSTEP
      IDONE=1
  315 TSTEP=TSTEP*FAC
      HSTEP=HSTEP*FAC
      MSTEP=0.
      DO 320 I=1,NCOMP
      MEV(I)=MEV(I)*FAC
      IF(MEV(I).GT.M(I)) MEV(I)=M(I)
      MSTEP=MSTEP+MEV(I)
  320 M(I)=M(I)-MEV(I)
      T=T+TSTEP
      H=HS-HSTEP
      MD=MD-MSTEP
      GO TO 140
C     INTERPOLATE POINT OF TERMINATION BY TIME
  321 FAC=(TMAX+TSTEP-T)/TSTEP
      IDONE=3
      T=T-TSTEP
      GO TO 315
  325 WRITE(6,85) NPAS
      IF(IND.EQ.1) GO TO 122
      GO TO 214
  330 WRITE(6,90)
      STOP
    5 FORMAT(*1*,//,47X,* COMPOSITION OF SIMULATED FUEL MIXTURE *,///,19
     2X,* COMPONENT*,35X,*VOLUME*,10X,*MOL*,10X,*BOILING*,7X,*DENSITY*,/
     3,20X,* NUMBER*,8X,*SPECIES*,22X,*PERCENT*,8X,*WEIGHT*,8X,*PT. (C)*
     4,8X,*G/CC*,/)
   10 FORMAT(I2)
   20 FORMAT(2A10,A9,F5.2,5X,2(F5.1,5X),F5.2)
   25 FORMAT(9I2)
   30 FORMAT(* *,22X,I2,10X,2A10,A9,1X,F5.2,10X,2(F5.1,9X),F5.2)
   31 FORMAT(I1)
   32 FORMAT(I2,8X,F5.0,5X,F5.0)
   34 FORMAT(5(F5.1,5X))
   36 FORMAT(////,56X,* DROPLET DISTRIBUTION *,///,56X,* DIAMETER*,5X,*W
     2EIGHT*,/,56X,* (MICRONS)*,4X,*PERCENT*,/)
```

```
38 FORMAT(* *,58X,F5.0,6X,F5.1)
40 FORMAT(10X,F6.0,4X,F5.0,5X,F5.0,5X,F5.0)
42 FORMAT(F5.0,5X,F6.0,4X,F5.0,5X,F5.0,5X,F5.0)
44 FORMAT(*1*,/,* DROPLET HISTORY FOR :*,/,10X,* INITIAL DIAMETER (MI
   2CRONS):*,5X,F5.0,/,10X,* DUMP ALTITUDE, MSL (METERS):*,3X,F6.0,/10
   3X,* LOCAL GROUND LEVEL (METERS):*, 3X,F6.0,/,10X,
   4* GROUND-LEVEL TEMPERATURE (C):*,4X,F4.0,///,46X,* RELATIVE*,4X,*I
   5N*,/,3X,* T*,6X,*ALTITUDE*,4X,*DIAMETER*,5X,*VELOCITY*5X,*MASS*,8X
   6,*COMPONENT*,/,*   (MIN)*4X,*(METERS)*,4X,*(MICRONS)*,4X,*(M/SEC)*,
   76X,*REMAINING... *)
46 FORMAT(*+*,62X,9(I2,4X))
48 FORMAT(*+*,120X,*DELTA T (C)*,/)
50 FORMAT(*1*,/,* DROPLET HISTORY FOR :*,/,10X,* DIAMETER INTERVAL (M
   2ICRONS):*,4X,F5.0,/,10X,* DUMP ALTITUDE, MSL (METERS):*,3X,F6.0,/1
   30X,* LOCAL GROUND LEVEL (METERS):*,3X,F6.0,/,10X,* GROUND LEVEL TE
   4MPERATURE(C):*,5X,F4.0,/,10X,* AIRCRAFT VELOCITY (MET/SEC):*,3X,F6
   5.0,///)
51 FORMAT(* INITIAL*,7X,*FINAL*,6X,*ELAPSED*,5X,*FINAL*,6X,*RELATIVE*
   2,4X,*IN*,56X,*PERCENT*,/,* DIAMETER*,5X,*DIAMETER*,5X,*TIME*,6X,*A
   3LTITUDE*,6X,*MASS*,6X,*COMPONENT*,49X,*OF TOTAL*,/,* (MICRONS)*,4X
   4,*(MICRONS)*,4X,*(MIN)*,5X,*(METERS)*,4X,*REMAINING...*)
55 FORMAT(*+*,62X,9(I2,4X))
56 FORMAT(*+*,116X,*INITIAL MASS*,/)
60 FORMAT(* *,F7.0,7X,F6.0,5X,F7.2,5X,F6.0,6X,F5.3)
61 FORMAT(*+*,58X,9(2X,F4.2))
65 FORMAT(*+*,118X,F6.2)
70 FORMAT(//,84X,* OVERALL PERCENT OF INITIAL MASS:  *,F6.2,//,* PERC
   2ENT OF INITIAL MASS REMAINING, BY COMPONENT NUMBER:*,//)
75 FORMAT(5(* #*,I2,*:*,F6.2,*%*,6X))
80 FORMAT(* *,F7.3,4X,F6.0,7X,F5.0,7X,F6.4,6X,F6.4,4X,9(2X,F4.2))
81 FORMAT(*+*,58X,9(2X,F4.2))
82 FORMAT(*+*,123X,F5.1)
85 FORMAT(//,9X,* TOTAL NUMBER OF ITERATIONS = *,I7)
90 FORMAT(*1    END OF JOB*)
   END
```

TABLE C-1. IDENTIFICATION OF PROGRAM VARIBLES

Name	Description
ALB	droplet albedo
CP	droplet heat capacity
CS	local speed of sound
D	droplet diameter
DCFB	density correction factor at boiling point
DCFD	density correction factor at droplet temperature
DCOOL	droplet cooling during interval
DCSAVE	same as DCOOL, for use during interval halving
DD	droplet diameter in microns (during input of distribution)
DENS(I)	density of component I
DENSA	density of air
DENSD	droplet density
DENSI	initial droplet density
DHMAX	maximum droplet fall during interval
DHMIN	minimum droplet fall during interval
DHVAP	heat of vaporization
DI	initial droplet diameter
DIFY	diffusivity
DMAX	diameter of largest droplet in distribution
DMIC	droplet diameter in microns
DMMAX	maximum evaporation during interval
DMMIN	minimum evaporataion during interval
DSAVE	diameter of smallest droplet in distribution

DT	difference between air and droplet temperature
DTNW	new guess for steady state droplet temperatuare
DTSAV	saved value of DT
DU	initial droplet diameter in microns
DX	diameter interval for distribution of droplets
EA	emissivity of air
ED	emissivity of droplet
FAC	fraction of interval before droplet reached the ground
H	droplet altitude
HG	altitude at ground
HH	heat transfer coefficient
HI	initial droplet altitude
HM	mass transfer coefficient
HS	saved value of H
HSTEP	change in altitude during interval
IDONE	flag for completion of calculation
IDS	flag for droplet cooling calculation
IND	flag for single droplet versus distribution
K(I)	number of component to be printed out in I'th position
KK	same as K(I) (during printout)
M(I)	mass of component I
MD	mass of droplet
MEV(I)	mass evaporated during interval (of component I)
MI	initial mass of droplet
MOLES	total number of moles in droplet
MOLF(I)	mole fraction of component I

MR(I)	fraction of mass remaining of component I
MREL	fraction of mass remaining of droplet
MS	saved value of MD
MSAVE(I)	saved value of M(I)
MSTEP	mass evaporated during interval (of droplet)
MW(I)	molecular weight of component I
NAM1	name of component (during input and printout)
NAM2	name of component (during input and printout)
NAM3	name of component (during input and printout)
NB	number of bins in droplet distribution
NCOMP	number of components
NMAX	maximum number of iterations
NPAS	number of iterations
NUH	Nusselt number for heat transfer
NUM	Nusselt number for mass transfer
OLDT	previous value of DT
PA	local air pressure
PCR(I)	fraction of mass remaining in droplet distribution bin I
PCT(J)	percent mass in droplet distribution bin J
PCV(I)	percent by volume of component I
PMR(I)	fraction of mass remaining of component I (during printout)
PR	Prandtl number
PV	vapor pressure
Q	variable used to calculate Reynolds number
QLN	log of Q
REY	Reynolds number

RMMIN	minimum fractional mass remaining of droplet
RS	solar insolation rate
T	time
TA	local air temperature
TB(I)	normal boiling point of component I
TD	droplet temperatuare
TF	temperature of evaporating film
TG	temperature at ground-level
TKA	thermal conductivity of air
TMAX	maximum time permitted
TOT	total mass reaching ground
TSAVE	saved value of time
TSTEP	duration of interval
TO	temperature at zero altitude
UT	terminal velocity of droplet
V	true airspeed of aircraft
VC(I)	molar volume of component I at its normal boiling point
VD	droplet volume
VISCA	local viscosity of air

APPENDIX D

SAMPLE FUEL DROPLET PROGRAM RESULTS

This appendix presents the predictions of the fuel droplet evaporation and free-fall program for five cases involving a single droplet and for five cases involving a distribution of droplets. The assumed initial droplet composition and, for the latter cases, the droplet size distribution is shown before the first case.

COMPOSITION OF SIMULATED FUEL MIXTURE

COMPONENT NUMBER	SPECIES	VOLUME PERCENT	MOL WEIGHT	BOILING PT. (C)	DENSITY G/CC
1	ISO-PENTANE	3.90	72.2	27.9	.62
2	ISO-HEXANE	8.10	86.2	60.2	.66
3	CYCLOHEXANE	2.10	84.2	80.7	.78
4	BENZENE	.30	78.1	80.1	.88
5	3-METHYLHEXANE	9.40	100.2	91.8	.69
6	METHYLCYCLOHEXANE	7.10	98.2	100.9	.77
7	TOLUENE	.70	92.1	110.8	.87
8	4-METHYLHEPTANE	10.10	114.2	117.7	.70
9	CIS-1,4-DIMETHYLCYCLOHEXANE	7.40	112.2	124.3	.78
10	M-XYLENE	1.60	106.2	139.1	.87
11	4-METHYLOCTANE	9.10	128.3	142.4	.72
12	ISOPROPYLCYCLOHEXANE	4.30	126.2	154.5	.80
13	1-ETHYL-2-METHYLBENZENE	2.40	120.2	165.2	.88
14	2,7-DIMETHYLOCTANE	7.30	142.3	159.6	.72
15	P-MENTHANE(CIS)	3.70	140.3	171.9	.80
16	P-CYMENE	1.80	134.2	177.1	.86
17	NAPTHALENE	.20	128.2	217.9	1.03
18	UNDECANE	4.80	156.3	195.9	.74
19	3-METHYLBUTYLCYCLOHEXANE	2.50	154.3	196.5	.80
20	2-METHYLENEDECALIN(TRANS)	3.40	150.3	201.8	.89
21	1-BUTYL-3-METHYLBENZENE	1.10	148.2	205.0	.86
22	1-METHYLNAPTHALENE	.20	142.2	244.6	1.02
23	DODECANE	2.60	170.3	216.3	.75
24	3-ETHYLBUTYLCYCLOHEXANE	1.20	168.3	211.8	.80
25	1,3,5-TRIETHYLBENZENE	.50	162.3	216.8	.86
26	2,3-DIMETHYLNAPTHALENE	.20	156.2	268.8	1.00
27	TRIDECANE	1.10	184.4	235.4	.76
28	3-ISOPROPYLBUTYLCYCLOHEXANE	.40	182.4	225.8	.80
29	3,5-DIETHYL-1-PROPYLBENZENE	.10	176.3	234.8	.87
30	TETRADECANE	.20	198.4	253.7	.76
31	PENTADECANE	.10	212.4	270.6	.77
32	PERHYDROPHENANTHRENE	1.60	192.4	290.8	.94
33	PYRENE	.10	202.3	393.0	1.27

DROPLET DISTRIBUTION

DIAMETER (MICRONS)	WEIGHT PERCENT
10.	.4
30.	1.6
50.	2.8
70.	2.8
90.	3.2
110.	4.8
130.	4.4
150.	4.4
170.	4.8
190.	4.8
210.	5.2
230.	5.6
250.	5.6
270.	6.0
290.	6.0
310.	6.4
330.	6.4
350.	6.4
370.	5.6
390.	4.4
410.	3.6
430.	2.8
450.	2.0
470.	1.2
490.	.4

DROPLET HISTORY FOR :
INITIAL DIAMETER (MICRONS): 270.
PUMP ALTITUDE, MSL (METERS): 1500.
LOCAL GROUND LEVEL (METERS): 0.
GROUND-LEVEL TEMPERATURE (C): 20.

T (MIN)	ALTITUDE (METERS)	DIAMETER (MICRONS)	VELOCITY (M/SEC)	RELATIVE MASS REMAINING	IN COMPONENT 2	5	8	11	14	18	23	27	32	DELTA T (C)
0.000	1500.	270.	0.0000	1.0000	1.00	1.00	1.00	1.00	1.00	1.00	1.00	1.00	1.00	-15.3
.000	1500.	267.	.8995	.9737	.90	.97	.99	1.00	1.00	1.00	1.00	1.00	1.00	-13.2
.001	1500.	262.	.8918	.9343	.73	.92	.97	.99	1.00	1.00	1.00	1.00	1.00	-5.6
.002	1500.	258.	.8791	.8961	.53	.85	.95	.98	.99	1.00	1.00	1.00	1.00	2.1
.004	1500.	253.	.8669	.8602	.33	.77	.92	.97	.99	1.00	1.00	1.00	1.00	7.1
.008	1500.	248.	.8538	.8139	.12	.65	.88	.96	.98	1.00	1.00	1.00	1.00	5.9
.012	1499.	245.	.8343	.7768	.03	.54	.83	.95	.98	1.00	1.00	1.00	1.00	4.5
.016	1499.	241.	.8181	.7462	.01	.43	.79	.93	.97	.99	1.00	1.00	1.00	4.8
.021	1499.	238.	.8044	.7199	.00	.35	.74	.91	.96	.99	1.00	1.00	1.00	3.6
.029	1499.	233.	.7921	.6722	0.00	.21	.65	.88	.95	.99	1.00	1.00	1.00	3.4
.037	1498.	228.	.7691	.6329	0.00	.11	.56	.84	.93	.99	1.00	1.00	1.00	2.4
.046	1498.	224.	.7494	.6003	0.00	.06	.48	.80	.91	.99	.99	1.00	1.00	2.1
.054	1497.	220.	.7324	.5727	0.00	.03	.40	.76	.89	.98	.99	1.00	1.00	1.8
.071	1497.	213.	.7175	.5252	0.00	0.00	.27	.69	.85	.97	.99	1.00	1.00	1.6
.087	1496.	208.	.6908	.4893	0.00	0.00	.18	.61	.81	.97	.99	1.00	1.00	1.1
.104	1495.	204.	.6696	.4599	0.00	0.00	.11	.54	.77	.96	.99	1.00	1.00	.9
.137	1494.	196.	.6514	.4104	0.00	0.00	.02	.41	.69	.94	.98	.99	1.00	.8
.171	1493.	190.	.6191	.3758	0.00	0.00	.00	.30	.61	.92	.97	.99	1.00	.5
.204	1492.	185.	.5948	.3484	0.00	0.00	.00	.21	.54	.91	.97	.99	1.00	.4
.271	1489.	176.	.5745	.3028	0.00	0.00	0.00	.08	.40	.87	.95	.98	1.00	.3
.337	1487.	169.	.5387	.2703	0.00	0.00	0.00	.03	.29	.83	.94	.98	1.00	.1
.471	1483.	158.	.5108	.2216	0.00	0.00	0.00	0.00	.11	.74	.90	.96	1.00	.0
.604	1479.	151.	.4648	.1923	0.00	0.00	0.00	0.00	.03	.66	.87	.95	1.00	-.1
.871	1472.	139.	.4339	.1538	0.00	0.00	0.00	0.00	0.00	.49	.79	.92	1.00	-.1
1.404	1460.	123.	.3875	.1058	0.00	0.00	0.00	0.00	0.00	.20	.63	.85	.99	-.1
1.937	1450.	109.	.3219	.0749	0.00	0.00	0.00	0.00	0.00	.06	.48	.76	.99	-.2
3.004	1432.	92.	.2714	.0469	0.00	0.00	0.00	0.00	0.00	0.00	.19	.61	.98	-.2
5.137	1405.	79.	.2108	.0314	0.00	0.00	0.00	0.00	0.00	0.00	0.00	.25	.95	-.2
9.404	1362.	72.	.1710	.0241	0.00	0.00	0.00	0.00	0.00	0.00	0.00	0.00	.87	-.2
17.937	1286.	65.	.1480	.0184	0.00	0.00	0.00	0.00	0.00	0.00	0.00	0.00	.71	-.2
26.471	1221.	60.	.1265	.0142	0.00	0.00	0.00	0.00	0.00	0.00	0.00	0.00	.55	-.2
35.004	1166.	54.	.1095	.0107	0.00	0.00	0.00	0.00	0.00	0.00	0.00	0.00	.40	-.1
52.071	1072.	40.	.0913	.0046	0.00	0.00	0.00	0.00	0.00	0.00	0.00	0.00	.13	-.1
69.137	1014.	27.	.0548	.0017	0.00	0.00	0.00	0.00	0.00	0.00	0.00	0.00	0.00	-.1
103.271	955.	27.	.0296	.0017	0.00	0.00	0.00	0.00	0.00	0.00	0.00	0.00	0.00	-.1
137.404	895.	27.	.0294	.0017	0.00	0.00	0.00	0.00	0.00	0.00	0.00	0.00	0.00	-.1
171.537	835.	27.	.0292	.0016	0.00	0.00	0.00	0.00	0.00	0.00	0.00	0.00	0.00	-.1
205.671	774.	27.	.0290	.0016	0.00	0.00	0.00	0.00	0.00	0.00	0.00	0.00	0.00	-.1
239.806	717.	26.	.0288	.0016	0.00	0.00	0.00	0.00	0.00	0.00	0.00	0.00	0.00	-.1
273.937	658.	26.	.0286	.0016	0.00	0.00	0.00	0.00	0.00	0.00	0.00	0.00	0.00	-.1
308.071	600.	26.	.0283	.0016	0.00	0.00	0.00	0.00	0.00	0.00	0.00	0.00	0.00	-.1
342.206	543.	26.	.0281	.0016	0.00	0.00	0.00	0.00	0.00	0.00	0.00	0.00	0.00	-.1
376.337	486.	26.	.0278	.0015	0.00	0.00	0.00	0.00	0.00	0.00	0.00	0.00	0.00	-.1
410.471	429.	26.	.0275	.0015	0.00	0.00	0.00	0.00	0.00	0.00	0.00	0.00	0.00	-.1
444.604	373.	26.	.0272	.0015	0.00	0.00	0.00	0.00	0.00	0.00	0.00	0.00	0.00	-.1
478.737	318.	26.	.0269	.0015	0.00	0.00	0.00	0.00	0.00	0.00	0.00	0.00	0.00	-.1
512.871	264.	26.	.0266	.0014	0.00	0.00	0.00	0.00	0.00	0.00	0.00	0.00	0.00	-.1
547.004	210.	25.	.0263	.0014	0.00	0.00	0.00	0.00	0.00	0.00	0.00	0.00	0.00	-.1
581.137	157.	25.	.0260	.0014	0.00	0.00	0.00	0.00	0.00	0.00	0.00	0.00	0.00	-.1
615.271	104.	25.	.0256	.0014	0.00	0.00	0.00	0.00	0.00	0.00	0.00	0.00	0.00	-.1
649.404	53.	25.	.0252	.0013	0.00	0.00	0.00	0.00	0.00	0.00	0.00	0.00	0.00	-.1
683.537	2.	25.	.0249	.0013	0.00	0.00	0.00	0.00	0.00	0.00	0.00	0.00	0.00	-.1
684.613	0.	25.	.0245	.0013	0.00	0.00	0.00	0.00	0.00	0.00	0.00	0.00	0.00	-.1

TOTAL NUMBER OF ITERATIONS = 77

DROPLET HISTORY FOR :
INITIAL DIAMETER (MICRONS): 270.
DUMP ALTITUDE, MSL (METERS): 1500.
LOCAL GROUND LEVEL (METERS): 0.
GROUND-LEVEL TEMPERATURE (C): 0.

T (MIN)	ALTITUDE (METERS)	DIAMETER (MICRONS)	VELOCITY (M/SEC)	RELATIVE MASS REMAINING...	IN COMPONENT 2	5	8	11	14	18	23	27	32	DELTA T (C)
0.000	1500.	270.	0.0000	1.0000	1.00	1.00	1.00	1.00	1.00	1.00	1.00	1.00	1.00	-15.3
.001	1500.	265.	.9272	.9586	.84	.96	.99	1.00	1.00	1.00	1.00	1.00	1.00	-8.2
.003	1500.	260.	.9150	.9217	.65	.91	.97	.99	1.00	1.00	1.00	1.00	1.00	2.4
.011	1499.	255.	.9047	.8745	.33	.81	.95	.98	.99	1.00	1.00	1.00	1.00	4.3
.020	1499.	252.	.8862	.8396	.16	.72	.92	.98	.99	1.00	1.00	1.00	1.00	1.8
.028	1498.	249.	.8718	.8121	.07	.64	.89	.97	.99	1.00	1.00	1.00	1.00	1.5
.045	1498.	244.	.8601	.7668	0.00	.48	.83	.95	.98	1.00	1.00	1.00	1.00	1.3
.061	1497.	240.	.8400	.7325	0.00	.35	.77	.93	.97	1.00	1.00	1.00	1.00	.9
.078	1496.	236.	.8240	.7026	0.00	.26	.72	.91	.97	1.00	1.00	1.00	1.00	.8
.095	1495.	233.	.8098	.6769	0.00	.18	.66	.90	.96	.99	1.00	1.00	1.00	.7
.128	1494.	228.	.7972	.6320	0.00	.07	.56	.86	.94	.99	1.00	1.00	1.00	.5
.161	1492.	223.	.7745	.5982	0.00	.03	.46	.82	.93	.99	1.00	1.00	1.00	.3
.195	1491.	220.	.7566	.5706	0.00	.01	.38	.78	.91	.99	1.00	1.00	1.00	.2
.261	1488.	213.	.7415	.5250	0.00	0.00	.24	.70	.87	.98	.99	1.00	1.00	.1
.328	1485.	209.	.7154	.4917	0.00	0.00	.15	.62	.84	.96	.99	1.00	1.00	-.0
.395	1482.	204.	.6954	.4646	0.00	0.00	.09	.55	.80	.97	.99	1.00	1.00	-.1
.528	1476.	197.	.6784	.4198	0.00	0.00	.01	.42	.73	.96	.99	1.00	1.00	-.1
.661	1471.	192.	.6489	.3893	0.00	0.00	.00	.32	.66	.95	.98	1.00	1.00	-.2
.928	1461.	184.	.6275	.3417	0.00	0.00	0.00	.15	.52	.92	.98	1.00	1.00	-.2
1.195	1452.	177.	.5918	.3080	0.00	0.00	0.00	.06	.41	.89	.97	.99	1.00	-.2
1.728	1434.	167.	.5645	.2582	0.00	0.00	0.00	0.00	.21	.84	.95	.98	1.00	-.3
2.261	1417.	160.	.5203	.2278	0.00	0.00	0.00	0.00	.10	.78	.93	.98	1.00	-.3
3.328	1386.	149.	.4904	.1867	0.00	0.00	0.00	0.00	0.00	.66	.89	.96	1.00	-.3
5.461	1329.	137.	.4455	.1446	0.00	0.00	0.00	0.00	0.00	.43	.79	.93	1.00	-.3
7.595	1278.	127.	.3927	.1162	0.00	0.00	0.00	0.00	0.00	.25	.69	.89	1.00	-.3
11.861	1188.	107.	.3520	.0720	0.00	0.00	0.00	0.00	0.00	.01	.49	.81	.99	-.3
16.128	1118.	97.	.2757	.0546	0.00	0.00	0.00	0.00	0.00	0.00	.29	.71	.99	-.3
20.395	1057.	91.	.2386	.0452	0.00	0.00	0.00	0.00	0.00	0.00	.15	.60	.98	-.2
24.661	1001.	86.	.2165	.0394	0.00	0.00	0.00	0.00	0.00	0.00	.06	.49	.98	-.2
28.928	950.	83.	.2015	.0358	0.00	0.00	0.00	0.00	0.00	0.00	.02	.39	.97	-.2
37.461	852.	79.	.1914	.0312	0.00	0.00	0.00	0.00	0.00	0.00	0.00	.22	.95	-.2
45.995	761.	76.	.1778	.0285	0.00	0.00	0.00	0.00	0.00	0.00	0.00	.11	.94	-.2
54.528	674.	75.	.1694	.0267	0.00	0.00	0.00	0.00	0.00	0.00	0.00	.05	.92	-.2
63.061	590.	73.	.1630	.0253	0.00	0.00	0.00	0.00	0.00	0.00	0.00	.02	.90	-.2
71.595	509.	72.	.1580	.0241	0.00	0.00	0.00	0.00	0.00	0.00	0.00	.01	.87	-.2
80.128	431.	71.	.1537	.0231	0.00	0.00	0.00	0.00	0.00	0.00	0.00	.00	.85	-.2
88.661	354.	70.	.1498	.0222	0.00	0.00	0.00	0.00	0.00	0.00	0.00	.00	.82	-.2
97.195	279.	69.	.1460	.0213	0.00	0.00	0.00	0.00	0.00	0.00	0.00	.00	.80	-.2
105.728	206.	68.	.1423	.0204	0.00	0.00	0.00	0.00	0.00	0.00	0.00	.00	.77	-.2
114.261	135.	67.	.1386	.0195	0.00	0.00	0.00	0.00	0.00	0.00	0.00	.00	.74	-.2
122.795	66.	66.	.1348	.0186	0.00	0.00	0.00	0.00	0.00	0.00	0.00	0.00	.71	-.2
131.241	0.	65.	.1311	.0177	0.00	0.00	0.00	0.00	0.00	0.00	0.00	0.00	.68	-.2

TOTAL NUMBER OF ITERATIONS = 58

DROPLET HISTORY FOR :
INITIAL DIAMETER (MICRONS): 270.
DUMP ALTITUDE, MSL (METERS): 1500.
LOCAL GROUND LEVEL (METERS): 0.
GROUND-LEVEL TEMPERATURE (C): -20.

T (MIN)	ALTITUDE (METERS)	DIAMETER (MICRONS)	VELOCITY (M/SEC)	RELATIVE MASS REMAINING...	IN COMPONENT 2	5	8	11	14	18	23	27	32	DELTA T (C)
0.000	1500.	270.	0.0000	1.0000	1.00	1.00	1.00	1.00	1.00	1.00	1.00	1.00	1.00	-15.3
.002	1500.	266.	.9564	.9720	.90	.98	.99	1.00	1.00	1.00	1.00	1.00	1.00	-3.3
.010	1499.	261.	.9507	.9353	.72	.94	.99	1.00	1.00	1.00	1.00	1.00	1.00	11.1
.027	1498.	259.	.9389	.9087	.51	.89	.97	.99	1.00	1.00	1.00	1.00	1.00	.6
.060	1497.	254.	.9285	.8641	.20	.80	.95	.99	1.00	1.00	1.00	1.00	1.00	.3
.094	1495.	251.	.9106	.8336	.07	.71	.93	.98	.99	1.00	1.00	1.00	1.00	.0
.160	1491.	246.	.8978	.7883	0.00	.53	.88	.97	.99	1.00	1.00	1.00	1.00	-.0
.227	1488.	242.	.8778	.7550	0.00	.40	.83	.96	.99	1.00	1.00	1.00	1.00	-.1
.294	1484.	239.	.8624	.7269	0.00	.29	.78	.94	.98	1.00	1.00	1.00	1.00	-.2
.427	1477.	234.	.8491	.6792	0.00	.13	.68	.92	.97	1.00	1.00	1.00	1.00	-.2
.560	1471.	229.	.8257	.6446	0.00	.06	.59	.89	.96	1.00	1.00	1.00	1.00	-.3
.694	1464.	226.	.8090	.6176	0.00	.02	.51	.86	.95	1.00	1.00	1.00	1.00	-.3
.960	1452.	220.	.7936	.5738	0.00	0.00	.37	.81	.93	.99	1.00	1.00	1.00	-.3
1.227	1439.	216.	.7693	.5427	0.00	0.00	.26	.75	.91	.99	1.00	1.00	1.00	-.4
1.494	1427.	212.	.7512	.5176	0.00	0.00	.18	.70	.89	.99	1.00	1.00	1.00	-.4
2.027	1404.	206.	.7361	.4754	0.00	0.00	.06	.59	.84	.98	1.00	1.00	1.00	-.4
2.560	1381.	201.	.7094	.4457	0.00	0.00	.02	.50	.80	.98	.99	1.00	1.00	-.4
3.627	1337.	194.	.6896	.4014	0.00	0.00	0.00	.33	.70	.97	.99	1.00	1.00	-.4
4.694	1295.	189.	.6580	.3711	0.00	0.00	0.00	.21	.62	.95	.99	1.00	1.00	-.4
6.827	1214.	180.	.6349	.3212	0.00	0.00	0.00	.05	.45	.93	.98	1.00	1.00	-.4
8.960	1138.	173.	.5942	.2886	0.00	0.00	0.00	.01	.31	.90	.97	.99	1.00	-.4
11.094	1065.	168.	.5648	.2642	0.00	0.00	0.00	.00	.21	.87	.97	.99	1.00	-.4
13.227	996.	164.	.5413	.2447	0.00	0.00	0.00	0.00	.13	.84	.96	.99	1.00	-.4
15.360	929.	160.	.5214	.2289	0.00	0.00	0.00	0.00	.08	.80	.95	.99	1.00	-.4
17.494	865.	157.	.5043	.2158	0.00	0.00	0.00	0.00	.04	.77	.93	.98	1.00	-.4
19.627	802.	154.	.4896	.2047	0.00	0.00	0.00	0.00	.02	.73	.92	.98	1.00	-.4
21.760	741.	152.	.4766	.1951	0.00	0.00	0.00	0.00	.01	.69	.91	.98	1.00	-.4
23.894	681.	149.	.4649	.1865	0.00	0.00	0.00	0.00	.01	.65	.90	.97	1.00	-.4
26.027	623.	147.	.4542	.1787	0.00	0.00	0.00	0.00	.00	.61	.88	.97	1.00	-.3
28.160	566.	145.	.4442	.1715	0.00	0.00	0.00	0.00	.00	.57	.87	.96	1.00	-.3
30.294	511.	143.	.4347	.1647	0.00	0.00	0.00	0.00	.00	.53	.85	.96	1.00	-.3
32.427	456.	141.	.4255	.1581	0.00	0.00	0.00	0.00	.00	.50	.84	.95	1.00	-.3
34.560	403.	139.	.4166	.1519	0.00	0.00	0.00	0.00	.00	.46	.82	.95	1.00	-.3
36.694	351.	137.	.4079	.1459	0.00	0.00	0.00	0.00	.00	.42	.80	.94	1.00	-.3
38.827	300.	135.	.3993	.1400	0.00	0.00	0.00	0.00	.00	.38	.78	.94	1.00	-.3
40.960	250.	134.	.3909	.1343	0.00	0.00	0.00	0.00	.00	.35	.76	.93	1.00	-.3
45.227	152.	130.	.3825	.1233	0.00	0.00	0.00	0.00	0.00	.28	.73	.92	1.00	-.3
49.494	58.	126.	.3657	.1129	0.00	0.00	0.00	0.00	0.00	.22	.68	.90	1.00	-.3
52.267	0.	123.	.3494	.1066	0.00	0.00	0.00	0.00	0.00	.19	.66	.89	1.00	-.3

TOTAL NUMBER OF ITERATIONS = 54

DROPLET HISTORY FOR :
INITIAL DIAMETER (MICRONS): 500.
DUMP ALTITUDE, MSL (METERS): 1500.
LOCAL GROUND LEVEL (METERS): 0.
GROUND-LEVEL TEMPERATURE (C): 0.

T (MIN)	ALTITUDE (METERS)	DIAMETER (MICRONS)	VELOCITY (M/SEC)	RELATIVE MASS REMAINING...	IN COMPONENT 2	5	8	11	14	18	23	27	32	DELTA T (C)
0.000	1500.	500.	0.0000	1.0000	1.00	1.00	1.00	1.00	1.00	1.00	1.00	1.00	1.00	-15.3
.002	1500.	491.	1.8782	.9521	.85	.96	.99	1.00	1.00	1.00	1.00	1.00	1.00	-7.8
.006	1499.	483.	1.8617	.9275	.68	.92	.98	.99	1.00	1.00	1.00	1.00	1.00	1.5
.023	1497.	473.	1.8471	.8792	.36	.82	.95	.99	.99	1.00	1.00	1.00	1.00	6.2
.040	1496.	467.	1.8167	.8466	.19	.74	.92	.98	.99	1.00	1.00	1.00	1.00	1.8
.056	1494.	462.	1.7944	.8201	.09	.66	.90	.97	.99	1.00	1.00	1.00	1.00	1.6
.090	1490.	453.	1.7756	.7757	0.00	.51	.84	.95	.98	1.00	1.00	1.00	1.00	1.4
.123	1487.	446.	1.7427	.7430	0.00	.39	.79	.94	.98	1.00	1.00	1.00	1.00	1.0
.156	1483.	440.	1.7171	.7141	0.00	.29	.74	.92	.97	1.00	1.00	1.00	1.00	.8
.190	1480.	435.	1.6934	.6890	0.00	.22	.69	.90	.96	.99	1.00	1.00	1.00	.7
.256	1473.	425.	1.6730	.6447	0.00	.10	.59	.87	.95	.99	1.00	1.00	1.00	.6
.323	1467.	417.	1.6349	.6109	0.00	.04	.50	.83	.93	.99	1.00	1.00	1.00	.5
.390	1460.	410.	1.6042	.5831	0.00	.02	.42	.80	.92	.99	1.00	1.00	1.00	.2
.523	1448.	398.	1.5780	.5370	0.00	0.00	.28	.72	.88	.98	1.00	1.00	1.00	.1
.656	1435.	389.	1.5322	.5035	0.00	0.00	.18	.65	.85	.98	.99	1.00	1.00	-.0
.790	1423.	382.	1.4969	.4763	0.00	0.00	.11	.58	.82	.97	.99	1.00	1.00	-.1
1.056	1400.	369.	1.4668	.4307	0.00	0.00	.02	.46	.75	.96	.99	1.00	1.00	-.1
1.323	1377.	359.	1.4135	.3992	0.00	0.00	.00	.35	.68	.95	.99	1.00	1.00	-.2
1.456	1333.	343.	1.3736	.3507	0.00	0.00	0.00	.18	.55	.93	.98	.99	1.00	-.3
2.390	1292.	331.	1.3072	.3160	0.00	0.00	0.00	.08	.43	.90	.97	.99	1.00	-.3
2.923	1251.	321.	1.2552	.2891	0.00	0.00	0.00	.03	.33	.87	.96	.99	1.00	-.3
3.990	1174.	304.	1.2118	.2470	0.00	0.00	0.00	0.00	.17	.81	.94	.98	1.00	-.3
5.056	1101.	292.	1.1372	.2193	0.00	0.00	0.00	0.00	.08	.75	.92	.97	1.00	-.4
6.123	1032.	282.	1.0823	.1990	0.00	0.00	0.00	0.00	.03	.69	.90	.97	1.00	-.4
7.190	965.	275.	1.0385	.1833	0.00	0.00	0.00	0.00	.01	.63	.87	.96	1.00	-.4
8.256	901.	268.	1.0020	.1702	0.00	0.00	0.00	0.00	.00	.57	.84	.95	1.00	-.4
9.323	839.	262.	.9699	.1588	0.00	0.00	0.00	0.00	.00	.51	.82	.94	1.00	-.4
10.390	779.	256.	.9407	.1485	0.00	0.00	0.00	0.00	.00	.45	.79	.93	1.00	-.4
11.456	721.	250.	.9132	.1391	0.00	0.00	0.00	0.00	.00	.39	.76	.92	1.00	-.4
12.523	664.	245.	.8869	.1304	0.00	0.00	0.00	0.00	.00	.34	.73	.90	1.00	-.4
13.590	609.	239.	.8615	.1222	0.00	0.00	0.00	0.00	.00	.30	.70	.89	1.00	-.4
14.656	555.	234.	.8368	.1145	0.00	0.00	0.00	0.00	0.00	.25	.66	.88	1.00	-.4
15.723	503.	229.	.8128	.1073	0.00	0.00	0.00	0.00	0.00	.21	.63	.86	.99	-.4
16.790	453.	224.	.7894	.1005	0.00	0.00	0.00	0.00	0.00	.18	.60	.85	.99	-.3
18.923	354.	214.	.7667	.0880	0.00	0.00	0.00	0.00	0.00	.12	.53	.82	.99	-.3
21.056	262.	204.	.7221	.0774	0.00	0.00	0.00	0.00	0.00	.07	.47	.78	.99	-.3
23.190	175.	196.	.6812	.0686	0.00	0.00	0.00	0.00	0.00	.04	.40	.75	.99	-.3
25.323	92.	188.	.6448	.0614	0.00	0.00	0.00	0.00	0.00	.02	.34	.71	.99	-.3
27.456	14.	182.	.6130	.0557	0.00	0.00	0.00	0.00	0.00	.01	.28	.67	.98	-.3
27.848	0.	181.	.5858	.0548	0.00	0.00	0.00	0.00	0.00	.01	.27	.66	.98	-.3

TOTAL NUMBER OF ITERATIONS = 56

DROPLET HISTORY FOR :
INITIAL DIAMETER (MICRONS): 100.
DUMP ALTITUDE, MSL (METERS): 1500.
LOCAL GROUND LEVEL (METERS): 0.
GROUND-LEVEL TEMPERATURE (C): 0.

T (MIN)	ALTITUDE (METERS)	DIAMETER (MICRONS)	VELOCITY (M/SEC)	RELATIVE MASS REMAINING	IN COMPONENT 2	5	8	11	14	18	23	27	32	DELTA T (C)
0.000	1500.	100.	0.0000	1.0000	1.00	1.00	1.00	1.00	1.00	1.00	1.00	1.00	1.00	-15.3
.000	1500.	98.	.2205	.9566	.83	.96	.99	1.00	1.00	1.00	1.00	1.00	1.00	-4.9
.001	1500.	96.	.2162	.9178	.63	.90	.97	.99	1.00	1.00	1.00	1.00	1.00	3.3
.003	1500.	94.	.2126	.8722	.32	.81	.95	.98	.99	1.00	1.00	1.00	1.00	2.7
.005	1500.	93.	.2070	.8367	.14	.72	.92	.98	.99	1.00	1.00	1.00	1.00	1.7
.007	1500.	92.	.2025	.8084	.06	.63	.89	.97	.99	1.00	1.00	1.00	1.00	1.4
.011	1500.	90.	.1988	.7623	0.00	.46	.83	.95	.98	1.00	1.00	1.00	1.00	1.3
.015	1500.	89.	.1927	.7268	0.00	.33	.77	.93	.97	1.00	1.00	1.00	1.00	.9
.020	1500.	87.	.1878	.6963	0.00	.24	.71	.91	.97	1.00	1.00	1.00	1.00	.6
.024	1500.	86.	.1835	.6700	0.00	.16	.65	.89	.96	.99	1.00	1.00	1.00	.7
.032	1500.	84.	.1797	.6244	0.00	.06	.54	.85	.94	.99	1.00	1.00	1.00	.5
.040	1500.	82.	.1729	.5903	0.00	.02	.44	.81	.92	.99	1.00	1.00	1.00	.3
.049	1499.	81.	.1677	.5627	0.00	.01	.36	.77	.90	.99	1.00	1.00	1.00	.3
.065	1499.	79.	.1633	.5167	0.00	0.00	.22	.68	.87	.98	.99	1.00	1.00	.2
.082	1499.	77.	.1558	.4831	0.00	0.00	.12	.61	.83	.98	.99	1.00	1.00	.1
.099	1499.	75.	.1501	.4558	0.00	0.00	.07	.53	.79	.97	.99	1.00	1.00	.0
.132	1499.	73.	.1453	.4108	0.00	0.00	.00	.40	.71	.96	.99	1.00	1.00	.0
.165	1498.	71.	.1370	.3805	0.00	0.00	0.00	.29	.64	.94	.98	.99	1.00	-.0
.232	1498.	67.	.1312	.3320	0.00	0.00	0.00	.12	.49	.92	.97	.99	1.00	-.1
.299	1497.	65.	.1214	.2980	0.00	0.00	0.00	.04	.37	.89	.97	.99	1.00	-.1
.432	1497.	61.	.1140	.2483	0.00	0.00	0.00	0.00	.17	.82	.94	.98	1.00	-.1
.565	1496.	58.	.1025	.2183	0.00	0.00	0.00	0.00	.07	.76	.92	.98	1.00	-.1
.832	1494.	54.	.0949	.1793	0.00	0.00	0.00	0.00	0.00	.63	.87	.96	1.00	-.1
1.365	1491.	50.	.0843	.1371	0.00	0.00	0.00	0.00	0.00	.38	.77	.92	1.00	-.1
1.899	1489.	46.	.0715	.1078	0.00	0.00	0.00	0.00	0.00	.20	.66	.88	1.00	-.1
2.965	1485.	39.	.0616	.0659	0.00	0.00	0.00	0.00	0.00	0.00	.44	.79	.99	-.1
7.232	1474.	30.	.0452	.0338	0.00	0.00	0.00	0.00	0.00	0.00	0.00	.34	.97	-.1
15.765	1459.	27.	.0296	.0254	0.00	0.00	0.00	0.00	0.00	0.00	0.00	0.00	.92	-.1
32.832	1433.	25.	.0245	.0203	0.00	0.00	0.00	0.00	0.00	0.00	0.00	0.00	.79	-.1
66.965	1390.	22.	.0210	.0134	0.00	0.00	0.00	0.00	0.00	0.00	0.00	0.00	.52	-.1
135.232	1326.	12.	.0157	.0028	0.00	0.00	0.00	0.00	0.00	0.00	0.00	0.00	.05	-.1
271.765	1285.	10.	.0050	.0017	0.00	0.00	0.00	0.00	0.00	0.00	0.00	0.00	0.00	-.0
544.832	1229.	10.	.0035	.0017	0.00	0.00	0.00	0.00	0.00	0.00	0.00	0.00	0.00	-.0
817.899	1171.	10.	.0035	.0017	0.00	0.00	0.00	0.00	0.00	0.00	0.00	0.00	0.00	-.0
*******	1133.	10.	.0034	.0016	0.00	0.00	0.00	0.00	0.00	0.00	0.00	0.00	0.00	-.0

TOTAL NUMBER OF ITERATIONS = 48

DROPLET HISTORY FOR :

DIAMETER INTERVAL (MICRONS):	20.
DUMP ALTITUDE, MSL (METERS):	1500.
LOCAL GROUND LEVEL (METERS):	0.
GROUND LEVEL TEMPERATURE(C):	20.
AIRCRAFT VELOCITY (MET/SEC):	175.

INITIAL DIAMETER (MICRONS)	FINAL DIAMETER (MICRONS)	ELAPSED TIME (MIN)	FINAL ALTITUDE (METERS)	RELATIVE MASS REMAINING...	IN COMPONENT 2	5	8	11	14	18	23	27	32	PERCENT OF TOTAL INITIAL MASS
10.	0.	11.38	1500.	.000	0.00	0.00	0.00	0.00	0.00	0.00	0.00	0.00	0.00	0.00
30.	1.	91.05	1499.	.000	0.00	0.00	0.00	0.00	0.00	0.00	0.00	0.00	0.00	0.00
50.	0.	364.17	1490.	.000	0.00	0.00	0.00	0.00	0.00	0.00	0.00	0.00	0.00	0.00
70.	0.	1456.48	1442.	.000	0.00	0.00	0.00	0.00	0.00	0.00	0.00	0.00	0.00	0.00
90.	5.	728.38	1398.	.000	0.00	0.00	0.00	0.00	0.00	0.00	0.00	0.00	0.00	0.00
110.	7.	916.22	1296.	.000	0.00	0.00	0.00	0.00	0.00	0.00	0.00	0.00	0.00	0.00
130.	6.	1465.30	1088.	.000	0.00	0.00	0.00	0.00	0.00	0.00	0.00	0.00	0.00	0.00
150.	9.	1567.70	882.	.000	0.00	0.00	0.00	0.00	0.00	0.00	0.00	0.00	0.00	0.00
170.	10.	1704.44	603.	.000	0.00	0.00	0.00	0.00	0.00	0.00	0.00	0.00	0.00	0.00
190.	11.	1774.34	293.	.000	0.00	0.00	0.00	0.00	0.00	0.00	0.00	0.00	0.00	0.00
210.	14.	1569.54	43.	.000	0.00	0.00	0.00	0.00	0.00	0.00	0.00	0.00	0.00	0.00
230.	18.	1167.43	0.	.001	0.00	0.00	0.00	0.00	0.00	0.00	0.00	0.00	0.00	.00
250.	22.	877.19	0.	.001	0.00	0.00	0.00	0.00	0.00	0.00	0.00	0.00	0.00	.01
270.	25.	684.41	0.	.001	0.00	0.00	0.00	0.00	0.00	0.00	0.00	0.00	0.00	.01
290.	27.	539.47	0.	.001	0.00	0.00	0.00	0.00	0.00	0.00	0.00	0.00	0.00	.01
310.	30.	428.47	0.	.002	0.00	0.00	0.00	0.00	0.00	0.00	0.00	0.00	0.00	.01
330.	32.	342.18	0.	.002	0.00	0.00	0.00	0.00	0.00	0.00	0.00	0.00	0.00	.01
350.	34.	272.57	0.	.002	0.00	0.00	0.00	0.00	0.00	0.00	0.00	0.00	0.00	.01
370.	36.	214.83	0.	.002	0.00	0.00	0.00	0.00	0.00	0.00	0.00	0.00	0.00	.01
390.	39.	166.77	0.	.002	0.00	0.00	0.00	0.00	0.00	0.00	0.00	0.00	0.00	.01
410.	41.	127.34	0.	.002	0.00	0.00	0.00	0.00	0.00	0.00	0.00	0.00	0.00	.01
430.	50.	97.77	0.	.002	0.00	0.00	0.00	0.00	0.00	0.00	0.00	0.00	.03	.01
450.	69.	80.75	0.	.005	0.00	0.00	0.00	0.00	0.00	0.00	0.00	0.00	.15	.01
470.	84.	70.07	0.	.008	0.00	0.00	0.00	0.00	0.00	0.00	0.00	0.00	.26	.01
490.	96.	62.03	0.	.010	0.00	0.00	0.00	0.00	0.00	0.00	0.00	0.00	.36	.00

OVERALL PERCENT OF INITIAL MASS: .11

PERCENT OF INITIAL MASS REMAINING, BY COMPONENT NUMBER:

# 1:	0.00%	# 2:	0.00%	# 3:	0.00%	# 4:	0.00%	# 5:	0.00%
# 6:	0.00%	# 7:	0.00%	# 8:	0.00%	# 9:	0.00%	#10:	0.00%
#11:	0.00%	#12:	0.00%	#13:	0.00%	#14:	0.00%	#15:	0.00%
#16:	0.00%	#17:	0.00%	#18:	0.00%	#19:	0.00%	#20:	0.00%
#21:	0.00%	#22:	0.00%	#23:	0.00%	#24:	0.00%	#25:	0.00%
#26:	.00%	#27:	0.00%	#28:	0.00%	#29:	0.00%	#30:	.00%
#31:	.00%	#32:	.02%	#33:	.09%	#			

DROPLET HISTORY FOR :

DIAMETER INTERVAL (MICRONS):	20.
DUMP ALTITUDE, MSL (METERS):	1500.
LOCAL GROUND LEVEL (METERS):	0.
GROUND LEVEL TEMPERATURE(C):	0.
AIRCRAFT VELOCITY (MET/SEC):	175.

INITIAL DIAMETER (MICRONS)	FINAL DIAMETER (MICRONS)	ELAPSED TIME (MIN)	FINAL ALTITUDE (METERS)	RELATIVE MASS REMAINING...	IN COMPONENT 2	5	8	11	14	18	23	27	32	PERCENT OF TOTAL INITIAL MASS
10.	1.	364.11	1500.	.000	0.00	0.00	0.00	0.00	0.00	0.00	0.00	0.00	0.00	0.00
30.	0.	*******	1458.	.000	0.00	0.00	0.00	0.00	0.00	0.00	0.00	0.00	0.00	0.00
50.	2.	9512.23	1238.	.000	0.00	0.00	0.00	0.00	0.00	0.00	0.00	0.00	0.00	0.00
70.	5.	*******	794.	.001	0.00	0.00	0.00	0.00	0.00	0.00	0.00	0.00	0.00	0.00
90.	9.	*******	135.	.001	0.00	0.00	0.00	0.00	0.00	0.00	0.00	0.00	0.00	0.00
110.	10.	5256.83	0.	.001	0.00	0.00	0.00	0.00	0.00	0.00	0.00	0.00	0.00	.00
130.	12.	3014.32	0.	.001	0.00	0.00	0.00	0.00	0.00	0.00	0.00	0.00	0.00	.01
150.	15.	1830.20	0.	.002	0.00	0.00	0.00	0.00	0.00	0.00	0.00	0.00	0.00	.01
170.	17.	1068.68	0.	.002	0.00	0.00	0.00	0.00	0.00	0.00	0.00	0.00	0.00	.01
190.	19.	587.52	0.	.002	0.00	0.00	0.00	0.00	0.00	0.00	0.00	0.00	0.00	.01
210.	20.	299.61	0.	.003	0.00	0.00	0.00	0.00	0.00	0.00	0.00	0.00	.07	.02
230.	45.	209.12	0.	.010	0.00	0.00	0.00	0.00	0.00	0.00	0.00	0.00	.36	.06
250.	56.	162.68	0.	.014	0.00	0.00	0.00	0.00	0.00	0.00	0.00	0.00	.55	.08
270.	65.	131.24	0.	.018	0.00	0.00	0.00	0.00	0.00	0.00	0.00	0.00	.68	.11
290.	73.	108.65	0.	.020	0.00	0.00	0.00	0.00	0.00	0.00	0.00	.00	.76	.12
310.	81.	91.43	0.	.022	0.00	0.00	0.00	0.00	0.00	0.00	0.00	.00	.82	.14
330.	88.	77.76	0.	.024	0.00	0.00	0.00	0.00	0.00	0.00	0.00	.02	.87	.15
350.	96.	66.71	0.	.026	0.00	0.00	0.00	0.00	0.00	0.00	.00	.05	.90	.17
370.	104.	57.77	0.	.028	0.00	0.00	0.00	0.00	0.00	0.00	.00	.11	.92	.19
390.	113.	50.51	0.	.030	0.00	0.00	0.00	0.00	0.00	0.00	.00	.20	.94	.13
410.	123.	44.54	0.	.033	0.00	0.00	0.00	0.00	0.00	0.00	.01	.29	.96	.12
430.	134.	39.60	0.	.037	0.00	0.00	0.00	0.00	0.00	.00	.05	.39	.97	.10
450.	146.	35.44	0.	.041	0.00	0.00	0.00	0.00	0.00	.00	.10	.48	.97	.08
470.	159.	31.99	0.	.046	0.00	0.00	0.00	0.00	0.00	.00	.16	.56	.98	.05
490.	173.	29.11	0.	.052	0.00	0.00	0.00	0.00	0.00	.00	.23	.63	.98	.02

OVERALL PERCENT OF INITIAL MASS: 1.55

PERCENT OF INITIAL MASS REMAINING, BY COMPONENT NUMBER:

# 1:	0.00%	# 2:	0.00%	# 3:	0.00%	# 4:	0.00%	# 5:	0.00%
# 6:	0.00%	# 7:	0.00%	# 8:	0.00%	# 9:	0.00%	#10:	0.00%
#11:	0.00%	#12:	0.00%	#13:	0.00%	#14:	0.00%	#15:	0.00%
#16:	0.00%	#17:	.00%	#18:	.00%	#19:	.00%	#20:	.00%
#21:	.00%	#22:	.02%	#23:	.02%	#24:	.00%	#25:	.00%
#26:	.08%	#27:	.07%	#28:	.01%	#29:	.01%	#30:	.04%
#31:	.04%	#32:	1.12%	#33:	.15%	#			

DROPLET HISTORY FOR :

DIAMETER INTERVAL (MICRONS):	20.
DUMP ALTITUDE, MSL (METERS):	1500.
LOCAL GROUND LEVEL (METERS):	0.
GROUND LEVEL TEMPERATURE(C):	-20.
AIRCRAFT VELOCITY (MET/SEC):	175.

INITIAL DIAMETER (MICRONS)	FINAL DIAMETER (MICRONS)	ELAPSED TIME (MIN)	FINAL ALTITUDE (METERS)	RELATIVE MASS REMAINING...	IN COMPONENT 2	5	8	11	14	18	23	27	32	PERCENT OF TOTAL INITIAL MASS
10.	1.	*******	1496.	.001	0.00	0.00	0.00	0.00	0.00	0.00	0.00	0.00	0.00	0.00
30.	3.	*******	1370.	.002	0.00	0.00	0.00	0.00	0.00	0.00	0.00	0.00	0.00	0.00
50.	5.	*******	848.	.002	0.00	0.00	0.00	0.00	0.00	0.00	0.00	0.00	0.00	0.00
70.	7.	8709.59	0.	.002	0.00	0.00	0.00	0.00	0.00	0.00	0.00	0.00	0.00	.00
90.	9.	1744.99	0.	.002	0.00	0.00	0.00	0.00	0.00	0.00	0.00	0.00	0.00	.01
110.	25.	711.87	0.	.015	0.00	0.00	0.00	0.00	0.00	0.00	0.00	0.00	.60	.06
130.	33.	425.92	0.	.022	0.00	0.00	0.00	0.00	0.00	0.00	0.00	0.00	.82	.10
150.	41.	276.51	0.	.026	0.00	0.00	0.00	0.00	0.00	0.00	0.00	.01	.92	.11
170.	49.	187.89	0.	.030	0.00	0.00	0.00	0.00	0.00	0.00	0.00	.12	.96	.14
190.	59.	132.69	0.	.036	0.00	0.00	0.00	0.00	0.00	0.00	.02	.39	.98	.17
210.	72.	97.77	0.	.047	0.00	0.00	0.00	0.00	0.00	.00	.16	.63	.99	.24
230.	88.	76.12	0.	.064	0.00	0.00	0.00	0.00	0.00	.02	.37	.77	.99	.36
250.	106.	61.91	0.	.085	0.00	0.00	0.00	0.00	0.00	.08	.54	.85	1.00	.48
270.	123.	52.27	0.	.107	0.00	0.00	0.00	0.00	0.00	.19	.66	.89	1.00	.64
290.	140.	45.18	0.	.126	0.00	0.00	0.00	0.00	.00	.30	.73	.92	1.00	.76
310.	157.	39.68	0.	.143	0.00	0.00	0.00	0.00	.00	.41	.79	.94	1.00	.92
330.	173.	35.37	0.	.158	0.00	0.00	0.00	0.00	.00	.49	.83	.95	1.00	1.01
350.	188.	31.89	0.	.171	0.00	0.00	0.00	0.00	.00	.57	.86	.96	1.00	1.10
370.	204.	29.03	0.	.184	0.00	0.00	0.00	0.00	.01	.63	.89	.97	1.00	1.03
390.	220.	26.64	0.	.196	0.00	0.00	0.00	0.00	.02	.68	.90	.97	1.00	.98
410.	236.	24.59	0.	.208	0.00	0.00	0.00	.00	.04	.73	.92	.98	1.00	.75
430.	252.	22.82	0.	.220	0.00	0.00	0.00	.00	.07	.76	.93	.98	1.00	.62
450.	268.	21.29	0.	.232	0.00	0.00	0.00	.00	.10	.79	.94	.98	1.00	.46
470.	285.	19.96	0.	.243	0.00	0.00	0.00	.00	.14	.82	.95	.99	1.00	.29
490.	302.	18.80	0.	.255	0.00	0.00	0.00	.00	.18	.84	.95	.99	1.00	.10

OVERALL PERCENT OF INITIAL MASS: 10.21

PERCENT OF INITIAL MASS REMAINING, BY COMPONENT NUMBER:

# 1:	0.00%	# 2:	0.00%	# 3:	0.00%	# 4:	0.00%	# 5:	0.00%
# 6:	0.00%	# 7:	0.00%	# 8:	0.00%	# 9:	0.00%	#10:	.00%
#11:	.00%	#12:	.01%	#13:	.05%	#14:	.07%	#15:	.17%
#16:	.15%	#17:	.13%	#18:	1.29%	#19:	.73%	#20:	1.26%
#21:	.45%	#22:	.18%	#23:	1.36%	#24:	.55%	#25:	.27%
#26:	.21%	#27:	.71%	#28:	.24%	#29:	.07%	#30:	.15%
#31:	.08%	#32:	1.96%	#33:	.16%	#			

DROPLET HISTORY FOR :

DIAMETER INTERVAL (MICRONS):	20.
DUMP ALTITUDE, MSL (METERS):	6000.
LOCAL GROUND LEVEL (METERS):	0.
GROUND LEVEL TEMPERATURE(C):	0.
AIRCRAFT VELOCITY (MET/SEC):	175.

INITIAL DIAMETER (MICRONS)	FINAL DIAMETER (MICRONS)	ELAPSED TIME (MIN)	FINAL ALTITUDE (METERS)	RELATIVE MASS REMAINING...	IN COMPONENT 2	5	8	11	14	18	23	27	32	PERCENT OF TOTAL INITIAL MASS
10.	1.	*******	5996.	.002	0.00	0.00	0.00	0.00	0.00	0.00	0.00	0.00	0.00	0.00
30.	3.	*******	5814.	.002	0.00	0.00	0.00	0.00	0.00	0.00	0.00	0.00	0.00	0.00
50.	5.	*******	5081.	.002	0.00	0.00	0.00	0.00	0.00	0.00	0.00	0.00	0.00	0.00
70.	7.	*******	3824.	.002	0.00	0.00	0.00	0.00	0.00	0.00	0.00	0.00	0.00	0.00
90.	9.	*******	2355.	.002	0.00	0.00	0.00	0.00	0.00	0.00	0.00	0.00	0.00	0.00
110.	11.	*******	754.	.001	0.00	0.00	0.00	0.00	0.00	0.00	0.00	0.00	0.00	0.00
130.	12.	7373.82	0.	.001	0.00	0.00	0.00	0.00	0.00	0.00	0.00	0.00	0.00	.01
150.	15.	4363.13	0.	.002	0.00	0.00	0.00	0.00	0.00	0.00	0.00	0.00	0.00	.01
170.	17.	2693.48	0.	.002	0.00	0.00	0.00	0.00	0.00	0.00	0.00	0.00	0.00	.01
190.	19.	1687.23	0.	.002	0.00	0.00	0.00	0.00	0.00	0.00	0.00	0.00	0.00	.01
210.	21.	1054.82	0.	.002	0.00	0.00	0.00	0.00	0.00	0.00	0.00	0.00	0.00	.01
230.	31.	667.91	0.	.003	0.00	0.00	0.00	0.00	0.00	0.00	0.00	0.00	.07	.02
250.	48.	505.71	0.	.009	0.00	0.00	0.00	0.00	0.00	0.00	0.00	0.00	.33	.05
270.	59.	407.90	0.	.013	0.00	0.00	0.00	0.00	0.00	0.00	0.00	0.00	.50	.08
290.	66.	338.87	0.	.016	0.00	0.00	0.00	0.00	0.00	0.00	0.00	.00	.63	.10
310.	77.	287.30	0.	.019	0.00	0.00	0.00	0.00	0.00	0.00	0.00	.00	.71	.12
330.	84.	247.22	0.	.021	0.00	0.00	0.00	0.00	0.00	0.00	0.00	.00	.78	.13
350.	92.	215.13	0.	.022	0.00	0.00	0.00	0.00	0.00	0.00	.00	.00	.83	.14
370.	99.	189.14	0.	.024	0.00	0.00	0.00	0.00	0.00	0.00	.00	.01	.86	.13
390.	107.	167.78	0.	.025	0.00	0.00	0.00	0.00	0.00	0.00	.00	.03	.89	.11
410.	115.	150.02	0.	.027	0.00	0.00	0.00	0.00	0.00	0.00	.00	.07	.91	.10
430.	123.	135.14	0.	.029	0.00	0.00	0.00	0.00	0.00	0.00	.00	.12	.93	.08
450.	132.	122.55	0.	.030	0.00	0.00	0.00	0.00	0.00	.00	.00	.19	.94	.06
470.	141.	111.77	0.	.032	0.00	0.00	0.00	0.00	0.00	.00	.01	.26	.95	.04
490.	151.	102.53	0.	.035	0.00	0.00	0.00	0.00	0.00	.00	.03	.34	.96	.01

OVERALL PERCENT OF INITIAL MASS: 1.22

PERCENT OF INITIAL MASS REMAINING, BY COMPONENT NUMBER:

# 1:	0.00%	# 2:	0.00%	# 3:	0.00%	# 4:	0.00%	# 5:	0.00%
# 6:	0.00%	# 7:	0.00%	# 8:	0.00%	# 9:	0.00%	#10:	0.00%
#11:	0.00%	#12:	0.00%	#13:	0.00%	#14:	0.00%	#15:	0.00%
#16:	0.00%	#17:	.00%	#18:	.00%	#19:	.00%	#20:	.00%
#21:	.00%	#22:	.01%	#23:	.00%	#24:	.00%	#25:	.00%
#26:	.05%	#27:	.02%	#28:	.00%	#29:	.00%	#30:	.02%
#31:	.03%	#32:	.92%	#33:	.14%	#			

DROPLET HISTORY FOR :

DIAMETER INTERVAL (MICRONS):	20.
DUMP ALTITUDE, MSL (METERS):	300.
LOCAL GROUND LEVEL (METERS):	0.
GROUND LEVEL TEMPERATURE(C):	0.
AIRCRAFT VELOCITY (MET/SEC):	175.

INITIAL DIAMETER (MICRONS)	FINAL DIAMETER (MICRONS)	ELAPSED TIME (MIN)	FINAL ALTITUDE (METERS)	RELATIVE MASS REMAINING...	IN COMPONENT 2	5	8	11	14	18	23	27	32	PERCENT OF TOTAL INITIAL MASS
10.	0.	182.06	300.	-.000	0.00	0.00	0.00	0.00	0.00	0.00	0.00	0.00	0.00	0.00
30.	0.	1456.45	291.	-.000	0.00	0.00	0.00	0.00	0.00	0.00	0.00	0.00	0.00	0.00
50.	0.	2912.92	211.	.000	0.00	0.00	0.00	0.00	0.00	0.00	0.00	0.00	0.00	0.00
70.	3.	4783.31	0.	.000	0.00	0.00	0.00	0.00	0.00	0.00	0.00	0.00	0.00	.00
90.	8.	1695.05	0.	.001	0.00	0.00	0.00	0.00	0.00	0.00	0.00	0.00	0.00	.00
110.	11.	797.88	0.	.002	0.00	0.00	0.00	0.00	0.00	0.00	0.00	0.00	0.00	.01
130.	13.	314.84	0.	.002	0.00	0.00	0.00	0.00	0.00	0.00	0.00	0.00	0.00	.01
150.	20.	109.72	0.	.004	0.00	0.00	0.00	0.00	0.00	0.00	0.00	0.00	.08	.02
170.	36.	64.96	0.	.013	0.00	0.00	0.00	0.00	0.00	0.00	0.00	0.00	.49	.06
190.	46.	48.32	0.	.018	0.00	0.00	0.00	0.00	0.00	0.00	0.00	0.00	.71	.09
210.	56.	35.93	0.	.022	0.00	0.00	0.00	0.00	0.00	0.00	0.00	0.00	.83	.12
230.	62.	27.18	0.	.025	0.00	0.00	0.00	0.00	0.00	0.00	0.00	0.00	.90	.14
250.	71.	20.62	0.	.029	0.00	0.00	0.00	0.00	0.00	0.00	0.00	.10	.94	.16
270.	81.	16.34	0.	.034	0.00	0.00	0.00	0.00	0.00	0.00	.00	.35	.96	.20
290.	95.	13.03	0.	.042	0.00	0.00	0.00	0.00	0.00	0.00	.10	.54	.98	.25
310.	110.	10.80	0.	.052	0.00	0.00	0.00	0.00	0.00	0.00	.25	.68	.98	.33
330.	127.	9.27	0.	.066	0.00	0.00	0.00	0.00	0.00	.02	.41	.76	.99	.42
350.	147.	8.07	0.	.084	0.00	0.00	0.00	0.00	0.00	.09	.53	.82	.99	.54
370.	165.	7.18	0.	.100	0.00	0.00	0.00	0.00	0.00	.17	.61	.85	.99	.56
390.	183.	6.46	0.	.116	0.00	0.00	0.00	0.00	0.00	.26	.68	.88	.99	.51
410.	200.	5.86	0.	.130	0.00	0.00	0.00	0.00	0.00	.34	.73	.90	1.00	.47
430.	217.	5.42	0.	.143	0.00	0.00	0.00	0.00	0.00	.42	.77	.92	1.00	.40
450.	233.	5.01	0.	.155	0.00	0.00	0.00	0.00	0.00	.49	.80	.93	1.00	.31
470.	249.	4.64	0.	.166	0.00	0.00	0.00	0.00	0.00	.55	.83	.94	1.00	.20
490.	266.	4.34	0.	.177	0.00	0.00	0.00	0.00	.00	.60	.85	.95	1.00	.07

OVERALL PERCENT OF INITIAL MASS: 4.87

PERCENT OF INITIAL MASS REMAINING, BY COMPONENT NUMBER:

# 1:	0.00%	# 2:	0.00%	# 3:	0.00%	# 4:	0.00%	# 5:	0.00%
# 6:	0.00%	# 7:	0.00%	# 8:	0.00%	# 9:	0.00%	#10:	0.00%
#11:	0.00%	#12:	0.00%	#13:	.00%	#14:	.00%	#15:	.01%
#16:	.01%	#17:	.06%	#18:	.34%	#19:	.19%	#20:	.37%
#21:	.15%	#22:	.12%	#23:	.63%	#24:	.23%	#25:	.12%
#26:	.16%	#27:	.43%	#28:	.13%	#29:	.04%	#30:	.11%
#31:	.07%	#32:	1.62%	#33:	.16%	#			

INITIAL DISTRIBUTION

Hq TAC/SGPA	1	USAF Hosp/SGB	2
Hq SAC/SGPA	1	R&D/EQ/DARD-ARE-E	1
Hq USAFE/SGB	1	Hq AFESC/RDVC	5
Hq PACAF/SGPE	1	AMD/RDB	1
Hq AAC/SGB	1	Hq AFSC/DEV	1
Hq AFLC/SGB	1	USAFSAM/VNL	1
FAA/AEQ-10	2	AFGL/LKD	5
Hq TAC/DEEV	1	ASD/DEP	1
Hq USAFE/DEPV	1	NEPSS	1
AMRL/CC	1	Hq SAC/DEV	1
USAFSAM/CC	1	Hq PACAF/DEEV	1
ASD/CC	1	AMRL/THE	1
AFOSR/CC	1	AFAPL/SFF	1
AEDC/CC	1	AFOSR/N	1
USAFRCE/WR/DEEV	1	AEDC/DOTR	1
USAFRCE/CR/DEEV	1	Hq MAC/DEEV	1
USAFRCE/ER/DEEV	1	AFOSR	1
DTIC/DDA	12	Hq USAFE/DEVS	1
Hq AFSC/SGB	1	Hq MAC/SGPE	1
NAPC/Code PE 71 AFK	1	23 CES/DEEV	1
Hq AFSC/DLWM	1	USCG (G-WEP-1/73)	1
Hq AFSC/SDNE	1	Hq AFESC/RD	1
Hq USAF/LEEV	1	Hq AFESC/RDVA	2
OSAF/MIQ	1	Army Environmental	
OSAF/OI	1	Hygiene Agency-HSE-EA	2
AFIT/LSGM	1	OASD/(I&L)EES	1
AFIT/Library	1	ARPA	1
AFIT/DE	1	AFMSC/SGPA	1
R&D/EQ/Code 3021	1	Hq AFRES/DE	1
OEHL/CC	4	EPA/ESRL	1
Hq AFESC/DEV	4	O'CGD9 (MEP)	1
USAFSAM/EDE	2	Hq AFESC/RDV	1
Hq AFISC		Hq AFESC/WE	2
AUL/LSE 71-249	1	AFATL/DLODL	1
HqUSAFA/Library	1	AFWL/SUL (Tech Lib)	1
Hq AFESC/TST	1	AFTEC/SGB	1
OL-AD/OEHL	1	Hq AFRES/SGB	1
OUSDR&E	1	4TFW/DOV	1
Hq AAC/DEV	1	Hq AFESC/RDVCA	9
Hq AFLC/DEPV	1	1 Med Svc Wg/SGB	1
Hq USAF/SGES	1	NAVFAC/Code 111	1
EPA/ORD	1	Chem Abstracts Ser	1
AMD/RDU	1	NCEL/Code 15111	1
Hq AFSC/SGPA	1	USCG/GDD	1
Hq USAF/LEEVP	1	EPA/Corvallis	1
Hq USAF/LGYF	1	EPA/Athens	1
AFIT/DEM	1	Hq ATC/SGPAP	1
Hq ATC/DEEV	1		

(The reverse of this page is blank)